PHYSIOLOGICAL FUNCTION OF RENAL H^+,K^+-ATPASES IN ELECTROLYTE AND ACID-BASE HOMEOSTASIS

By

MEGAN MICHELLE GREENLEE

A DISSERTATION PRESENTED TO THE GRADUATE SCHOOL
OF THE UNIVERSITY OF FLORIDA IN PARTIAL FULFILLMENT
OF THE REQUIREMENTS FOR THE DEGREE OF
DOCTOR OF PHILOSOPHY

UNIVERSITY OF FLORIDA

2011

ACKNOWLEDGMENTS

First and foremost, I acknowledge and thank Jeremiah, my husband and best friend, for he is the foundation upon which I stood during graduate school and still stand in life. Secondly, I thank my parents, Michael and Deborah Greenlee, for their unfaltering love and encouragement. I most certainly could not have succeeded in my career and life goals without both of them by my side. I also thank the IDP program for providing me not only the opportunity to pursue science but also to develop strong friendships and collaborations.

As for my coworkers, I first thank Jeanette Lynch for she suggested I start along the scientific path of whole animal studies, an area that has not only provided for a great dissertation but also greatly added to the field of renal and gastrointestinal physiology. I do appreciate her continuing support with laboratory techniques and long conversations about science. Most of all, I appreciate her companionship including taking coffee and lunch breaks together and discussing life issues (the good and bad). She was quite patient with me. At times, she “put on her hard hart” with a smile to survive my frustrations with graduate school and lab. I will never forget her.

Secondly, I thank Michelle Gumz. Not only did she provide great advice and mentored me in the laboratory but she has become a really great friend of mine. I admire her passion for both science and family and her ability to see the good side of most situations. She has been my champion and, I believe, made me the scientist I am today. I hope for nothing but the best in her new faculty position.

As for my progress in graduate school, I sincerely thank my committee members, Brian Cain, Chris Baylis, and Jill Verlander. All three of them have offered such great suggestions and comments on my dissertation work and also, on my pursuit of a post-

doctoral fellowship. It is surprising and extraordinary how much each one of them cares about my success. Above all, I thank Brian for teaching me how to perform experiments and to be a scientist. He is the reason why I ended up in graduate school and not pharmacy or medical school. I also thank him for this continued guidance and support in my graduate work.

Finally, I thank my committee chair and mentor, Charles Wingo, for he provided me with vast resources to accomplish my graduate dissertation project. He also taught me a considerable amount about clinical observations that really helped me to understand and discuss my own data and that of other investigators. He allowed and encouraged my development as a scientist by letting me design experiments, make mistakes, and then make even better experiments. Overall, I thank him for his immense support of both my work and life endeavors.

TABLE OF CONTENTS

page

LIST OF TABLES

LIST OF FIGURES

LIST OF ABBREVIATIONS

µEq	microequivalent(s)
µg	microgram(s)
µL	microliter(s)
µM	micromolar
µm	micrometer
ADP	adenosine diphosphate
AE1–2	anion exchanger 1 and 2
Aldo	aldosterone
Ang II	angiotensin II
ANOVA	analysis of variance
ANP	atrial natriuetic peptide
ATP	adenosine triphosphate
ATPase	adenosine triphosphatase
AQP1–4	aquaporin 1, 2, 3, and 4
AVP	arginine vasopressin
B	binding of sample
B_o	maximum binding
BCA	bicinchoninic acid
BK	big conductance potassium channel
BLAST	basic local alignment search tool
bp	basepair(s)
C	Celsius
Ca^{2+}	calcium

Ca^{2+}-ATPase	calcium translocating adenosine triphosphatase
CAII, CAIV	carbonic anhydrase 2 and 4
cAMP	cyclic adenosine monophosphate
cDNA	complementary deoxyribonucleic acid
Cl^-	chloride
CO_2	carbon dioxide
CpG	cytosine-phosphate-guanidine
Ct	cycle threshold
CTX	cortex
DNA	deoxyribonucleic acid
DNase	deoxyribonuclease
dNTPs	deoxynucleotide triphosphates
DOCP	desoxycorticosterone pivalate
EDTA	ethylenediaminetetraacetic acid
EIA	enzyme immunoassay
ENaC	epithelial sodium channel
ET-1	endothelin 1
ETAR	endothelin a receptor
ETBR	endothelin b receptor
Eq	equivalent(s)
g	gram(s), gravitational force
GAPD	glyceraldehye 3-phosphatase dehydrogenase
GFR	glomerular filtration rate

H^+	hydrogen; proton; acid
H^+-ATPase	proton translocating adenosine triphosphatase
H^+,K^+-ATPase	proton and potassium translocating adenosine triphosphatase
H_2O	water
HCl	hydrochloric acid
HCO_3^-	bicarbonate
Hct	hematocrit
HKα	H^+,K^+-ATPase α subunit
$HK\alpha_1$	H^+,K^+-ATPase α_1 subunit
$HK\alpha_2$	H^+,K^+-ATPase α_2 subunit
$HK\alpha_1^{-/-}$	$HK\alpha_1$ null
$HK\alpha_{1,2}^{-/-}$	$HK\alpha_1$ and $HK\alpha_2$ null
$HK\alpha_2^{-/-}$	$HK\alpha_2$ null
HKβ	H^+,K^+-ATPase β subunit
$HK\beta^{-/-}$	HKβ null
HRE	hormone response element
HRP	horseradish peroxidase
IC	intercalated cell
i.m.	intramuscular
IM	inner medulla
IMCD3	inner medullary collecting duct 3 cell line
i.p.	intraperitoneal
K^+	potassium

KCC	potassium and chloride cotransporter
KCl	potassium chloride
kDa	kiloDalton(s)
kg	kilogram
KHP	potassium hydrogen phthalate
L	liter(s)
ln	natural log
MAPK	mitogen activated protein kinase
Med	medulla
mEq	miliequivalent(s)
mg	miligram(s)
miRNA	microribonucleic acid (microRNA, miR)
mL	mililiter(s)
mM	milimolar
mmHg	millimeters of mercury
mOsm	miliosmoles
MR	mineralocorticoid receptor
mRNA	messenger ribonucleic acid
N	number
Na^+	sodium
Na^+,K^+-ATPase	sodium and potassium translocating adenosine triphosphatase
NaCl	sodium chloride
$NaK\alpha_1$	Na^+,K^+-ATPase α 1 subunit

$NaK\beta_1$	Na^+,K^+-ATPase β_1 subunit
NaOH	sodium hydroxide
NBCe1	electrogenic sodium bicarbonate cotransporter 1
NCBI	National Center of Biotechnology Information
NCC	sodium and chloride cotransporter
NDCBE	sodium dependent (or driven) chloride and bicarbonate exchanger
NF-κB	nuclear factor light-chain-kappa of activated B cells
NH_3	ammonia
NH_4^+	ammonium
NH_4Cl	ammonium chloride
NHE1	sodium and hydrogen exchanger 1
NHE3	sodium and hydrogen exchanger 3
NKCC2	sodium, potassium, two chloride cotransporter 2
NSB	non-specific binding
NT	no template
nM	nanomolar
OM	outer medulla
$OMCD_1$	outer medullary collecting duct 1 cell line
P	probability of null hypothesis
PBS	phosphate buffered saline
PC	principal cell
pCO_2	partial pressure of carbon dioxide
PCR	polymerase chain reaction

PKA	protein kinase A
PKC	protein kinase C
P-type	phosphorylated-type
qPCR	quantitative polymerase chain reaction
R1	reaction 1
R2	reaction 2
RAAS	renin-angiotensin-aldosterone system
Rhbg	Rhesus associated blood group factor b
Rhcg	Rhesus associated blood group factor c
RNA	ribonucleic acid
RNase	ribonuclease
ROMK	renal outer medullary potassium channel
rpm	revolutions per minute
RT	reverse transcriptase
SCH-28080	Schering-28080
SDS	sodium dodecyl sulfate
SEM	standard error of the mean
Sp1	specificity protein 1
TBS	tris buffered saline
TBS-S	tris buffered saline with 0.05% Saddle Soap®
TESS	Transcription Element Search Software
TD	Teklad
TF	transcription factor

UTR	untranslated region
V1R	vasopressin receptor 1
V1aR	vasopressin receptor 1a
V2R	vasopressin receptor 2
V-type	vacuolar-type
WNK1	with-no-lysine kinase 1
WT	wild type

Abstract of Dissertation Presented to the Graduate School
of the University of Florida in Partial Fulfillment of the
Requirements for the Degree of Doctor of Philosophy

PHYSIOLOGICAL FUNCTION OF RENAL H^+,K^+-ATPASES IN ELECTROLYTE AND ACID-BASE HOMEOSTASIS

By

Megan Michelle Greenlee

May 2011

Chair: Charles S. Wingo
Major: Medical Science – Physiology and Pharmacology

Mineralocorticoid excess and dietary potassium (K^+) depletion cause hypokalemia, metabolic alkalosis, and hypertension. These effects are thought to arise from urinary K^+ and acid/proton (H^+) loss and enhanced urinary sodium (Na^+) retention. Hypokalemia activates H^+,K^+-ATPase-mediated K^+ reabsorption and H^+ secretion in the renal collecting duct. Studies have also shown that H^+,K^+-ATPases (in the colon) are required for maximal ENaC-mediated Na^+ transport. Therefore, we hypothesized that H^+,K^+-ATPases and ENaC in the collecting duct functionally associate and cause the alkalosis and Na^+-retaining effects of both mineralocorticoids and dietary K^+ depletion. To test this hypothesis, we examined the stimulation of renal H^+,K^+-ATPase expression by the long-acting mineralocorticoid, desoxycorticosterone pivalate (DOCP). We also compared the systemic and renal response of wild type (WT), $HK\alpha_1^{-/-}$ and $HK\alpha_{1,2}^{-/-}$ mice to DOCP. Secondly, we compared the systemic and renal response of WT, $HK\alpha_1^{-/-}$ and $HK\alpha_{1,2}^{-/-}$ mice to dietary K^+ depletion. Finally, we examined ENaC subunit expression, the effect of dietary Na^+ depletion, and food restriction in the WT and knockout mice. We observed that DOCP stimulated renal medullary $HK\alpha_2$ expression in a K^+ dependent manner. In contrast to WT and $HK\alpha_1^{-/-}$ mice, DOCP did not cause metabolic alkalosis

and urinary Na^+ retention in $HK\alpha_{1,2}^{-/-}$ mice. However, the double knockouts exhibited no significant defects in urinary K^+ or Na^+ retention during dietary K^+ depletion. Finally, we observed that renal medullar αENaC subunit protein expression was less in $HK\alpha_{1,2}^{-/-}$ mice. The double knockouts also had a higher hematocrit during dietary Na^+ depletion and displayed greater aldosterone excretion with food restriction, suggesting fluid volume loss and salt wasting. Overall, we conclude that renal H^+,K^+-ATPases, most likely $HK\alpha_2$-containing, are required for mineralocorticoid-induced alkalosis and renal Na^+ retention. The mechanism more than likely involves dysregulation of ENaC in the collecting duct. Our results are important for understanding mechanisms of renal salt transport and suggest that renal $HK\alpha_2$-containing H^+,K^+-ATPases may have an important role in blood pressure regulation.

CHAPTER 1
INTRODUCTION

Renal Physiology

Organs of the urinary (or excretory) system include the kidneys, ureters, and urinary bladder.[1] These organs produce and eliminate urine in order to excrete excess metabolic products, toxins, electrolytes, fluid and more from the body. In contrast to the ureters and bladder which are responsible for urine elimination, the kidneys are responsible for urine production, filtration of blood, regulation of electrolyte, acid-base and fluid balance, and adjustment of blood pressure. The kidneys also generate and are influenced by hormones that control many of these functions.

Basic Structure of the Kidney

The kidneys are bilateral, bean shaped organs located in the retroperitoneal space.[1] A capsule covers and visceral fat surrounds each kidney. The hilus, a slit in the capsule, serves as the entry and exit site for the renal artery, vein, nerves and the ureter. The functional unit of the kidney is termed the nephron, which consists of the renal corpuscle followed by several tubular structures in this order: the proximal convoluted tubule, proximal straight tubule, thin descending and thin ascending limbs of Henle's loop, thick ascending limb of Henle's loop, and the distal convoluted tubule. All nephrons converge into the collecting duct system, which consists of the connecting segment, initial collecting tubule, followed by the cortical, outer medullary and inner medullary collecting ducts. The renal corpuscle is the filtering unit whereas the nephron and collecting duct systems facilitate ion and fluid reabsorption and secretion to produce urine.

Kidneys have three distinct divisions called the cortex (the outer portion), outer medulla (the middle portion) and inner medulla (the inner portion) classified by the presence or absence of particular tubular structures. [1] The cortex contains the renal corpuscles and most of the tubular segments except for the thin descending and ascending limbs of Henle's loop and the outer and inner medullary collecting ducts. The cortex also contains several structures that compose the juxtaglomerular apparatus including the extraglomerular mesangial cells, macula densa cells adjacent to the thick ascending limb, granular cells in the afferent arteriole, and both the afferent and efferent arterioles. All of these structures participate in renal autoregulation and a tubuloglomerular feedback system to stabilize renal blood flow and glomerular filtration. The outer medulla contains proximal straight tubules, thin descending limbs, medullary thick ascending limbs, and outer medullary collecting ducts. The outer medulla is further divided into the outer and inner stripe based on the confinement of proximal straight tubules only in the outer stripe. The inner medulla contains only thin descending and ascending limbs and inner medullary collecting ducts.

Filtration

Arterial blood reaches the renal corpuscle through a series of arteries that begin with the renal artery followed by the segmental, interlobar, arcuate, and interlobular arteries.[1] The interlobular arteries, also called the cortical radial arteries, split into individual afferent arterioles which provide systemic blood to individual renal corpuscles. The renal corpuscles consist of the glomerulus, Bowman's capsule, and Bowman's space which function together to filter incoming blood.[2] The differences in glomerular capillary and interstitial hydrostatic and oncotic pressures determine the net force of glomerular filtration. The glomerular capillary hydrostatic pressure and oncotic pressure

in Bowman's space promote filtration whereas the glomerular capillary oncotic pressure and hydrostatic pressure in Bowman's space resist filtration. Filtrate passes through the glomerular filtration barrier which includes the glycocalyx-covered endothelial cells, epithelial podocytes, and the glomerular basement membrane. This filtration barrier prevents filtration of most plasma proteins and other large macromolecules. This restriction of plasma protein filtration increases glomerular capillary oncotic pressure and reduces filtration by the end of the glomerular capillaries. The filtered blood next enters the efferent arteriole where the arteriolar resistance decreases intravascular hydrostatic pressure. This generation of low intravascular hydrostatic pressure creates favorable conditions for fluid and solute reabsorption by the peritubular capillaries and vasa recta that provide nutrients to surrounding tubules. The interlobular, arcuate, interlobar, and segmental veins return the filtered blood to the renal vein for recirculation.

The glomerular filtration rate (GFR) is regulated by afferent and efferent arteriolar resistances and is ~125 mL/min in normal adult humans [2] and 360 to 1,700 µL/min/g kidney weight in the mouse. [3] Constriction of the afferent arteriole decreases GFR whereas efferent arteriolar constriction increases GFR. [2] GFR autoregulation, which occurs in the afferent arteriole, sustains renal blood flow and GFR over a very small range. Constriction or relaxation of the afferent arteriole occurs in response to altered systemic blood pressure or renal perfusion pressure and change glomerular capillary hydrostatic pressure to affect glomerular filtration. Inherent myogenic, Ca^{2+} dependent responses of the arteriolar smooth muscle cells and a tubuloglomerular feedback system are responsible for vasoconstriction or vasodilation of the afferent arteriole. In

the feedback system, macula densa cells detect changes in salt and fluid composition in the thick ascending limb tubular fluid. In response, the cells secrete paracrine molecules that stimulate afferent arteriole contraction or relaxation.

Several other factors adjust renal blood flow and GFR including sympathetic nerve activity, the renin-angiotensin-aldosterone system (RAAS), arginine vasopressin (AVP), and atrial natriuetic peptide (ANP).[2] Renal sympathetic nerve activity increases in response to stressful situations including decreased plasma volume. The stimulated renal sympathetic nerves release norepinephrine which increases afferent and efferent arteriole resistances decreasing GFR. RAAS, ANP, and AVP action will be discussed latter in this chapter.

Ion and Water (H_2O) Transport

The renal tubules are primarily responsible for reabsorption of the filtered load including ions and H_2O.[1] However, the tubules also participate in ion secretion. The tubular fluid remaining at the end of the collecting duct is essentially the final urine composition because the ureters and bladder modify the filtrate very little. This section discusses the known mechanisms for sodium (Na^+), H_2O, potassium (K^+), and acid-base transport within the nephron and collecting duct.

Na^+ and H_2O

Na^+ is the most abundant cation in extracellular fluid with a concentration ranging from 142-145 mM in humans.[4] The total body content of Na^+ determines extracellular fluid volume. Changes in extracellular fluid volume will affect circulating blood volume and, in turn, blood pressure.

The kidney is the major organ that regulates total body Na^+ content.[5] The proximal tubule isosmotically reabsorbs ~ 67% of filtered Na^+ through paracellular transport and

both passive and active intracellular transport. The Na^+ and hydrogen (H^+) exchanger named NHE3 and other Na^+-coupled cotransporters are responsible for passive intracellular Na^+ uptake at the apical plasma membrane. The Na^+,K^+-adenosine triphosphatase (ATPase) and electrogenic Na^+ and bicarbonate (HCO_3^-) cotransporter (NBCe1) on the basolateral plasma membrane facilitate Na^+ exit into the interstitium. Na^+ transport in the thin limbs is primarily passive and presumed to be through paracellular mechanisms. In the thick ascending limb, an Na^+,K^+,$2Cl^-$ cotransporter named NKCC2 and NHE3 on the apical plasma membrane mediate passive luminal Na^+ uptake with extrusion into the interstitium through a basolateral Na^+,K^+-ATPase. Paracellular transport of Na^+ also occurs within this segment. Overall, the loop of Henle reabsorbs approximately 25% of the filtered Na^+ load. Within the distal convoluted tubule, the apical Na^+ and Cl^- cotransporter (NCC) and basolateral Na^+,K^+-ATPase facilitate Na^+ reabsorption. The connecting segment, initial collecting tubule, and cortical collecting ducts possess an apical epithelial Na^+ channel (ENaC) that facilitates electrogenic Na^+ reabsorption with a basolateral Na^+,K^+-ATPase. The distal convoluted tubule, connecting segment, initial collecting tubule, and cortical collecting ducts absorb ~ 5% of the filtered Na^+ load. The final segments involved in Na^+ transport are the medullary collecting ducts where it appears ENaC and Na^+,K^+-ATPase reabsorb the remaining Na^+ (~3%) left in the filtered load. The amount of Na^+ left in the urine filtrate largely depends on the dietary Na^+ load.

In contrast to Na^+ transport, cellular H_2O transport always occurs passively through channels called aquaporins.[4, 5] Dissociation of Na^+ and H_2O reabsorption in the thick ascending limb is used to create an osmotic gradient in the kidney.[5] The

osmolality of interstitial fluid increases from the cortex to the medulla and this is necessary for concentration of the urine filtrate. Urine concentration and dilution are regulated by the hormonal actions of vasopressin in the collecting duct.

The proximal tubule has a large capacity for isosmotic Na^+ and H_2O reabsorption. Aquaporin 1 (AQP1), constitutively present on both the apical and basolateral plasma membrane of proximal tubule cells, is responsible for H_2O transport in this segment. The thick ascending limb and distal convoluted tubule are relatively impermeable to H_2O leading to H_2O-free Na^+ reabsorption in these segments. The accumulated interstitial Na^+ is greatest in the medulla and progressively decreases by the end of the distal convoluted tubule. The H_2O-free Na^+ reabsorption generates an osmotic gradient that is highest in the inner medulla and causes the distal tubular luminal fluid to be hyposmotic. The connecting segment, initial collecting tubule, and collecting duct receive the hyposmotic filtrate and, in the presence of AVP, these segments reabsorb the majority of the remaining H_2O in the filtrate. AVP increases H_2O reabsorption through the apical plasma membrane AQP2 channel. AVP release from the posterior pituitary inversely correlates with H_2O intake such that H_2O restriction increases and H_2O loading decreases circulating AVP levels. These conditions produce a maximally concentrated urine or diluted urine, respectively.

K^+

Unlike Na^+, K^+ is the most abundant intracellular cation with a concentration of ~120 mM.[4] In contrast, extracellular fluid has a $[K^+]$ of 3.5 to 5.0 mM. The Na^+,K^+-ATPase generates this plasma membrane $[K^+]$ gradient and thereby maintains cellular membrane potential. The membrane potential is especially important for the development of an action potential in excitable cells such as those found in the heart,

muscle, and brain. The body regulates K^+ homeostasis through modulation of excretion and extracellular to intracellular redistribution.[7, 8]

The kidneys are the organs with the major responsibility to maintain K^+ balance.[7, 8] The proximal tubule reabsorbs ~ 80% of filtered K^+ through solvent drag and electrodiffusion. In the thin descending limb, K^+ secretion occurs passively and paracellularly because of a high medullary [K^+] gradient. High medullary [K^+] is maintained by paracellular K^+ reabsorption in the thin and thick ascending limbs. Paracellular K^+ reabsorption in thin ascending limb is driven by the high tubular [K^+] and decreasing interstitial [K^+] gradient upon approach to the cortex. In the thick ascending limb, about half of K^+ reabsorption occurs through passive diffusion driven by a lumen positive voltage. The thick ascending limb also reabsorbs K^+ through NKCC2 on the apical plasma membrane and K^+ channels on the basolateral membrane. A K^+ channel called ROMK (renal outer medullary K^+) is also present in the apical membrane to provide for K^+ recycling within the thick ascending limb. Overall, the loop of Henle reabsorbs ~10% of the filtered K^+.

Cells of the connecting segment, initial collecting tubule and cortical and outer medullary collecting ducts secrete K^+ into the tubule lumen primarily through two apical K^+ channels, ROMK and BK (big-conductance K^+),[6] and possibly through a K^+ and Cl^- cotransporter (KCC).[7, 8] Electrogenic Na^+ reabsorption through ENaC and the Na^+,K^+-ATPase generates a net negative luminal charge that drives K^+ secretion through ROMK and possibly other apical K^+ channels.[7] In contrast, BK channels primarily respond to luminal flow rate.[9, 10] K^+ reabsorption occurs within intercalated cells (ICs) of the collecting duct system through coupling of apical H^+,K^+-ATPases and

basolateral K^+ channels.[11] H^+,K^+-ATPases also mediate K^+ recycling in cooperation with apical K^+ channels.[12] The renal H^+,K^+-ATPases will be described in more detail in a later section.

Dietary K^+ intake regulates urinary K^+ excretion through modulation of K^+ transport in the collecting tubules.[6, 13] A high K^+ diet favors K^+ secretion so that the kidney excretes 10 to 150% of the filtered K^+ load. A low K^+ diet favors K^+ reabsorption so that the kidney excretes only 2 to 3% of the filtered load.

Acids and bases

The kidneys are important regulators of acid-base balance and ensure that the body maintains blood pH around 7.4.[14] In humans, a typical diet and normal metabolism create an acid load of ~70mmols acid or protons (H^+) per day. The kidney responds to this acid load by increased urinary acid excretion and renal reabsorption of all the filtered bicarbonate (HCO_3^-).

The proximal tubule reabsorbs ~ 80% of filtered HCO_3^-.[14] In early parts of this segment, both the apical NHE3 and proton translocating (H^+)-ATPase secrete H^+ that titrate luminal HCO_3^-. Extracellular carbonic anhydrase 4 (CAIV) catalyzes the conversion of H^+ and HCO_3^- to H_2O and carbon dioxide (CO_2). CO_2 then diffuses across the cell membrane and intracellular carbonic anhydrase 2 (CAII), present in all tubule cells, converts it back to H^+ and HCO_3^-. The apical NHE3 recycles the H^+ for further HCO_3^- reclamation and a basolateral NBCe1 transports the intracellular HCO_3^- into the interstitium. In the late proximal tubule, NHE3 and H^+-ATPase secrete net H^+.

The proximal tubule also produces new HCO_3^-.[14, 15] Glutaminase in the proximal tubule converts glutamine to ammonium (NH_4^+) and α-ketoglutarate. Gluconeogenesis indirectly generates HCO_3^- from α-ketogluturate in a 1:1 ratio with the NH_4^+. Apical

NHE3 and H^+-ATPases secrete the newly formed NH_4^+ into the tubule lumen and basolateral NBCe1 transports the newly formed HCO_3^- into the interstitium. In the thick ascending limb, apical NHE3 and H^+-ATPases participate in net H^+ secretion and the basolateral Cl^- and HCO_3^- exchanger, anion exchanger 2 (AE2), reabsorbs the remaining intracellular HCO_3^-.

The collecting duct is necessary for maximal urinary acidification.[16] Net H^+, HCO_3^- and ammonia (NH_3) secretion are important in urinary acidification by the collecting duct. These transport processes depend upon the plasma membrane localization of H^+, HCO_3^- and NH_3 secreting transporters. Apical H^+-ATPases or H^+,K^+-ATPases and basolateral Cl^-, HCO_3^- exchangers mediate net H^+ secretion in some cells whereas apical Cl^-, HCO_3^- exchangers and basolateral H^+-ATPase mediate net HCO_3^- secretion in other cells of the collecting duct. The mechanism of acid-base transport in the collecting duct will be described in more detail in a later section.

Hormonal Regulation

Glomerular filtration and renal ion and H_2O transport are highly regulated processes. Hormones are central to regulation of these processes and act in an endocrine, paracrine, and autocrine fashion to modulate renal filtration and transport. Several of these hormones and their actions in the kidney are described below.

RAAS

The RAAS system functions to modulate renal blood flow, glomerular filtration, and renal Na^+ transport.[2, 5] Low intravascular volume activates central and renal baroreceptors which increase renal sympathetic nerve activity leading to renin secretion by granular cells of the afferent arteriole.[17] Less sodium chloride (NaCl) delivery to the macula densa cells also increases granular cell renin release. The released renin

enzymatically converts circulating angiotensinogen into angiotensin I. Angiotensin converting enzyme then cleaves plasma angiotensin I into the biologically active peptide, angiotensin II (Ang II). Ang II stimulates adrenal aldosterone and pituitary AVP release, vasoconstriction, and increased proximal tubule NHE3-mediated Na^+ reabsorption. The adrenal glomerulosa cells produce the mineralocorticoid, aldosterone, in response to Ang II or low circulating $[K^+]$.[18, 19] Aldosterone acts on the distal convoluted tubule and collecting duct to facilitate Na^+ reabsorption through NCC[20] and ENaC.[21] It has also been shown to activate NHE3-mediated Na^+ reabsorption. [22-24] Combined, RAAS modulates filtration and corrects circulating volume to maintain blood pressure and tissue perfusion.

In addition to increasing blood pressure, aldosterone excess results in hypokalemic metabolic alkalosis.[25-27] Aldosterone and other mineralocorticoids have pronounced effects on K^+ homeostasis. Mineralocorticoids activate K^+ secretion in the cortical collecting duct [28, 29] and proximal colon. [30] The hormones also modulate transcellular K^+ redistribution.[31] Mineralocorticoid-induced K^+ secretion is only observed with chronic mineralocorticoid exposure not acute.[32] Mineralocorticoids also have not consistently been shown to increase urinary K^+ excretion. [28, 33]

The effect of mineralocorticoids to promote K^+ secretion is thought to be secondary to electrogenic Na^+ reabsorption. Consistent with this concept, urinary K^+ excretion in animals on a normal diet is primarily amiloride sensitive (ENaC inhibitor) and Na^+-dependent.[34] However, with high K^+ intake and thus greater plasma aldosterone levels, the proportion of amiloride insensitive and Na^+-independent K^+

excretion increases. The evidence suggests that dietary K^+ intake has a greater impact on renal K^+ transport than aldosterone alone.

The effect of aldosterone to cause metabolic alkalosis is thought to result from enhanced urinary acid excretion. Aldosterone stimulates ammoniagenesis in the proximal tubule.[35] The hormone also increases acidification by the distal nephron and collecting duct.[36, 37] Several studies have shown aldosterone-mediated stimulation of NHE3- and H^+-ATPase-mediated H^+ secretion in these segments.[38-41]

AVP

The posterior pituitary releases AVP, also known as antidiuretic hormone, in response to increased plasma osmolality or low intravascular volume.[17, 42, 43] In the collecting duct, AVP stimulates H_2O reabsorption through AQP2 [44]and can also increase ENaC-mediated Na^+ reabsorption.[45] Thus, AVP corrects high plasma osmolality and low extracellular fluid volume.[17] These actions also maintain or correct blood pressure.

ANP

Atrial myocytes synthesize and release ANP in response to increased stretch or filling pressure within the atrium.[17] Thus, greater circulating fluid volume and blood pressure will stimulate ANP release. ANP acts in the kidney to promote Na^+ excretion by increasing GFR and renal blood flow, decreasing renin and AVP, and inhibiting ENaC-mediated Na^+ reabsorption in the collecting duct. These actions stimulate natriuresis and diuresis to eliminate the extra circulating volume.

Endothelin

Endothelin 1 (ET-1) is a peptide hormone produced primarily in the renal medulla.[46] ET-1 action is unique because the hormone promotes systemic

vasoconstriction [47] and natriuresis.[46] These two actions occur because of the differential localization and function of two endothelin receptors, A (ETAR) and B (ETBR). ETARs are expressed in vascular smooth muscle cells and, upon binding ET-1, cause vasoconstriction.[48] ET-1 through ETBRs reduces medullary Na^+ reabsorption, causing natriuresis.[49, 50]

Several studies now show that ET-1 enhances acidification by the proximal tubule and collecting duct.[51, 52] ET-1 appears to be important in urinary acidification during acid challenges such as high protein intake. Dietary acid loading increases ET-1 mRNA and protein expression in the kidney.[53, 54] The dietary acid-induced ET-1 activates proximal tubule NHE3 [54, 55] and collecting duct H^+-ATPase-mediated H^+ secretion. [56]

The Renal Collecting Duct

Fine regulation of the final urine content occurs in the collecting duct.[1] The collecting duct is a highly heterogeneous structure with many different cell types that perform distinct functions. Hormones such as those described above regulate transport within the collecting duct. Many renal diseases result from dysregulation of collecting duct transport.

Structure and Function

Cells within the collecting duct system are quite heterogeneous. In the cortical and outer medullary collecting duct and initial portion of the inner medullary collecting duct, the majority cell type is called the principal cell (PC) and the minority cell type, an intercalated cell (IC). The cells in the terminal portion of the inner medullary collecting duct (IMCD) are called inner medullary collecting duct cells. The PCs, ICs, and IMCD cells possess distinct ultrastructural and functional characteristics. The collecting duct ultrastructure has been most extensively examined in the rat and rabbit.

PCs of the cortical, outer medullary, initial portion of the inner medullary collecting ducts are structurally quite similar and possess a mostly flat apical plasma membrane and many infoldings on the basolateral plasma membrane but there are slight structural differences between the PCs of these segments.[57] IMCD cells are very different than PCs in that the apical projections increase in number, the cell height increases, and the basolateral plasma membrane infoldings decrease. PCs and IMCD cells are also distinguished by the expression and location of ENaC and AQP2 in the apical plasma membrane. Functionally, the PCs and IMCD cells primarily participate in Na^+ and H_2O reabsorption. PCs in the cortical and outer medullar collecting duct also participate in K^+ secretion. Figure 1-1 depicts the known transporters present in cortical collecting duct PCs.

ICs in the cortical, outer medullary, and inner medullary collecting ducts have greater mitochondrial density than PCs and possess numerous tubulovesicles, microplicae, and microvilli at the apical plasma membrane.[57] There are three types of ICs that have been described in the mouse cortical collecting duct using immunohistochemistry and electron microscopy: the A-type, B-type, and non A-, non B-type.[16] The A-type and non A-, non B- type ICs possess many apical plasma membrane microprojections and apically localized cytoplasmic tubulovesicles. [57] The A-type ICs also display subapical and apical plasma membrane H^+-ATPase localization.[16] In contrast to the A-type ICs, the non A-, non B- cells do not express basolateral AE1, but have an subapical and apical plasma membrane localization of the Cl^- and HCO_3^- exchanger named pendrin. A-type ICs are present in the cortical, outer and initial portion of the inner medullary collecting duct. The non A-, non B- type ICs do

not extend farther than the cortical collecting duct. In contrast, B-type ICs have a flatter apical membrane with fewer apical plasma membrane microprojections. [57] H^+-ATPase localizes to the subbasolateral vesicles and basolateral plasma membrane and pendrin to the subapical vesicles and apical plasma membrane.[16] B-type ICs only appear in the cortical collecting duct and exhibit decreased abundance at distal portions of the cortical collecting duct with eventual disappearance by the outer medullary collecting duct. The A-type IC is believed to participate in H^+ secretion, the B-type HCO_3^- secretion, and the non A-, non B-type may participate in both local H^+ and HCO_3^- secretion, based on acid-base transporter localization. Figures 1-2, 1-3, and 1-4 depict transporters present in A-, B-, and non A-, non B- type ICs, respectively.

Mechanisms and Regulation of Ion and H_2O Transport

Dietary and hormonal influence of ion and H_2O transport in the collecting duct is quite important for maintenance of Na^+, H_2O, K^+, and acid-base homeostasis. Dysfunction and dysregulation of these transporters have many pathophysiological consequences, especially regarding blood pressure.

Na^+

PCs are the primary cell types thought to be involved in Na^+ transport in the collecting duct.[5] ENaC is present in the apical plasma membrane of these cells and in a concerted action with the basolateral Na^+,K^+-ATPase electrogenically reabsorbs Na^+ from the luminal filtrate. ENaC is heteromultimeric and composed of an α, β, and γ subunit.[21, 58] While the αENaC subunit is constitutively present at the apical plasma membrane, βENaC and γENaC traffic to the apical plasma membrane in response to certain stimuli, including the mineralocorticoid, aldosterone. The latter two subunits

primarily regulate assembly and plasma membrane trafficking of functional ENaC channels.

Under normal conditions, ENaC-mediated Na^+ reabsorption in the collecting duct is low and sometimes undetectable. [59] Aldosterone greatly stimulates PC mRNA and protein expression of αENaC, Na^+,K^+-ATPase α_1 subunit ($NaK\alpha_1$), and serum and glucocorticoid regulated kinase 1(SGK-1).[60-63] To increase transcription of these genes, aldosterone binds the mineralocorticoid receptor (MR), causing the complex to translocate to the nucleus.[21, 26] In the nucleus, the aldosterone-MR complex binds to hormone response elements (HREs) in a target gene's promoter altering transcription.[64] Aldosterone also causes decreased retrieval of ENaC channels from the apical plasma membrane through SGK-1 mediated shutdown of retrieval/degradation mechanisms.[21, 58] Aldosterone rapidly stimulates activity of ENaC channels already in the apical plasma membrane through a phosphoinositide dependent mechanism.[65] A low Na^+ diet, which produces secondary hyperaldosteronism, also increases ENaC subunit expression and apical plasma membrane abundance and stimulates Na^+ reabsorption through ENaC.[59]

The importance of ENaC to urinary Na^+ retention is highlighted by two different genetic diseases, pseudohypoaldosteronism type 1 and Liddle's syndrome.[58] In pseudohypoaldosteronism type 1, patients exhibit symptoms of low plasma aldosterone which include low blood pressure and urinary salt wasting. In reality, the patients display hyperaldosteronism. The salt wasting phenotype results from genetic mutations in MR or ENaC subunits, which decrease channel activity and Na^+ reabsorption. The converse is true in Liddle's syndrome in which mutations in β- or γENaC constitutively

activate ENaC- mediated Na^+ reabsorption. The excessive Na^+ retention leads to hypertension.

Interestingly, collecting duct specific knockout (Hoxb7 promoter) of the αENaC in mice does not appear to significantly impair urinary Na^+ retention under normal or Na^+ restricted conditions.[66] This is in contrast to data showing that whole body disruption of βENaC in mice causes salt wasting during Na^+ restricted conditions.[67] The differences between collecting duct specific knockout of the αENaC and total body βENaC knockout may be a consequence of the presence of ENaC channels in the connecting segment, in addition to the collecting duct. Indeed, a recent study showed that connecting segment and collecting duct specific (AQP2 promoter) knockout of αENaC in mice caused increased urinary Na^+ excretion, polyuria, and greater plasma aldosterone levels than control mice under normal or Na^+ restricted conditions.[68] Taken together, the studies suggest particular importance of ENaC channels in the connecting segment for maintenance of Na^+ balance.

Under normal conditions, a large majority of Na^+ transport in the collecting duct is insensitive to amiloride. [69] However, it is sensitive to thiazide diuretics (NCC inhibitor) and this thiazide sensitivity is present despite the lack of evidence for NCC in collecting duct cells. In fact, the electroneutral Na^+ dependent Cl^-, HCO_3^- exchanger (NDCBE) expressed in the collecting duct was recently found to be thiazide sensitive and to mediate electroneutral Na^+ reabsorption in ICs. This transporter also displayed increased activity during dietary Na^+ restriction. These data indicate that ENaC is not the only Na^+ reabsorptive mechanism present in the collecting duct.

H_2O

PCs express an AVP regulated apical AQP2 channel that facilitates luminal H_2O reabsorption.[44] AVP release increases in response to decreased H_2O intake, increased plasma osmolality, and decreased effective circulating volume. In the collecting duct, AVP stimulates translocation and insertion of intracellular AQP2-containing tubulovesicles into the apical plasma membrane of PCs, increasing H_2O reabsorption. This effect occurs through binding of AVP to basolateral AVP V2 receptors (V2R) in PCs, which subsequently increase cyclic adenosine monophosphate (cAMP) levels.[70] The cAMP-activated protein kinase A (PKA) phosphorylates AQP2 causing membrane translocation and insertion of the H_2O channels.

The V1aR AVP receptor is also expressed in the collecting duct.[71] V1aR localizes to both PCs and ICs of the cortical collecting duct and exclusively in A-type ICs in medullary collecting ducts.[72] However, the exact role of V1aR in H_2O transport is not entirely clear. V1aR appears to antagonize V2R action in collecting duct cells.[73] The physiological effect of V1aR- mediated antagonism of V2R to alter H_2O homeostasis has not yet been investigated.

Dysregulation of AQP2 results in altered urinary H_2O excretion and disturbs H_2O homeostasis.[44] An example of AQP2 malfunction is congenital nephrogenic diabetes insipidus, where mutations in AQP2 or V2R disrupt trafficking of AQP2 channels to the apical plasma membrane. Thus, patients with this disease display decreased urinary concentrating ability, polyuria, and polydipsia. Conditions of hypokalemia have also been shown to decrease AQP2 expression leading to acquired nephrogenic diabetes insipidus. [74]

AQP3 and AQP4 are present in the basolateral plasma membrane of PCs, where they facilitate H_2O exit into the interstitium.[44] AVP regulates AQP3 trafficking to the basolateral plasma membrane and knockout of AQP3 in mice produces nephrogenic diabetes insipidus.[75] In contrast, AVP has not been shown to regulate AQP4 and knockout of AQP4 in mice produces a much less severe H_2O handling phenotype.[76]

K^+

The collecting duct participates in both K^+ secretion and K^+ reabsorption.[6, 13, 77] K^+ secretion occurs in both PCs and ICs through two distinct K^+ channels, ROMK and BK, respectively.[78-82] ROMK is present and active in the apical plasma membrane of PCs under normal conditions.[81] BK localizes to the apical plasma membrane of ICs.[82] Although quiescent under normal conditions, increased luminal flow rate and high dietary K^+ intake stimulate K^+ secretion through BK.[83, 84] As mentioned previously, there is a large component of K^+ secretion in the collecting duct that is Cl^- dependent and potentially mediated by KCCs.[8, 85] The identity of the KCC has not been determined.

The only identified transporter for K^+ reabsorption in the collecting duct is the H^+,K^+-ATPase.[86, 87] H^+,K^+-ATPases are expressed and active in A- and B- type ICs.[88, 89] These transporters are composed of an α and β subunit and two different α subunits are expressed in the kidney.[87] The H^+,K^+-ATPase α 2 ($HK\alpha_2$) subunit also localizes to the apical plasma membrane of PCs in the cortical and outer medullary collecting duct of rabbit.[90] The role of H^+,K^+-ATPases in K^+ reabsorption by the collecting duct will be discussed later in this chapter.

Dietary K^+ intake and hormones influence K^+ transport in the collecting duct.[77] High dietary K^+ intake stimulates expression and activity of ROMK and BK whereas a low K^+ diet shuts down K^+ secretion through these channels. The with-no-lysine kinase

(WNK) system has also been shown to control ROMK activity in the collecting duct.[91] High dietary K^+ increases expression of a cleavage product of WNK1, called kidney specific WNK1, which inhibits long WNK1 and prevents WNK1-mediated inactivation of ROMK channels.[92] High dietary K^+ intake also increases circulating aldosterone levels.[77] Some studies suggest that aldosterone is required for collecting duct K^+ secretion [28, 93] whereas many others do not.[29, 32, 78, 94, 95] Overall, the data indicate a complicated interplay between dietary K^+ load and aldosterone to modify K^+ transport in the collecting duct.

A low K^+ diet decreases K^+ secretion by ROMK and BK in the collecting duct.[77] One potential mechanism involves repression of kidney specific WNK1 expression relieving inhibition of long WNK1.[92] Long WNK1 can then inactivate ROMK and shut down K^+ secretion. Furthermore, low dietary K^+ stimulates mitogen-activated protein kinase (MAPK) pathways, at least partially through AngII, which inhibit ROMK and BK channel activity.[96, 97]

In contrast to the regulation of apical K^+ channels, a high dietary K^+ intake decreases and a low dietary K^+ intake increases K^+ reabsorptive activity and expression of H^+,K^+-ATPases of the collecting duct.[86, 87] This is described in more detail in a later section.

Acid-base

Acid-base transport primarily occurs within ICs of the collecting duct and involves complicated interplays between H^+, HCO_3^- and NH_3 secretion.[36] Acid-base transporters localize to specific membranes of each differentiated IC subtype (A-, B-, and non A-,non B- type; Figure 1-2, 1-3, and 1-4, respectively).[16] The plasma membrane distribution of these transporters is such that the connecting segment and cortical collecting tubule

can secrete net H^+ or HCO_3^- as needed whereas the medullary collecting duct secretes net H^+ into the tubular fluid. The expression and activity of these transporters depends upon dietary acid-base intake, systemic acid-base balance and hormonal status of the animal.

H^+ secretion and reabsorption. In A-type and non A-, non B- type ICs, an apical vacuolar(V)-type H^+-ATPase mediates electrogenic H^+ secretion into the tubule lumen.[16] In B-type ICs, H^+-ATPases localize to the basolateral plasma membrane where they reabsorb H^+ into the interstitium. In the A- and B-type ICs, the H^+-ATPases coordinate net H^+ secretion or reabsorption with a Cl^-,HCO_3^- exchanger on the opposite membrane. These Cl^-,HCO_3^- exchangers are discussed below. A- and B- type ICs also express apical H^+,K^+-ATPases that mediate H^+ secretion throughout the collecting duct.[86, 87] Involvement of H^+,K^+-ATPases in normal and stimulated H^+ secretion by the collecting duct will be discussed later.

V-type H^+-ATPases are multisubunit complexes that have many different isoforms for each subunit.[36] The B_1 and a_4 subunits specifically localize to ICs. [98, 99] States of metabolic acidosis activate the apical H^+-ATPase and increase apical plasma membrane insertion of H^+-ATPase-containing vesicular pools in A-type ICs to achieve greater net H^+ secretion.[100-105] Conditions of metabolic alkalosis activate the basolateral H^+-ATPase and increase basolateral plasma membrane insertion of intracellular H^+-ATPase-containing vesicular pools in B-type ICs to mediate greater net H^+ reabsorption.[101, 106-108] Humans with null mutations in the B_1 H^+-ATPase subunit display distal renal tubular acidosis with an inability to acidify their urine despite the presence of metabolic acidosis.[99] In mice, knockout of the B_1 H^+-ATPase subunit produces alkaline

urine but no systemic acid-base disturbances unless the mice are challenged by a dietary acid load. [109]

The RAAS system is quite important for the regulation of H^+-ATPase-mediated H^+ secretion. Both Ang II and aldosterone increase H^+-ATPase mediated H^+ secretion in A-type ICs.[38, 110, 111] Aldosterone has been shown to stimulate H^+-ATPase activity rapidly (<15 min) through a non-genomic mechanism in isolated outer medullary collecting ducts. [38] The hormone also appears to activate H^+-ATPases within 24 hr via an MR-dependent mechanism using an *in vitro* renal cell line.[39] Patients with pseudohypoaldosteronism quite often present with symptoms of distal renal tubular acidosis, assumed to result from decreased apical H^+-ATPase-mediated H^+ secretion in A-type ICs.[58, 112]

HCO_3^- secretion and reabsorption. Cl^-,HCO_3^- exchangers present on the opposite side of the plasma membrane from the H^+-ATPase complement the net H^+ secretory or reabsorptive actions of the H^+-ATPase in A- and B-type ICs. In A-type ICs, basolateral AE1 mediates HCO_3^- reabsorption and, similar to the apical H^+-ATPase, dietary acid loading stimulates AE1 activity, expression, and basolateral plasma membrane trafficking. [103, 106, 107]Thus, AE1 knockout mice and humans with AE1 mutations exhibit a distal renal tubular acidosis.[113, 114] Conversely, in B-type ICs, the apical Cl^-,HCO_3^- exchanger, pendrin, mediates net HCO_3^- secretion.[16, 115] Metabolic alkalosis, dietary base loading, dietary Na^+ and Cl^- restriction, and mineralocorticoids increase expression and apical localization of pendrin.[116-120]

Mineralocorticoids stimulate net H^+ secretion by the collecting duct. However, the long-acting mineralocorticoid, desoxycorticosterone pivalate (DOCP), accompanied with

a greater NaCl intake, has been shown to increase pendrin-mediated HCO_3^- secretion and density at the apical plasma membrane of B-type ICs.[118] Pendrin activity appears to be required for maximal ENaC- mediated Na^+ reabsorption, potentially through a luminal HCO_3^- dependent mechanism.[121, 122] In contrast to WT mice, pendrin null mice did not exhibit increased blood pressure with DOCP treatment.[118, 122] Several lines of evidence indicate that acid-base transporters, like pendrin and NDCBE, are not only involved in regulation of acid-base balance but also are required for Na^+ reabsorption and blood pressure regulation.

NH_3 secretion. The collecting duct has a large capacity for NH_4^+ secretion, mediated by simultaneous secretion of ammonia (NH_3) and H^+.[15] Rhesus associated glycoproteins, Rhbg and Rhcg, are transporters that facilitate NH_3 secretion and both localize to the collecting duct. Rhbg is present in the basolateral plasma membrane of cells in the distal tubule and collecting duct, whereas Rhcg localizes to both the apical and basolateral plasma membrane of these segments.[123, 124] In the collecting duct, Rhbg and Rhcg staining is greatest in A- and non A-, non B- type ICs but also present in PCs. In non A-, non B-type ICs, Rhcg only localizes to the apical plasma membrane. B-type ICs do not appear to express Rhbg or Rhcg. In the inner medullary collecting duct, Rhbg and Rhcg are only localized to ICs present in the initial portion of this collecting duct segment.

Metabolic acidosis appears to stimulate both Rhbg and Rhcg expression and membrane localization.[125-127] Recently, investigators showed that HCl-induced metabolic acidosis stimulated Rhbg expression in the kidney.[125] IC specific Rhbg knockout mice also displayed reduced urinary NH_3 excretion with acid loading. Similarly,

the same group showed that Rhcg protein expression and apical localization increase with metabolic acidosis and that IC specific Rhcg knockout mice exhibit less urinary NH_3 excretion than control mice with HCl loading.[126, 128] These data demonstrate that both Rhbg and Rhcg are essential for acidosis-induced NH_3 excretion.

The Renal H^+,K^+-ATPases

As described above, transporters within the renal collecting duct are quite important for the regulation of Na^+, H_2O, K^+, and acid-base balance. Several lines of evidence indicate that H^+,K^+-ATPases in the collecting duct are important in K^+ and acid-base transport. Some data suggest that the H^+,K^+-ATPases may also directly or indirectly participate in Na^+ transport. This section discusses the history and characteristics of H^+,K^+-ATPases and their role in renal solute transport.

Discovery of H^+,K^+-ATPases

In the 1970s, it was first recognized that gastric acid secretion was dependent on a K^+-stimulated ATPase, an activity discovered to be a H^+,K^+-ATPase in the apical plasma membrane of gastric parietal cells.[129, 130] This discovery sparked interest in whether the H^+,K^+-ATPase represented the mechanism of K^+ absorption in the colon and kidney. Distal colon plasma membranes from rabbits were found to possess a K^+-stimulated ATPase and K^+-dependent H^+ secretion inhibited by Schering (SCH)- 28080, similar to the gastric H^+,K^+-ATPase.[131, 132] K^+-ATPase activities in the distal nephron and collecting duct of rats and rabbits were also found to be sensitive to the gastric H^+,K^+-ATPase inhibitors, omeprazole and SCH-28080; and dietary K^+ restriction increased pump activity.[133, 134] These data only suggested the presence of an H^+,K^+-ATPase in the collecting duct. In 1989, Charles Wingo reported that active net H^+ secretion and K^+ absorption were both sensitive to omeprazole in the rabbit outer

medullary collecting duct.[135] That study confirmed the presence and activity of H^+,K^+-ATPases in the collecting duct. All these observations fueled many years research into the physiological function and regulation of gastric, colonic and renal H^+,K^+-ATPases.

Structure and Transport Characteristics

H^+,K^+-ATPases are part of the type II class of phosphorylated (P)-type ATPases which include the Na^+,K^+-ATPase, and calcium (Ca^{2+})-ATPase.[4] P-type ATPases are named as such because of the phosphorylated intermediate produced during their enzymatic cycle. The P-type ATPase enzymatic cycle involves conversion from an E1 (adenosine triphosphate (ATP) bound) to E2 (phosphorylated) state. In the E1 conformation, ATP is bound to the pump and intracellular cations (H^+ in the case of H^+,K^+-ATPases) enter the intracellular ion binding sites. The γ phosphate of ATP is used to phosphorylate the pump inducing a conformational change that occludes the bound cations from the intracellular and extracellular fluid. Another conformational change causes a shift into the E2 state where the occluded cations become exposed to the extracellular fluid. The conformational change also reduces the ion affinity for the pump releasing the H^+ into the extracellular fluid. At the same time, extracellular cations (K^+ in the case of the H^+,K^+-ATPases) bind to the pump and dephosphorylation causes occlusion of these ions. Dephosphorylation allows ATP to rebind the enzyme, shifting the pump into an E1 conformation. This conformation exposes the occluded cations to the intracellular fluid and reduces their affinity for the pump. Ion dissociation places the enzyme back in the starting E1-ATP bound conformation. H^+,K^+-ATPases use the E1-E2 ATPase cycle to secrete H^+ from the cell and absorb K^+ into the cell across their concentration gradients in an approximate $2H^+$:$2K^+$ ratio per hydrolyzed ATP.[136]

P-type ATPases are primarily composed of an α and β subunit.[4] However, some accessory γ subunits have been identified for the Na^+,K^+-ATPase.[137] The 10 transmembrane spanning α subunit catalyzes ion translocation and contains the ATP binding and phosphorylation sites.[138] The single transmembrane spanning β subunit regulates membrane trafficking, assembly, and degradation of the α subunit.[139-141]

Two distinct H^+,K^+-ATPase α subunits have been described and two distinct genes encode these subunits.[86, 87] The murine *Atp4a* gene encodes the H^+,K^+-ATPase α 1 ($HK\alpha_1$) subunit and murine *Atp12a* gene encodes the H^+,K^+-ATPase α 2 ($HK\alpha_2$) subunit. In the mouse, the two H^+,K^+-ATPase α (HKα) subunits have 63% peptide sequence homology as determined by sequence comparison on the National Center for Biotechnology Information (NCBI) website (www.ncbi.nlm.nih.gov). The *Atp4b* gene encodes the only known H^+,K^+-ATPase specific β subunit (HKβ). Several studies have shown that HKβ pairs with $HK\alpha_1$ and Na^+,K^+-ATPase β 1 ($NaK\beta_1$) and/or HKβ subunits pair with $HK\alpha_2$.[140-146] In the kidney, most data suggests that $NaK\beta_1$ is the partner for $HK\alpha_2$.

H^+,K^+-ATPase specific activity has classically been studied using inhibitors. Based on tissue expression of HKα subunit, the gastric H^+,K^+-ATPase is assumed to only contain $HK\alpha_1$ subunits. The gastric enzyme is sensitive to omeprazole and SCH-28080 but insensitive to ouabain.[147] That study also showed that amiloride inhibits the gastric $HK\alpha_1$-containing H^+,K^+-ATPase. The colonic H^+,K^+-ATPase is assumed to only contain $HK\alpha_2$ subunits. In contrast, this enzyme may or may not be sensitive to SCH-28080 and is partially sensitive to ouabain, the canonical Na^+,K^+-ATPase inhibitor.[132, 134, 142, 143, 148-151]

The crystal structures for the E2-phosphorylated state and SCH-28080 bound gastric H^+,K^+-ATPase have recently been resolved.[152-154] It is apparent from those studies that, in addition to its other responsibilities, the HKβ subunit is important for promotion of the catalytic cycle. Its N-terminal tail interacts with the $HK\alpha_1$ subunit and prevents cycle reversal.[154] A crystal structure for the colonic H^+,K^+-ATPase has not been published. Homology modeling of rabbit $HK\alpha_2$ to the known Ca^{2+}-ATPase structure has shown that the two P-type ATPases share significant structural homology.[138] The crystal structure for the $HK\alpha_2$-containing H^+,K^+-ATPases may prove useful to further define the diverse inhibitor profiles and cation specificities (as described below) of $HK\alpha_1$- and $HK\alpha_2$-containing H^+,K^+-ATPases.

H^+,K^+-ATPases were originally thought to secrete only H^+ and reabsorb only K^+. However, several studies now suggest that the both the $HK\alpha_1$- and $HK\alpha_2$-containing H^+,K^+-ATPases transport other cations. The first such studies observed that, in addition to K^+ flux, SCH-28080 inhibited Na^+ flux in microperfused cortical collecting ducts from dietary K^+ and Na^+ restricted rabbits.[155, 156] This SCH-28080 sensitive Na^+ flux was also inversely correlated with luminal $[K^+]$. It has also been found that Na^+ stimulates type III K^+-ATPase activity in microdissected collecting ducts from dietary K^+ depleted rats.[148] This type III activity, defined as sensitivity to ouabain and low sensitivity to SCH-28080, was only present in K^+ restricted animals and the inhibitor profile of type III activity is consistent with an $HK\alpha_2$-containing H^+,K^+-ATPase. In vitro analysis of $HK\alpha_2$-containing H^+,K^+-ATPase cation specificity in heterologous expression systems has also shown that both the rat and human enzymes can transport Na^+ on the K^+ binding site.[157] It was also observed that the gastric $HK\alpha_1$-containing H^+,K^+-ATPase transported Na^+ on the K^+

binding site.[158] However, the binding affinity of H^+,K^+-ATPases for Na^+ is much less than for K^+. To achieve a similar K^+-ATPase activity in *in vitro* expression systems or microdissected tubule, it requires as much as 14 times more Na^+ than K^+.

K^+ and NH_4^+ have very similar biophysical properties.[15] Therefore, it is not surprising that studies have also shown the H^+,K^+-ATPases to transport NH_4^+ on the K^+ binding site. This transport was first reported in the rat distal colon where NH_4^+ aptly substituted for K^+ in K^+-ATPase assays.[159] In a heterologous expression system, NH_4^+ and K^+ have been found to possess similar affinity for the $HK\alpha_2$-containing H^+,K^+-ATPase with NH_4^+ actually having greater efficacy for the pump.[157, 160] Overall, these data suggest that H^+,K^+-ATPases have the ability to reabsorb Na^+ and NH_4^+ in addition to K^+.

Genomic Organization

The cDNAs encoding for $HK\alpha_1$, $HK\beta$, and $HK\alpha_2$ have been cloned.[161-163] In the mouse, the mRNA nucleotide sequences for *Atp4a*, which encodes $HK\alpha_1$, and *Atp12a,* which encodes $HK\alpha_2$, are ~ 60% homologous. *Atp4a* localizes to chromosome 7 and has 22 exons. The human *ATP4A* gene localizes to chromosome 19 and also has 22 exons. Promoter analysis of the mouse *Atp4a* gene has not been published. However, promoter analyses for this gene in other species have been reported.[164, 165] Those studies identified putative cAMP response elements. $HK\alpha_1$ regulation by cAMP and its associated signaling molecules will be discussed later.

The mouse *Atp12a* gene is located on chromosome 14 and has 23 exons. The human gene *ATP12A* localizes to chromosome 13 and also has 23 exons. Promoter analysis of mouse *Atp12a* has demonstrated putative cAMP response elements, specificity protein 1(Sp1) sites, HREs, and nuclear factor kappa-light-chain-enhancer of

activated B cells (NF-κB) sites.[166] The regulation of HKα_2 by these pathways will also be discussed later. A putative cytosine-phosphate-guanine (CpG) island was detected in 5' flanking region of the human HKα_2 gene (*ATP12A* or *ATP1AL1*).[167] The methylation of CpG sites within the 5' promoter of a gene causes repression of gene expression.[168] However, a similar CpG island has not been detected in the proximal 5' region of the mouse *Atp12a* gene.[166]

The gene *Atp4b* localizes to chromosome 8 and has 7 exons encoding the mouse HKβ subunit. The human gene *ATP4B* localizes to chromosome 13, similar to *ATP12A*. HKβ genes from several species have been cloned and characterized.[162, 169-171] The promoter region of rat gastric HKβ gene has many potential transcription factor binding sites including a potential HRE.[171]

Tissue Localization

The stomach and colon were the first places where expression and activity of HKα_1-/HKβ- and HKα_2-containing H^+,K^+-ATPases were detected, respectively. Expression or activity of HKα_1- containing H^+,K^+-ATPases has since been observed in the kidney, cochlea, adrenal gland, and brain.[88, 89, 172, 173] HKβ mRNA and protein expression have been detected in the kidney and colon.[144, 174, 175] HKα_2-containing H^+,K^+-ATPases have been detected in the kidney, prostate, uterus, skin, and brain.[176-179]

The localization of these transporters in the kidney has been examined using pharmacology, expression analysis, and *in situ* hybridization, and immunolocalization. Expression or activity of renal HKα_1- and HKα_2-containing H^+,K^+-ATPases have been detected in the macula densa, proximal tubule, thick ascending limb, connecting segment, and the entire collecting duct.[88-90, 180-186] By *in situ* hybridization, HKβ

transcripts have been localized to the proximal tubule, thick ascending limb, connecting segment, and entire collecting duct also.[175]

The activity and expression of H^+,K^+-ATPases in the collecting duct has been the most well studied. H^+,K^+-ATPase activity (omeprazole and SCH-28080 sensitive) was originally detected in the outer medullary collecting ducts of rabbits fed a low K^+ diet.[135] Subsequent studies found $HK\alpha_1$ mRNA and protein expression in the cortex and medulla of rabbit, rat, and mouse.[180, 182, 186] Renal $HK\alpha_2$ mRNA and protein expression and activity (ouabain sensitive) in the rat, rabbit, and mouse are low under normal conditions but have been more readily detected in K^+ deplete animals. [90, 181, 184, 185, 187, 188]

Two studies of H^+,K^+-ATPase activity more closely defined the enzymatic characteristics and localization of $HK\alpha_1$- and $HK\alpha_2$-containing H^+,K^+-ATPases in the proximal tubule, thick ascending limb, and collecting duct. The first study examined pharmacological inhibition of K^+-ATPase activity in microdissected cortical and outer medullary collecting ducts, proximal tubules and thick ascending limbs from rats fed a normal or low K^+ diet.[148] Type I K^+-ATPase activity, defined as high sensitivity to SCH-28080 and insensitivity to ouabain, was observed in both segments of the collecting duct under normal conditions. Type II activity which was relatively insensitive to SCH-28080 and sensitive to ouabain was detected in the proximal tubule and thick ascending limb of normal rats. Type III activity which was sensitive to high ouabain and SCH-28080 was detected in the collecting duct of K^+ depleted rats. Type I and II activity significantly decreased in rats fed a low K^+ diet. The second study used HKα knockout mice to decipher the identities of type I and type III K^+-ATPase activity.[151] Under normal

conditions, type I activity was absent in $HK\alpha_1$ null ($HK\alpha_1^{-/-}$) mice but still present in $HK\alpha_2$ null ($HK\alpha_2^{-/-}$) mice. Under low K^+ conditions, type III activity was present in $HK\alpha_1^{-/-}$ mice but absent in $HK\alpha_2^{-/-}$ mice. This study did not address type II activity. It is important to note that these two studies were performed in different species. However, similar H^+,K^+-ATPase enzyme characteristics were observed. The two studies are consistent with only $HK\alpha_1$- containing H^+,K^+-ATPases being active in the collecting duct of normal animals and only $HK\alpha_2$-containing H^+,K^+-ATPases being active in the collecting duct of K^+ depleted animals.

The close homology of HKα and Na^+,K^+-ATPase α subunit peptide sequences have made it difficult to generate antibodies specific for the different HKα subunits. However, a few studies have examined HKα subunit protein localization by immunohistochemistry. Immunolocalization experiments have detected unpolarized $HK\alpha_1$ expression in ICs of the cortical and outer medullary collecting duct in rat, rabbit, and human.[185, 186] One study reported similar distribution of $HK\alpha_1$ and the H^+-ATPase, with basolateral detection in B-type ICs.[182] However, analysis of $HK\alpha_1$-like (SCH-28080-sensitive) H^+,K^+-ATPase-mediated K^+ flux and HCO_3^- reabsorption (equamolar with H^+ secretion) in the cortical and outer medullary collecting duct of rabbits suggests that $HK\alpha_1$-containing H^+,K^+-ATPases reside predominately on the IC apical plasma membrane.[12, 155, 189] $HK\alpha_2$ immunoreactivity has been detected in the apical membrane of connecting segment cells and ICs of the rabbit collecting duct.[90, 183] Immunostaining appears to be greatest in the connecting segment. Qualitatively less apical plasma membrane staining in cortical collecting duct PCs and light staining in the thick ascending limb and macula densa have also been observed for $HK\alpha_2$.[90]

Physiological Function and Dietary Regulation

Many years research has shown that H^+,K^+-ATPase activity in the collecting duct selectively increases with dietary K^+ depletion.[86, 87] This activity includes greater K^+ flux and H^+ secretion. In particular, $HK\alpha_2$ mRNA and protein expression are dramatically up-regulated in animals fed a low K^+ diet, especially in the medulla.[181, 187] One study has shown that $HK\alpha_1$ mRNA expression increased in the cortex of K^+ depleted rats.[190] No reports of $HK\alpha_1$ protein expression in K^+ depleted animals have been published.

Under normal conditions, H^+,K^+-ATPases coupled with an apical K^+ channel in the collecting duct appear to facilitate net HCO_3^- reabsorption via apical K^+ recycling. Data supporting this model came from the examination of H^+,K^+-ATPase-mediated HCO_3^- and K^+ flux in cortical collecting ducts from rabbits.[12] It was observed that apical application of the K^+ channel inhibitor, barium, decreased SCH-28080 sensitive HCO_3^- flux. In a separate study, basolateral barium application inhibited SCH-28080 sensitive H^+,K^+-ATPase activity (HCO_3^- and K^+ flux) in the cortical collecting duct of dietary K^+ restricted rabbits.[11] The latter study suggested that renal H^+,K^+-ATPases mediate net K^+ reabsorption under dietary K^+ restricted conditions.

As described in earlier sections, both $HK\alpha_1$- and $HK\alpha_2$-containing H^+,K^+-ATPases exhibit Na^+ transport on the K^+ binding site and inhibition of H^+,K^+-ATPases by SCH-28080 reduces Na^+ flux in the collecting duct. A low NaCl diet has also been shown to increase ouabain-sensitive H^+ secretion, indicative of $HK\alpha_2$-containing H^+,K^+-ATPases, in ICs of the rat cortical collecting duct.[191] A subsequent study that examined $HK\alpha_2$ mRNA and protein expression in the kidneys from Na^+ restricted rats observed no change in $HK\alpha_2$ expression.[192] It is possible that dietary Na^+ restriction

augments $HK\alpha_2$-containing H^+,K^+-ATPase activity in the collecting duct via alterations of membrane trafficking or activity without changes in expression.

The H^+,K^+-ATPase inhibitors, omeprazole and SCH-28080, both inhibit HCO_3^- reabsorption and H^+ secretion in the cortical, outer medullary, and inner medullary collecting duct.[135, 155, 193, 194] Using $HK\alpha_1^{-/-}$, $HK\alpha_2^{-/-}$, and $HK\alpha_1$ and $HK\alpha_2$ double null ($HK\alpha_{1,2}^{-/-}$) mice, our lab has more recently demonstrated that both A- and B- type ICs in the cortical collecting duct possess substantial H^+,K^+-ATPase-mediated H^+ secretion via both $HK\alpha_1$- and $HK\alpha_2$-containing H^+,K^+-ATPases.[89] Some studies have observed increased H^+,K^+-ATPase activity in the collecting duct or greater HKα subunit expression in kidneys from acidotic animals. Increased H^+,K^+-ATPase activity has been detected in collecting ducts from rats with chronic metabolic acidosis derived from dietary NH_4Cl loading, lithium treatment, and during respiratory acidosis.[193, 195-198] All of those studies observed stimulation of SCH-28080-sensitive H^+,K^+-ATPase activity, suggesting stimulation of $HK\alpha_1$-containing H^+,K^+-ATPases. Other investigators have observed increased $HK\alpha_2$ mRNA expression in the medulla of NH_4Cl loaded animals.[199] NH_3 can activate SCH-28080 and ouabain-sensitive H^+,K^+-ATPase H^+ secretion in ICs of the rabbit cortical collecting duct, suggesting that both H^+,K^+-ATPase isoforms are involved.[200, 201] A more recent study also indicates that dietary acid-induced acidosis stimulates both $HK\alpha_1$- and $HK\alpha_2$-containing H^+,K^+-ATPases expression in the kidney. Differences in mRNA expression of many different acid-base transporters were measured in isolated outer medullary collecting ducts from normal and NH_4Cl -loaded animals.[100] Within 3 days of an acid-loaded diet, there was a ~15 and 2 fold stimulation of $HK\alpha_1$ and $HK\alpha_2$ mRNA expression, respectively, in the mouse outer medullary

collecting duct. With 2 weeks on an acid-loaded diet, only $HK\alpha_2$ expression remained elevated (~3 fold). The accumulated evidence indicates that both the $HK\alpha_1$- and $HK\alpha_2$-containing H^+,K^+-ATPases participate in acidosis-induced H^+ secretion by the collecting duct in a time-dependent manner. The studies suggest that $HK\alpha_1$-containing H^+,K^+-ATPases exhibit a more acute (earlier) response to acidosis whereas $HK\alpha_2$-containing H^+,K^+-ATPases exhibit a more prolonged response.

Hormonal Regulation

Aldosterone stimulates luminal acidification by the distal nephron and collecting duct and only a few studies have examined the role of renal H^+,K^+-ATPases in this effect. Early studies suggested that aldosterone activated H^+,K^+-ATPases in the collecting duct.[134, 202] However, subsequent analyses of H^+,K^+-ATPase activity in response to aldosterone produced negative results. Most of the studies focused on early aldosterone effects (1–2 days) and used SCH-28080 inhibition to measure H^+,K^+-ATPase activity.[39, 41, 203] In one such study, H^+,K^+-ATPase-mediated (SCH-28080-sensitive) ATPase activity was measured in microdissected cortical and medullary collecting ducts from adrenalectomized rats given zero, normal, or supraphysiological doses of aldosterone and a low, normal, or high dietary K^+ intake for a week.[41] The activity of SCH-28080-sensitive H^+,K^+-ATPases did not correlate with aldosterone levels but inversely correlated with dietary K^+ intake. Also, a low NaCl diet has been found to increase SCH-28080 and ouabain-sensitive H^+,K^+-ATPase-mediated H^+ secretion in rat collecting duct ICs.[191] Since low NaCl diets increase plasma aldosterone, it seemed plausible that this was a mineralocorticoid effect. However, aldosterone replacement (at the levels induced by 2 weeks of dietary NaCl deficiency) in adrenalectomized rats did not increase SCH-28080- or ouabain- sensitive

H^+,K^+-ATPase-mediated H^+ secretion. The results suggest that chronic dietary NaCl depletion-induced H^+,K^+-ATPase activity is mineralocorticoid independent.

Ang II has direct effects on the collecting duct to stimulate H^+ secretion. More specifically, Ang II appears to stimulate H^+-ATPase mediated H^+ secretion in A-type ICs of the cortical collecting duct.[110, 111] However, no effect of Ang II on SCH-28080-sensitive H^+,K^+-ATPase activity in the collecting duct has been observed.[204] Likewise, ET-1 induces distal nephron acidification through augmented apical H^+-ATPase mediated H^+ secretion.[56] However, H^+,K^+-ATPase-mediated H^+ secretion (SCH-28080-sensitive) does not appear to be sensitive to the non-selective ET-1 receptor antagonist, bosentan. The data suggest that ET-1 does not regulate H^+,K^+-ATPase activity in the collecting duct. However, the effect of Ang II and ET-1 on specifically $HK\alpha_2$-containing H^+,K^+-ATPase activity and expression has not been investigated.

Recent data demonstrate that tissue kallikrein and the sex hormone, progesterone, regulate $HK\alpha_2$-containing H^+,K^+-ATPases in the kidney. Circulating tissue kallikrein levels were shown to directly correlate with dietary K^+ intake.[205] In this same study, tissue kallikrein null mice became hyperkalemic when given a large dietary K^+ load, suggesting maladaptive renal K^+ excretion. The data showed abnormal activation of H^+,K^+-ATPase activity and $HK\alpha_2$ mRNA expression in the cortical collecting duct of the knockout mice. Thus, tissue kallikrein appears to negatively regulate $HK\alpha_2$-containing H^+,K^+-ATPases. Therefore, the knockout of tissue kallikrein in mice appears to cause excessive urinary K^+ retention through renal $HK\alpha_2$-containing H^+,K^+-ATPases.

In contrast to tissue kallikrein, recent evidence showed that plasma progesterone increased with dietary K^+ restriction and that progesterone directly stimulated urinary K^+ retention in mice.[206] Progesterone also stimulated $HK\alpha_2$ mRNA expression in an *in vitro* cell line and $HK\alpha_2^{-/-}$ mice did not exhibit progesterone-induced urinary K^+ retention. Although previously unrecognized, these studies support important roles for hormones other than aldosterone to modify K^+ balance, specifically through renal $HK\alpha_2$-containing H^+,K^+-ATPase-mediated K^+ reabsorption.

Molecular Regulation

As mentioned earlier, cAMP response elements have been detected in promoters of both the $HK\alpha_1$ and $HK\alpha_2$ genes in many species. This suggested that cAMP and its associated pathways are important to the regulation of H^+,K^+-ATPases. A few studies have examined cAMP and Ca^{2+} dependent regulation of renal $HK\alpha_1$ and $HK\alpha_2$ gene expression or activity. cAMP generating agents such as isoproterenol, calcitonin, and AVP have been shown to activate renal H^+,K^+-ATPase K^+-stimulated ATPase activity.[207] In that study, cAMP through a PKA-dependent mechanism increased type I H^+,K^+-ATPase activity in the cortical collecting duct of rats fed a normal K^+ diet. AVP-mediated PKA activation was also shown to stimulate type III H^+,K^+-ATPase activity in collecting ducts from K^+ depleted rats. This same group later reported that cAMP also regulated SCH-28080 sensitive H^+,K^+-ATPase activity through the extracellular-signal regulated kinase cascade in addition to PKA.[208, 209] cAMP response element binding protein has also been shown to bind to the $HK\alpha_2$ promoter and induce $HK\alpha_2$ gene expression in the mouse inner medullary collecting duct cell line (IMCD3).[210]

Putative Sp1 and NF-κB response elements were also detected in the mouse *Atp12a* promoter. In IMCD3 cells, both Sp1 and NF-κB have been shown to bind to their

proposed putative elements within the $HK\alpha_2$ gene promoter.[211, 212] However, Sp1 increased and NF-κB inhibited $HK\alpha_2$ gene expression. The physiological implications of Sp1 and NF-κB regulation of $HK\alpha_2$ have not been explored.

Physiology of H^+,K^+-ATPase Null Mice

Gene targeting strategies have been used to create HKα and HKβ subunit null mice. The genetic disruption of mouse *Atp4a* gene involved insertion of a neomycin resistance gene into exon 8 with replacement of codons 360-390.[213] The removed nucleotide sequences encode for part of the fourth transmembrane and a conserved phosphorylation site (asparagine 385) essential for activity. $HK\alpha_1^{-/-}$ mice exhibited normal plasma [K^+] and [HCO_3^-]. The knockouts displayed reduced gastric acidification or achloryhydria and increased gastric HKβ expression. $HK\alpha_1^{-/-}$ also had gastrinemia, abnormal parietal cell structure, and gastric metaplasia.

$HK\beta^{-/-}$ mice were generated by disruption of exon 1 in the *Atp4b* gene and replacement of 35 bp with the phosphoglycerate kinase I-neomycin gene.[214, 215] Expression of HKβ mRNA and protein were not detected in stomachs from $HK\beta^{-/-}$ mice. Similar to $HK\alpha_1^{-/-}$ mice, $HK\beta^{-/-}$ mice exhibited achloryhydria, gastrinemia, and altered parietal cell ultrastructure. The renal physiology of $HK\alpha_1^{-/-}$ and $HK\beta^{-/-}$ mice was not investigated in those studies.

Mice with a HKβ transgene linked to the cytomegaolovirus promoter have been generated.[216, 217] The transgene has a mutation of tyrosine 20 to an alanine in the HKβ cytoplasmic tail peptide sequence. Replacement of tyrosine 20 with alanine caused constitutive expression of $HK\alpha_1$/HKβ in the apical plasma membrane of gastric parietal cells. It was also shown that the HKβ transgenic mice displayed excessive gastric acid secretion and developed ulcers.[216] Furthermore, the transgenic mice had a slight

hyperkalemia and reduced urinary K^+ excretion, suggesting that renal HKα/HKβ-containing H^+,K^+-ATPases are physiologically important to the regulation of K^+ homeostasis.[217]

$HK\alpha_2^{-/-}$ mice were generated by disruption of exon 20 of the *Atp12a* gene which encodes for important transmembrane segments.[218] The knockout mice still exhibited mRNA expression of the mutated $HK\alpha_2$ transcript in the colon but not in the kidney. $HK\alpha_2^{-/-}$ mice developed more severe hypokalemia and had excessive fecal K^+ wasting when fed a K^+ depleted diet, consistent with the loss of colonic ($HK\alpha_2$) H^+,K^+-ATPase-mediated K^+ reabsorption. However, $HK\alpha_2^{-/-}$ mice did not exhibit urinary K^+ loss or altered systemic acid-base parameters on a normal or K^+ restricted diet. Interestingly, $HK\alpha_2^{-/-}$ mice also exhibited significant fecal K^+ loss with dietary Na^+ restriction.[219] Additionally, the knockout mice showed fecal Na^+ loss and reduced amiloride-sensitive short circuit current in their colons, suggesting that $HK\alpha_2$-containing H^+,K^+-ATPases are required for maximal ENaC activity.

Summary and Hypothesis

Much research over the past 30 years has examined the physiological function of renal H^+,K^+-ATPases in K^+ and H^+ transport by the collecting duct. Although controversial, some evidence suggests that mineralocorticoids activate renal H^+,K^+-ATPases. In contrast, it is well established that dietary K^+ depletion induces H^+,K^+-ATPase activity and expression in the collecting duct. Interestingly, both mineralocorticoids and dietary K^+ depletion cause hypokalemia, metabolic alkalosis, and stimulate urinary Na^+ retention resulting in increased blood pressure.[220, 221] Since many studies suggest that the renal H^+,K^+-ATPases participate either directly or indirectly in Na^+ reabsorption, we hypothesize that, in addition to K^+ reabsorption and H^+ secretion,

either or both of the renal H^+,K^+-ATPases are required for Na^+ reabsorption during mineralocorticoid excess and dietary K^+ depletion.

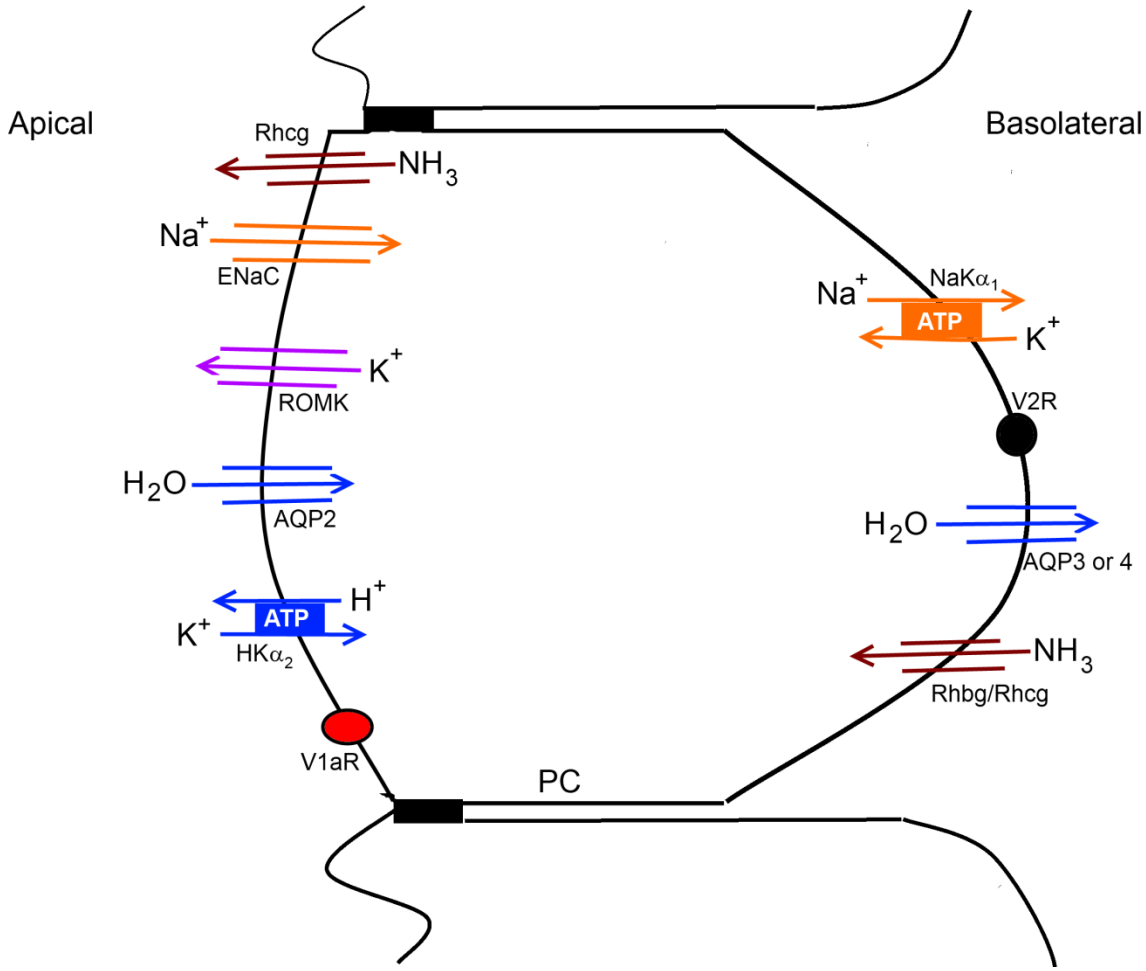

Figure 1-1. Model of collecting duct PC. An apical ENaC channel reabsorbs Na^+ from the tubular fluid and the basolateral Na^+,K^+-ATPase extrudes the Na^+ into the interstitium. An apical ROMK channel mediates K^+ secretion and an apical $HK\alpha_2$- containing H^+, K^+-ATPase reabsorbs K^+ and secretes H^+. The apical AQP2 and basolateral AQP3 or AQP4 channels reabsorb H_2O into the interstitium in response to V2R activation by vasopressin. V1aR inhibits the action of V2R and AVP.

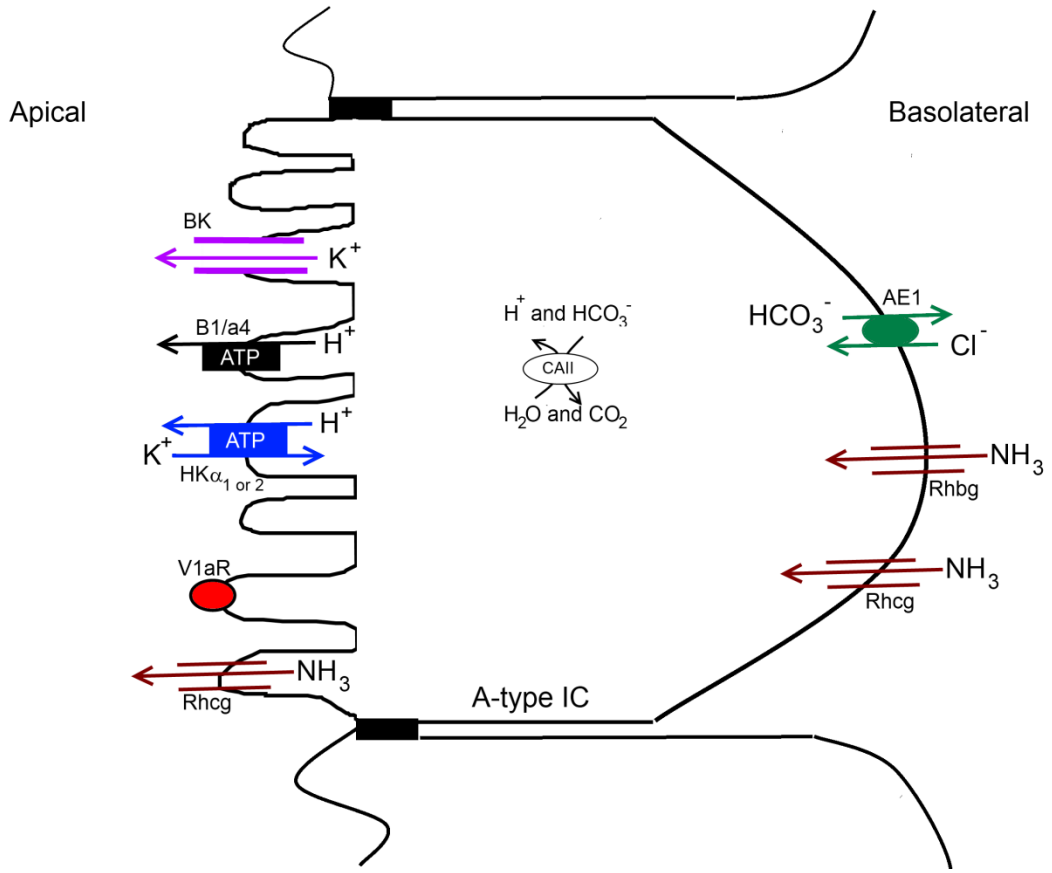

Figure 1-2. Model of collecting duct A-type IC. This IC subtype primarily participates in net acid secretion. An apical H^+-ATPase (B_1 and a_4) secretes H^+ into the luminal fluid. The basolateral Cl^-,HCO_3^- exchanger, AE1, reabsorbs the remaining intracellular HCO_3^- into the interstitium. Apical $HK\alpha_1$- and $HK\alpha_2$-containing H^+,K^+-ATPases reabsorb K^+ from and secrete H^+ into the lumen. The apical BK channel secretes K^+ in response to increased luminal flow. Rhcg, apical and basolateral, and basolateral Rhbg secrete NH_3 into the tubular fluid.

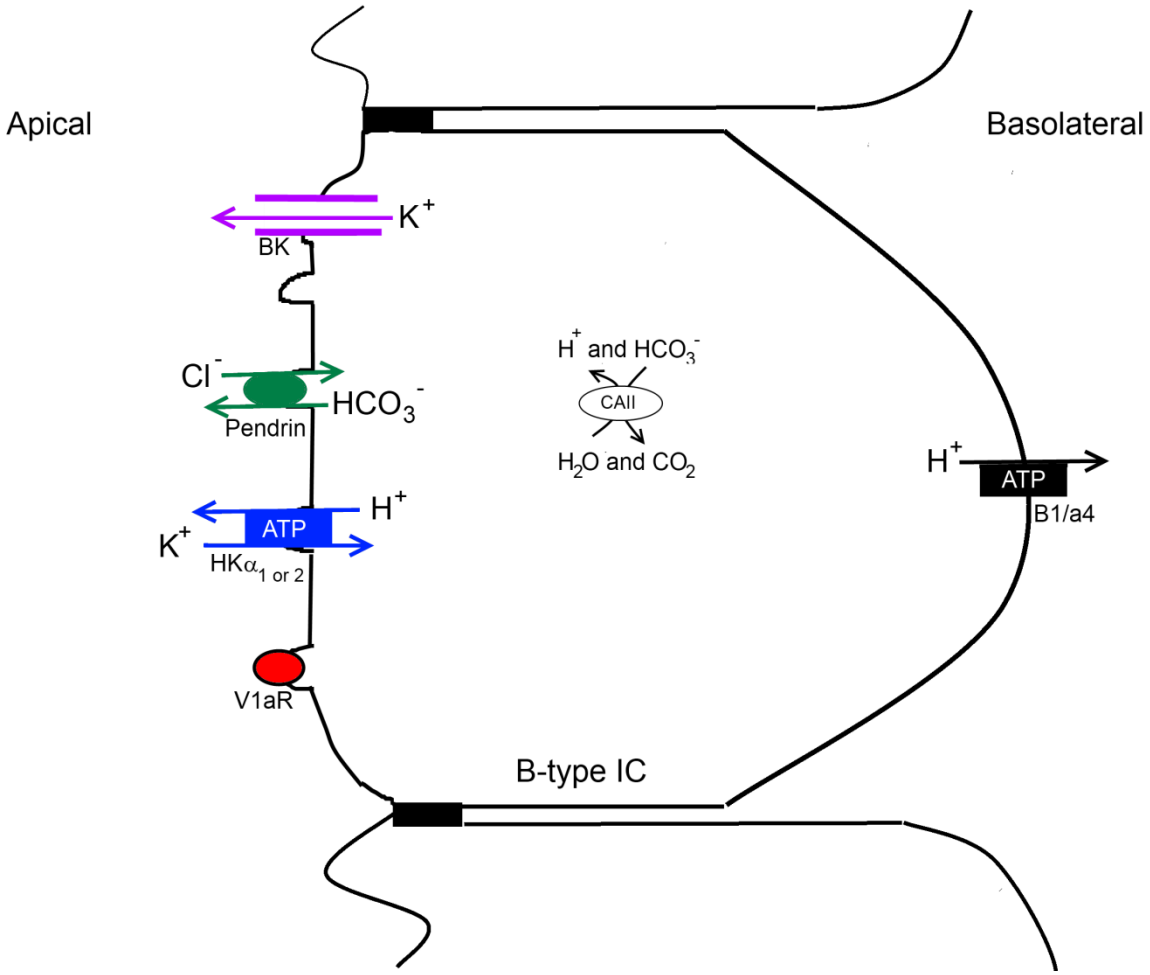

Figure 1-3. Model of collecting duct B-type IC. This IC subtype primarily participates in net base secretion. The apical Cl^-,HCO_3^- exchanger, Pendrin, secretes HCO_3^- into luminal fluid. A basolateral H^+-ATPase (B_1 and a_4) reabsorbs the remaining intracellular H^+ into the interstitium. Apical $HK\alpha_1$- and $HK\alpha_2$-containing H^+,K^+-ATPases reabsorb K^+ from and secrete H^+ into the lumen. The apical BK channel secretes K^+ in response to increased luminal flow.

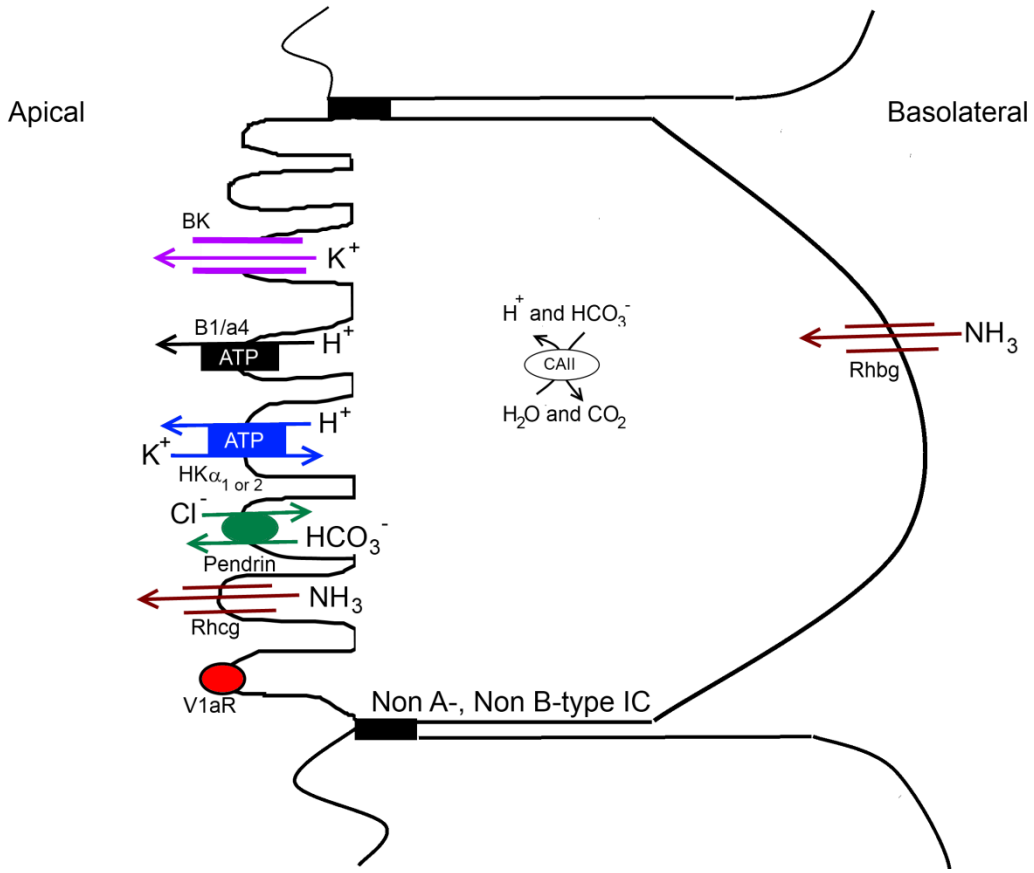

Figure 1-4. Model of collecting duct non A-, non B-type IC. This IC subtype can mediate net acid or base secretion. The apical Cl^-,HCO_3^- exchanger, Pendrin, secretes HCO_3^- into luminal fluid. The apical H^+-ATPase (B_1 and a_4) secretes H^+ into the lumen. Apical $HK\alpha_1$- and $HK\alpha_2$-containing H^+,K^+-ATPases reabsorb K^+ from and secrete H^+ into the lumen as well. The apical BK channel secretes K^+ in response to increased luminal flow. An apical Rhcg and basolateral Rhbg facilitate NH_3 secretion into the tubular fluid.

CHAPTER 2
MATERIALS AND METHODS

Animals

All animal use was approved by the Institutional Animal Care and Use Committee at the North Florida/South Georgia Veteran's Administration Medical Center in Gainesville, Florida and performed in accordance with the National Institute of Health's Guide for the Care and Use of Laboratory Animals. WT mice (C57BL/6J) were purchased from the Jackson Laboratory (Bar Harbor, Maine) or bred in house. $HK\alpha_1^{-/-}$ and $HK\alpha_{1,2}^{-/-}$ mice, originally acquired from Dr. Gary Shull (University of Cincinnati), were bred in house. $HK\alpha_1^{-/-}$ and $HK\alpha_2^{-/-}$ mice were bred and backcrossed onto the C57BL/6J background strain to create $HK\alpha_{1,2}^{-/-}$ mice. Both male and female mice (2-4 months old) from each genotype were used in experimental studies as designated below.

Genotyping

Tail snips (~ 0.25 cm) were taken from individual mice under isoflurane anesthesia and digested in a lysis buffer (0.2% sodium dodecyl sulfate or SDS, 0.2 M NaCl, 0.1 M Tris pH 7.5, 5 mM ethylenediaminetetraacetic acid or EDTA pH 8.0, 100 µg/ml proteinase K) at 55°C overnight. The sample was centrifuged at 13,000 rpm for 5 min and supernatant removed. An equal volume of isopropanol was added to the supernatant and the sample was incubated on ice for 30 min. The genomic deoxyribonucleic acid (DNA) was pelleted at 4°C for 30 min at 13,000 rpm, supernatant removed, and washed in equal volume of 75% ethanol. DNA was again pelleted at room temperature for 10 min at 13,000 rpm, supernatant removed, and allowed to air dry overnight. The DNA pellet was dissolved in sterile H_2O. Two separate triplex

polymerase chain reactions (PCR) were used to amplify genomic DNA from the *Atp4a* and *Atp12a* genes. Primer sequences are shown in Table 2-1. The $HK\alpha_1F$, $HK\alpha_1R$, and Neo primers were used to amplify genomic DNA from *Atp4a* and $HK\alpha_2F$, $HK\alpha_2R$, and Neo primers to amplify genomic DNA from *Atp12a*. HotStart Taq-polymerase (Qiagen, Valencia, CA) was used for DNA amplification. The kit supplied a 10X PCR buffer, 25 mM magnesium chloride ($MgCl_2$) , and 10 mM deoxynucleotide triphosphates (dNTPs) mixture. The reaction sample contained 1X buffer, 0.5mM $MgCl_2$, 0.2 mM dNTPs, 200 nM of each primer, and 1 unit of polymerase. The reaction cycle was as follows: 1 cycle at 94°C for 10 min; 40 cycles of 94°C for 30 s, 56°C for 30 s for *Atp4a* or 60°C for 1 min for *Atp12a*, 72°C for 1 min for *Atp4a* and 30 s for *Atp12a*; final 1 min extension at 72°C. PCR products were separated on a 2% agarose gel containing 0.1% ethidium bromide. Photographs were taken on Kodak Image Station 4000M using ultraviolet illumination (excitation 535nm and emission 600nm). As shown in Figure 2-1, WT mice displayed a 189 bp band for the *Atp4a* reaction whereas $HK\alpha_1^{-/-}$ and $HK\alpha_{1,2}^{-/-}$ mice displayed a 310 bp band due to the insertion of the neomycin gene. For the *Atp12a* reaction, WT and $HK\alpha_1^{-/-}$ mice displayed a 117 bp band whereas $HK\alpha_{1,2}^{-/-}$ mice displayed a 307 bp band indicative of neomycin insertion.

Diets, Treatments, and Metabolic Studies

Mice were housed in either their normal cage with bedding or in a metabolic cage (Nalgene) as designated in each individual experiment. The animals either received a normal pelleted diet supplied by the housing facility (Harlan Laboratories, Teklad (TD) 2016S/2018, 0.25% Na^+ and 0.53% K^+) or a gel diet consisting of 45% powered food (see experiments below for details), 1% agar, and 54% deoinized H_2O. Food intake and body weight were measured daily. For metabolic cage experiments, 24 hr urine and

fecal collections were performed. Urine was accumulated under H_2O-equilibrated mineral oil over the 24 hr period. At the end of the experiments, mice were anesthetized with 3-4% isoflurane and arterial blood was quickly and anaerobically collected through aortic cannulation. Blood [Na^+], [K^+], [Cl^-], pH, pCO_2, and hematocrit (Hct) were measured on a Stat Profile pHOx Plus C analyzer (Nova Biomedical; Waltham, MA) immediately after collection. Blood [HCO_3^-] was calculated on the instrument using the Henderson–Hasselbalch equation ($pH = 6.1 + \log([HCO_3^-]/[0.03*pCO_2])$. Kidneys were removed, weighed, and immediately frozen in liquid nitrogen and stored at -80°C.

DOCP experiments

Female mice between 8-16 weeks were used for DOCP experiments. For DOCP time course experiments and normal blood analysis, mice were fed normal lab chow and given free access to H_2O. One half the mice were given an intramuscular injection of 1.7 mg DOCP (Percorten V, Novartis Pharmaceuticals) under isoflurane anesthesia. For microperfusion and expression studies, another group of animals was treated with DOCP for eight days and sacrificed via Na^+ pentobarbital (i.p. 120 mg/kg) and cervical dislocation. One kidney was used for perfusion and the other for mRNA expression studies for day 8 of DOCP treatment.

For the high K^+ experiments, WT mice were fed a powdered diet (TD 99131; 0.2% Na+ and 0.6% K^+) supplemented with potassium chloride (KCl) to total 5% K^+ for 11 days in normal cages. The diet was made as a gel and mice were given free access to a H_2O bottle. On the third day, half of the mice were injected with DOCP.

In the last experiment, WT, $HK\alpha_1^{-/-}$, and $HK\alpha_{1,2}^{-/-}$ mice were housed in metabolic cages for 13 days and fed a powdered diet (TD 99131; 0.2% Na^+ and 0.6% K^+) made as a gel with free access to a H_2O bottle. $HK\alpha_1^{-/-}$ and $HK\alpha_{1,2}^{-/-}$ mice were pair fed with WT

mice of a similar body weight. Mice were injected with DOCP on day 5 of the experiment. In addition to food intake and body weight, H_2O intake was measured daily.

K^+ depletion experiments

Male mice between 12-16 weeks were used for K^+ depletion experiments. WT and $HK\alpha_{1,2}^{-/-}$ mice were housed in metabolic cages for 8 days and fed a normal gel diet (TD 99131) or a K^+ depleted gel diet (TD 99134, 0.2% Na^+ and ~ 0% K^+). Both KCl and $KHCO_3$ were removed to create the K^+-depleted diet. In an alternate experiment, mice were pair fed a normal gel diet for 4 days then switched to a K^+ depleted gel diet for 4 days. H_2O intake was from gel diet alone. In a separate experiment, WT, $HK\alpha_1^{-/-}$, and $HK\alpha_{1,2}^{-/-}$ mice were housed in normal cages and fed a K^+ depleted gel diet with free access to H_2O for 11 days. After 3 days on the diet, one half the animals were injected with DOCP (1.7 mg).

Na^+ depletion experiments

Male WT and $HK\alpha_{1,2}^{-/-}$ mice between 12-16 weeks were fed a normal gel diet (TD 99131) ad libitum for 7 days in regular cages. The mice were then placed in metabolic cages and pair fed the normal gel diet for 7 days and then switched to a Na^+ depleted gel diet (TD 03582, ~0% Na^+ and 0.6% K^+) for 7 days. Both NaCl and $NaHCO_3$ were removed to create the Na^+-depleted diet. H_2O intake was from gel diet alone.

NH_4Cl loading experiments

Male WT and $HK\alpha_1^{-/-}$ mice between 12-16 weeks were pair fed a normal gel diet (TD 99131) for 4 days then switched to the same gel diet supplemented with 0.28 M NH_4Cl for 6 days. H_2O intake was from gel diet alone. Mice were housed in normal cages for the first 2 days then placed in metabolic cages for the remainder of the experiment.

Urinalysis

Collected urine was centrifuged at 1000 x g for 5 min to remove debris and separate urine and oil. Urine pH was determined with an Accumet Model 25 pH meter (Fisher Scientific). Urine electrolytes ($[Na^+]$, $[K^+]$, and $[Cl^-]$) were measured using ion-sensitive electrodes on a Nova 16 clinical analyzer (Nova Biomedical, Waltham, MA). If concentration was too low for detection with Nova 16 instrument then urine Na^+ and K^+ were measured by spectrophotometric analysis on a digital flame photometer (Cole Parmer, Model 2655-00; see protocol in fecal analysis). Aliquoted urine samples were frozen at -80°C for later use.

The Ammonia Reagent Set (Pointe Scientific Inc., Canton, MI) was used to determine $[NH_4^+]$ in urine samples. This kit utilizes the enzymatic conversion of NH_4^+, α-ketoglutarate, and reduced nicotinamide adenine dinucleotide phosphate to L-glutamate, nicotinamide adenine dinucleotide phosphate, and H_2O catalyzed by glutamate dehydrogenase. The enzymatic conversion results in a decrease in absorbance at 340 nm. Thawed urine samples were diluted in deionized H_2O and $[NH_4^+]$ standards were made from 50 to 250 µM. The two reaction solutions provided with the kit were diluted in H_2O according to the manufacturer's protocol. Blank (H_2O), standards, and samples (40 µL) were pipetted in duplicate or triplicate onto a standard 96 well ultraviolet plate. For the first reaction, 200 µL of solution 1 was quickly mixed with each well and incubated for 7 min. The absorbance was read at 340 nm in a SpectraMax M5 plate reader (Molecular Devices). For the next reaction, 10 µL of solution 2 was added to each well, incubated for 7 min, and read at 340 nm. The reading of the first reaction (R1) was multiplied by 0.96 to correct for volume changes. The second reading (R2) was subtracted from the corrected R1 to calculate the change

in absorbance (R1-R2). A standard curve was generated for the change of absorbencies of each standard and used to calculate the [NH_4^+] in the samples.

To determine titratable acidity, equal volumes of 0.1M HCl and urine or blank (H_2O) were boiled for 2 minutes then cooled to 37 ºC. Titratable acidity (µmol/day) was calculated as the difference between the moles of standardized 0.1 M sodium hydroxide (NaOH) used to titrate the sample and the blank to pH 7.4. Potassium hydrogen phthalate (KHP) was used to standardize 0.1 M NaOH using the indicator, phenolphthalein (2%). KHP (0.8 g) was dissolved in 50 ml deionized H_2O and 4 drops of indicator were added. A measured volume of 0.1 M NaOH was used to titrate the KHP solution until the appearance of pink. At titration, the moles of KHP in the solution equals the moles of NaOH added. The moles and volume of NaOH added to the KHP solution were used to calculate the real molar concentration of prepared NaOH.

Urine [Ca^{2+}] was determined by modification of the Calcium (Arsenazo) Reagent Set (Pointe Scientific, Canton, MI). The kit utilizes the reaction of Ca^{2+} and Arsenazo III reagent in an alkaline solution to form a purple complex with absorbance at 650 nm. Standards were diluted in a range from 1 to 5 mM. Standards and samples (5 µL) were diluted and pipetted into a 96 well clear plate. The Arsenazo reagent (500 µL) was added to each well and incubated with sample for 10 min. The absorbance was read at 650 nm. A standard curve was generated and sample concentrations calculated.

Fecal analysis

Feces were weighed, baked overnight at 200°C in covered container, and weighed again. Dried fecal material was digested in 3 mL of 0.75 M nitric acid overnight at 37°C in a shaker. The digested material was homogenized using a mortar and pestle and

centrifuged at 1000 x g for 5 to 10 min to remove sediment. The supernatant was removed and stored at -20°C.

$[Na^+]$ and $[K^+]$ in digested fecal samples (and some urine samples) were determined by analysis on a digital flame photometer (Model 2655-00, Cole Parmer Instrument Company). Standards (1000 ppm Na^+ or K^+) and samples were diluted in diluent provided by Cole Parmer. The standards were diluted to a range of 0 to 40 ppm for K^+ and 0 to 20 ppm for Na^+. The flame photometer was allowed to equilibrate with a constant flow of diluent for 20-30 min before use. The appropriate spectrophotometric filter (Na^+ or K^+) was selected on front of photometer. The blank (diluent) was set to zero and the highest standard was set to a desired reading. Standards and samples were aspirated and a read in duplicate or triplicate. Standards were always rerun at the end of the experiment to correct for instrument drift. A standard curve was generated and the $[Na^+]$ or $[K^+]$ calculated for each sample.

Cell Culture

The immortal cell line, outer medullary collecting duct 1 ($OMCD_1$), was used for cell culture experiments. Guntupalli and colleagues generated the $OMCD_1$ cell line from the inner stripe of the outer medullary collecting duct of transgenic mice expressing the simian virus 40 T and large T antigens.[222] The cells exhibited phenotypic characteristics of outer medullary collecting duct ICs with microprojections and tubulovesicles near the plasma membrane and exhibited SCH-28080 sensitive K^+ flux and H^+ secretion, indicative of H^+,K^+-ATPases.[88, 222] In our studies, $OMCD_1$ cells were grown at 37°C on Costar transwell dishes to induce polarization. The cells were supplied with 4-(2-hydroxyethyl)-1-piperazineethanesulfonic acid-buffered Dulbecco's modified eagle medium: nutrient mixture F-12 supplemented (Invitrogen) with 10% fetal bovine serum

(Invitrogen) and 50 µg/ml gentamycin (Sigma). Once the cells reached 100% confluency, the cells were incubated in the same media without phenol red and supplemented with 10% cesium stripped fetal bovine serum for 24 hr. The cells were then treated with vehicle (ethanol) or 1 µM aldosterone replaced daily for 7 days. On the last day, cells were washed with phosphate buffered saline (PBS) and RNA was collected as described below.

RNA

RNA Extraction

TRIzol® reagent (Invitrogen) was used to extract RNA from tissues and cells. Tissues were homogenized using a glass dounce in TRIzol® reagent. Cells in transwells were incubated with TRIzol™ reagent for a few minutes, then detached using a cell scraper, and pipetted into a microcentrifuge tube. The homogenized tissue or cells were incubated at room temperature for 5 min. After the addition of an appropriate amount of chloroform, the sample was gently mixed three times and allowed to incubate for 2-3 min at room temperature. The sample was then centrifuged at 12,000 x g for 15 min at 4°C to separate the organic and aqueous phases. The aqueous phase (top clear phase containing RNA) was placed in a new tube and the organic phase (bottom phenol layer containing protein) was stored at 4°C for protein extraction. Isopropanol was added to the aqueous phase to precipitate RNA and stored at -80°C overnight. The following day, the sample was thawed and centrifuged at 12,000 x g for 10 min at 4°C. The supernatant was removed and the pelleted RNA washed with 75% ethanol. The sample was centrifuged at 7500 x g for 5 min, supernatant removed, and the pellet allowed to air dry for 5-10 min. The RNA pellet was dissolved in ribonuclease (RNase)-free H_2O and stored at -80°C. The RNA concentration was determined by

analysis on a spectrophotometer. RNA samples were treated with deoxyribonuclease (DNase) to remove DNA contaminants (DNA Free, Ambion). Approximately 10 µg RNA was diluted with a provided buffer to 50 µL total volume and 1 µL DNase 1 was added. The sample was incubated at 37°C for 20-30 min and then 5 µL inactivating reagent was added. The sample was incubated at room temperature for ~ 2 min and mixed often by flicking the tube. The inactivating reagent was separated from the RNA by centrifugation at 12,000 x g for 2 min. The supernatant containing RNA was removed and stored at -80°C. The RNA concentration and quality were determined by spectrophotometric analysis (absorbance 260 nm/ 280 nm from 1.9-2.0). RNA (1 or 2 µg) was converted to complementary DNA (cDNA) using SuperScript® III First Strand Synthesis SuperMix for quantitative reverse transcriptase (RT)-PCR (Invitrogen). RNA was mixed with a 2X reaction mixture and 6X enzyme mixture. The mixture was incubated at 25°C for 10 min, 50°C for 30 min, 85°C for 5 min, then held at 4°C. The cDNA was incubated in RNase H at 37°C for 20 min to degrade any remaining RNA. The cDNA was diluted to 4 ng/µL and stored at -20°C.

The TaqMan® MicroRNA RT Kit and TaqMan® MicroRNA Assays (Applied Biosystems) were used to convert microRNA into cDNA. Each 15 µL reaction included 1 mM dNTP, 3 units RT, RT buffer, 0.25 units RNase inhibitor, 3 µL primer, and 10 ng RNA. The primers were supplied with the specific TaqMan® MicroRNA Assay used (mmu-mir-505, assay # 001655; snoRNA-202, assay # 001232). The reaction mixture was incubated on ice for 5 min. The samples were then amplified using the following cycle parameters: 16°C for 30 min, 42°C for 30 min, 85°C for 5 min, and held at 4°C.

RT-PCR

HotStartTaq® DNA polymerase (Qiagen) was used for RT-PCR. Primers (MMG15 to 18 and GAPDHF/R) used for the reactions are shown in Table 1-1. The reaction mixture is the same as for genotyping except no additional magnesium chloride was added and 100 ng template DNA was used. The reaction cycle included: 1 cycle of 95°C for 15 min; 30-37 (30 for GAPDH, 37 for $HK\alpha_1$ and $HK\alpha_2$) cycles of 94°C for 30 s, 55°C for 1 min (65°C for GAPDHF/R primers), and 72°C for 1 min; 1 cycle of 72°C for 10 min then held at 4°C indefinitely. The PCR products were separated on a 2% agarose gel containing ethidium bromide. Photographs were taken on Kodak Image Station 4000M using ultraviolet illumination (excitation 535nm and emission 600nm).

Quantitative Real Time PCR (qPCR)

TaqMan® Gene Expression Assays (Applied Biosystems) were used for qPCR experiments. The primer/probe sets used include Atp4a (Mm00444423_m1), Atp12a (Mm0131809_m1), Atp6v1b1 (Mm00460320_g1), Atp6v0a4 (Mm00459882_m1), Slc4a1 (Mm00441492_m1), Slc26a4 (Mm00442308_m1), Rhbg (Mm00491234_m1), Rhcg (Mm00451199_m1), Slc9a3 (Mm01352473_m1), Slc9a2 (Mm01237129_m1), Scnn1a (Mm00803386_m1), Scnn1b (Mm00441215_m1), Scnn1g (Mm00441228_m1), and Actb (Mm00607939_s1). The 2X TaqMan® Universal PCR Mix- No AmpErase® Ung, a 20X primer/probe set (see above), and 20 ng cDNA were used in a 25 µL real time PCR reaction. The reaction was run in an Applied Biosystems 7500 Real Time PCR machine using the following cycle parameters: 1 cycle of 95°C for 10 min and 40 cycles of 95°C for 15 s and 60°C for 1 min. Each probe for every sample was run in duplicate. For qPCR of microRNA, the TaqMan® MicroRNA Assays (Applied Biosystems) were used (as described previously). The 20X probe/primer set for

mmu-mir-505 or snoRNA-202, 2X TaqMan® Universal PCR Mix-No AmpErase® Ung, and 1:15 dilution of microRNA cDNA product were mixed and run in duplicate. The ΔΔ cycle threshold (Ct) method was used to determine relative expression. Ct values were normalized to the endogenous control gene, Actb, for gene expression assays or snoRNA-202 for microRNA assays. The ΔΔCt was calculated by subtraction of each individual ΔCt (experimental gene Ct – endogenous gene Ct of each sample) from the average ΔCt of the control samples. Relative fold change in expression was calculated using $2^{-\Delta\Delta Ct}$. The fold change for control samples (control, cortex, or WT) is expressed as 1 or 100%.

Protein

Total Protein Extraction

Ethanol was added to the organic layer reserved from RNA extraction to precipitate DNA. The sample was gently mixed and incubated at room temperature for 3 min. The sample was centrifuged at 2000 x g for 5 min at 4°C and the supernatant placed in a fresh tube. Protein was precipitated by the addition of isopropanol and incubation at room temperature for 10 min. The protein was pelleted by centrifugation at 12,000 x g for 10 min at 4°C. After removal of the supernatant, the protein pellet was washed in 0.3 M guanidine HCl in 95% ethanol. The pellet was sonicated at 50% amplitude for < 10 s and incubated at room temperature for 20 min. The protein was repelleted by centrifugation at 7500 x g for 5 min at 4°C. The supernatant was removed and the pellet was washed 4 more times. After the last guanidine wash, the pellet was washed and sonicated twice in 95% ethanol. At the end of the washes, the pellet was allowed to air dry for 5-10 min. The protein was dissolved in 5% SDS and sonicated at 10% amplitude for 5 s. The sample was frozen overnight. After thawing, the sample was

boiled for 5 min and centrifuged at 10,000 x g for 10 min to remove insoluble material. The supernatant was aliquoted and frozen at -80°C.

Membrane Protein Extraction

For membrane protein, frozen tissue was dissected and immediately dounced in a glass homogenizer in solution A (10 mM Tris pH 7.4, 1 mM EDTA, 50 mM sucrose with 0.1 mg/ml Sigma protease inhibitor cocktail). After homogenization, an equal volume of solution B (10 mM Tris pH 7.4, 1 mM EDTA, 250 mM sucrose with 0.1 mg/ml Sigma protease inhibitor cocktail) was added and gently mixed with homogenate. The sample was centrifuged at 1000 x g for 5 min at 4°C to remove nuclei. The supernatant was centrifuged twice more at 10,000 x g for 20 min at 4°C to remove organelles. The remaining supernatant was centrifuged at 37,000 rpm overnight at 4°C in the Ti70.1 rotor of a Beckman ultracentrifuge. The membrane pellet was gently dissolved in solution B without protease inhibitors and subsequently stored at -80°C.

Bicinchoninic acid (BCA) Assay

Both total protein and membrane protein concentration were determined by BCA assay (Thermo Scientific Pierce). Bovine serum albumin standard (2 mg/ml) was diluted over a range of 0.1 to 1.6 mg/mL. Samples were diluted as appropriate. The standards and samples (10 µL) were run in triplicate. The standards and samples were pipetted into a 96 well clear plate and 200 µL of the reaction solution (50 parts solution A to 1 part solution B) were added to each well. The plate was covered with foil to protect from the light and incubated at 37°C for ~ 10 min. The absorbance at 540 nm was read on a plate reader (SpectraMax M5, Molecular Devices). A standard curve was generated from the absorbance of the bovine serum albumin standards and used to calculate the sample protein concentration.

Western Blot Analysis

Proteins (25 to 50 µg) were denatured at 95°C for 10 min in lithium dodecyl sulfate sample buffer (NuPage® LDS Sample Buffer, Invitrogen) with 5% 2-mercaptoethanol. The protein samples and protein ladder (Dual Color Precision Plus Protein Standard, Bio-Rad) were loaded onto a 4-20% gradient or 7.5% Tris-HCl polyacrilamide gel (Ready Gel, Bio-Rad) in Tris-glycine SDS buffer. The gels were run at 50 V until the ladder cleared the stacking gel then at 100-120 V until dye front reached the bottom of the gel. The proteins were transferred to polyvinylidene fluoride membranes in tris-glycine-methanol at 50 V for 3 hr at 4°C. The transferred proteins were washed in tris-buffered saline (TBS) for 5 min then blocked in 2% Rodeo® blocker (USB) in TBS with 0.05% Saddle Soap® (USB) (TBS-S) for 1 hr at room temperature. The membrane was incubated overnight in primary antibody (Table 2-2) diluted in blocking buffer. The membrane was washed twice in TBS-S for 10 min each and incubated in secondary antibody (Table 2-2) for 1 hr at room temperature. The membrane was washed again in TBS-S three times for 10 min each and rinsed in TBS. The membrane was incubated in Rodeo® electrochemiluminescence reagent (USB) for 5 min. For detection, two methods were employed. The membrane was exposed to x-ray film which was developed in a x-ray developer or chemiluminescent light on the membrane was detected by a digital camera (Kodak 4000M). The detection time was dependent upon the protein amount and primary antibody used. To reprobe the same blot with a different primary antibody, the blot was incubated in stripping solution (2% SDS, 100 mM 2-mercaptoethanol, 62.5 mM Tris (pH 6.7)) for 30 min at 70°C. The blots were washed in TBS twice for 5 min and then reblocked and probed as per above protocol.

To compare expression between genotypes, densitometric values for each band detected with each primary antibody were measured using the Un-Scan-It Gel Analysis software (Silk Scientific). The densitometric values obtained for a band detected with an experimental primary antibody (anti-αENaC and anti-γENaC) were divided by the values obtained for the loading control primary antibody (anti-β-actin) to correct for protein loading differences between samples. The percent differences in the corrected values were compared between WT (set at 100%) and knockout mice.

Enzyme Immunoassay (EIA)

The Aldosterone and AVP EIA Kits (Cayman Chemical) were used to determine urine concentrations of aldosterone and AVP. These kits utilize competitive binding of the hormone in a sample (or standard) and a hormone conjugated to acetylcholinesterase (tracer) to a hormone-specific primary antibody. The bound antibody and hormone will bind to secondary antibody bound to the provided 96 well plate. Ellman's reagent (acetylcholinesterase substrate) is used to develop the wells and the absorbance (yellow) is read at 410 nm. The concentration of hormone in the sample is therefore inversely proportional to the detected tracer. For aldosterone, the standards are diluted over a range of 7.8 to 1000 pg/ml and, for vasopressin, 23.4 to 1500 pg/ml. The standards and samples are diluted in a provided EIA buffer and run in duplicate or triplicate. Several other controls include blank, non-specific binding (NSB, EIA buffer only), binding maximum (B_o, tracer and antibody), and total activity (tracer at development). The controls, standards, and samples (50 µL) were pipetted onto the provided 96 well plate. Tracer and then antibody (50 µL) were added to all standards and samples and to the B_o wells. The plate was covered with film and incubated at 4°C overnight. The plate was washed 5 times with EIA wash buffer and Ellman's reagent

(200 µL) was added to each well. The plate was covered with plastic film and developed in the dark for 1.5 hr with shaking at 200 rpm. The absorbance at 410 nm was read on a plate reader (SpectraMax M5, Molecular Devices). The NSB absorbance was subtracted from B_o to correct the B_o absorbance values. The % binding (B) of samples and standards is determined by B/B_o and used to create the standard curve. The equation, $\text{logit}(B/B_o)=\ln[B/B_o/(1- B/B_o)]$, was first used to linearize the data. The resultant logit values were plotted versus log concentration and a linear regression was performed. The standard curve is used to calculate concentration of each sample.

In Silico Sequence Analyses

Promoter Analysis

The proximal 2000 bp promoter region of *Atp4a* and *Atp12a* were downloaded from the NCBI website (www.ncbi.nlm.nih.gov). The mRNA and genomic DNA sequences for each gene were aligned using NCBI basic local alignment search tool (BLAST). The alignment provided the exact position of the transcription start site in the genomic DNA for each gene. This information was used to extract 2000 bp upstream of the transcription start site within the genomic DNA sequence. The promoter sequence was then run through two online software programs, Transcription Element Search Software (TESS, www.cbil.upenn.edu/cgi-bin/tess/tess) and Transcription Factor (TF) Search (www.cbrc.jp/research/db/TFSEARCH.html) that detect putative transcription factor binding sites by two different algorithms. Percent match was set at 75%.

MicroRNA Target Analysis

Putative microRNA binding sites were determined in the 3' untranslated region (UTR) of *Atp4a* and *Atp12a*. The sequences were extracted and binding sites determined by the software program, TargetScanMouse, www.targetscan.org. Only

conserved sites and those with high context score percentiles were considered as potential binding sites.

Statistical Analyses

Origin 8 and SigmaPlot 11 were used for statistical analyses. Origin 8, Adobe Photoshop, and Paint.Net were used to create graphs and figures. All data are represented as mean ± standard error of the mean (SEM). Two-tailed Student's *t*-Test was used to compare two different groups. A one-way analysis of variance (ANOVA) with or without repeated measures was used to compare three or more groups with one effect. Two-way ANOVA with or without repeated measures was performed to compare two effects such as genotype, diet, treatment, and time. If significance was found, then an appropriate post-hoc test was performed. P values less than 0.05 were considered significant.

Table 2-1. Primer sequences

Primer name	Sequence (5' to 3')	T_m (°C)	Use
$HK\alpha_1F$	GCCTGTCACTGACAGCAAAGAGG	64	Genotyping
$HK\alpha_1R$	GGTCTTCTGTGGTGTCCGCC	64	Genotyping
$HK\alpha_2F$	CTGGAATGGACAGGCTCAACG	64	Genotyping
$HK\alpha_2R$	GTACCTGAAGAGCCCCTGCTG	63	Genotyping
Neo	CTGACTAGGGGAGGAGTAGAAGG	58	Genotyping
MMG15	GTTCCTGATGCTGTGCTCAA	59	RT-PCR
MMG16	TCGAGCAAACACCATCTCAG	59	RT-PCR
MMG17	GCCATACTTGTCCTGGTCGT	59	RT-PCR
MMG18	CTGAAGCCAAGGAGGCTATG	59	RT-PCR
GAPDHF	AGACACGATGGTGAAGGTCGGAGTGAAC	71	RT-PCR
GAPDHR	GTGGCACTGTTGAAGTCGCAGGAG	68	RT-PCR

T_m denotes melting temperature.

Table 2-2. Antibodies

Antibody name	Supplier	Dilution
Rabbit polyclonal anti-αENaC	Ecelbarger	1:1000
Rabbit polyclonal anti-γENaC	Ecelbarger	1:1000
Rabbit polyclonal anti-H^+-ATPase B1/B2	Santa Cruz, sc-20943	1:250
Goat polyclonal anti-β-actin	Santa Cruz, sc-1616	1:500
Anti-rabbit IgG HRP conjugate	USB, Rodeo® ECL kit	1:5000
Donkey anti-goat HRP conjugate	Santa Cruz, sc-2020	1:5000

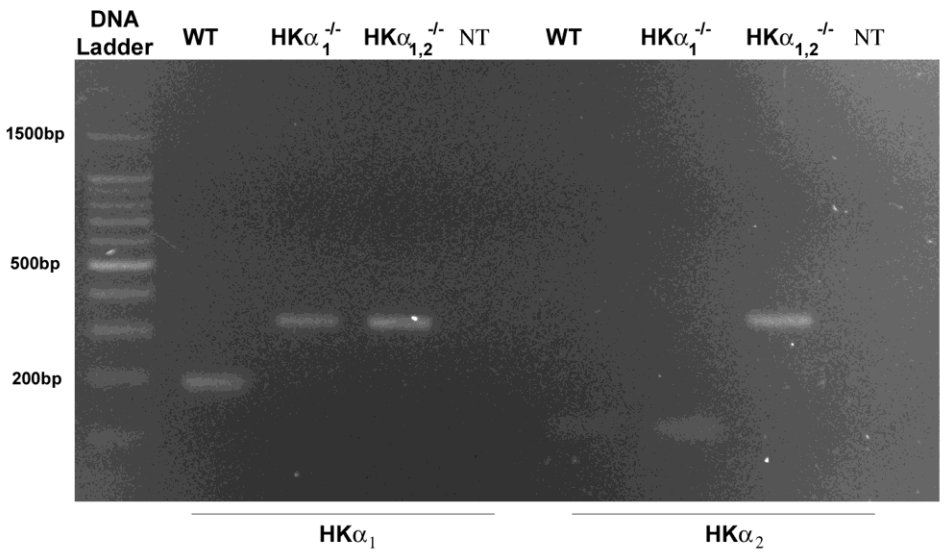

Figure 2-1. Representative genotyping PCR gel. Triplex PCR was used to amplify genomic DNA for HKα$_1$ (*Atp4a*) and HKα$_2$ (*Atp12a*) from tail snips of WT, HKα$_1^{-/-}$, and HKα$_{1,2}^{-/-}$ mice. The WT band for HKα$_1$ runs at 189 bp and for HKα$_2$ runs at 117 bp. The knockout band for HKα$_1$ runs at 310 bp and for HKα$_2$ runs at 307 bp. NT denotes no template control.

CHAPTER 3
EFFECT OF MINERALOCORTICOIDS ON RENAL H^+,K^+-ATPASES

Chronic mineralocorticoid excess* causes hypokalemia and metabolic alkalosis.[25, 27, 223] The mechanism responsible for mineralocorticoid-induced metabolic alkalosis is through increased urinary acidification, particularly by the renal collecting duct. [36] It is known that mineralocorticoids stimulate H^+ secretion by A-type ICs of the renal collecting duct in part through apical H^+-ATPases. [38, 224] Although there is not significant evidence that mineralocorticoids directly regulate renal H^+,K^+-ATPases, it is possible that mineralocorticoid-induced hypokalemia secondarily activates renal H^+,K^+-ATPases. Since a study has shown that H^+,K^+-ATPases are required for ENaC-mediated Na^+ reabsorption in the colon,[219] it is also possible that the renal H^+,K^+-ATPases are required for the mineralocorticoid stimulation of renal ENaC-mediated Na^+ retention.

In this study, the chronic effects of mineralocorticoids on renal H^+,K^+-ATPases were investigated in cell culture and animal models. To induce chronic mineralocorticoid excess, we treated mice with a one-time i.m. injection of DOCP, an ester analog of the mineralocorticoid, desoxycorticosterone. DOCP has long-lasting (~25-30 days) action resulting from esterase cleavage in muscle to desoxycorticosterone. This drug is clinically used for treatment of canine Addison's disease.[225-227] One week past DOCP treatment, mice have been shown to display increased blood pressure and hypokalemia with slight metabolic alkalosis. [118]

In the present study, the timings of DOCP-induced disturbances in body weight, Na^+, K^+, and acid-base homeostasis in mice were determined and correlated with renal

* The data contained within this chapter have been previously published. Greenlee MM, Lynch IJ, Gumz ML, Cain BD, Wingo CS: Mineralocorticoids stimulate the activity and expression of renal H^+,K^+-ATPases. *J Am Soc Nephrol*, 2011

HKα subunit expression. In a separate experiment, we examined the effect of a high K^+ diet to abolish the effect of DOCP on blood [K^+] and HKα subunit expression. The effect of chronic aldosterone exposure (7 days) on HKα subunit expression was also investigated using the *in vitro* OMCD1 cell line that is known to possess H^+,K^+-ATPase activity.[222] Finally, our study compared the physiological (systemic, renal, and gastrointestinal) responses of WT, $HK\alpha_1^{-/-}$, and $HK\alpha_{1,2}^{-/-}$ to DOCP treatment.

Results

Mineralocorticoid Excess in WT Mice

The first goal of these studies was to characterize the temporal changes in body weight, Na^+, K^+, and acid-base homeostasis during chronic mineralocorticoid excess in WT mice and to relate these changes to mRNA expression of renal H^+,K^+-ATPases. The second goal was to evaluate whether a high K^+ diet abolished the physiological effect of mineralocorticoids in WT mice and suppressed changes in renal H^+,K^+-ATPase expression.

Body weight and blood chemistries were measured over an 8 days in control and DOCP-treated female WT mice. DOCP treatment caused a considerable increase in body weight apparent by day 4 but control mice exhibited no significant change in body weight over this time period (Table 3-1). The minor body weight gain observed in control mice is consistent with normal growth in these young animals. The extra body weight gain in DOCP-treated mice is consistent with the known effect of DOCP to enhance Na^+ and fluid volume retention.

By day 4, DOCP treatment caused a slight, but statistically significant increase in blood [Na^+] and this effect started to decline by day 8 (Table 3-2). Moreover, DOCP treatment caused a considerable reduction in blood [K^+] that was statistically significant

at day 6 after treatment. Blood [HCO_3^-] was significantly increased by day 8 after DOCP treatment. The timing and magnitude of increased blood [HCO_3^-] were reflected in a reciprocal decrease in blood [Cl^-] by approximately 7mM.

To examine the contribution of hypokalemia to the physiological effects of DOCP, body weight change and blood chemistries were compared in control and DOCP-treated WT mice fed a high K^+ diet. A high K^+ diet abrogated the effect of DOCP on body weight gain (Table 3-3). The high K^+ fed mice did not display a reduction in blood [K^+] with DOCP treatment. Greater blood [HCO_3^-] and a reciprocal lower blood [Cl^-] were also not apparent in DOCP-treated mice fed a high K^+ diet.

Induction of Renal HKα_2 Expression

It is possible that up-regulation of HKα subunit mRNA occurs as a secondary response to DOCP-induced hypokalemia. Therefore, the next experiments evaluated the effect of DOCP treatment (8 days) on renal HKα_1 and HKα_2 mRNA expression in mice fed a normal diet and whether these effects were altered by a high K^+ diet or by time.

RT- and real time qPCR were used to investigate changes in steady state mRNA levels of H^+,K^+-ATPase α subunits, HKα_1 and HKα_2, in cortex, outer medulla, and inner medulla of control and DOCP-treated (8 days) mice fed a normal diet. In control mice, the relative expression of HKα_1 and HKα_2 differed between the three kidney segments (Figure 3-1). Expression for both α subunits was greatest in the cortex followed by the outer then inner medulla (Figure 3-1 A and B). HKα_1 was more highly expressed than HKα_2 in each segment (Figure 3-1 C).

Figures 3-2 and 3-3 depict HKα subunit mRNA expression in kidneys from control and DOCP-treated mice as detected by RT-PCR and real time PCR, respectively.

Neither $HK\alpha_1$ nor $HK\alpha_2$ mRNA expression in the renal cortex were significantly changed in DOCP-treated mice compared to control (Figure 3-3 A and B). In the outer medulla, DOCP did not affect $HK\alpha_1$ mRNA expression but increased $HK\alpha_2$ expression ~ 2-fold. DOCP also did not significantly affect $HK\alpha_1$ mRNA expression in the inner medulla (Figure 3-2 and 3-3 A). In contrast, DOCP dramatically stimulated $HK\alpha_2$ mRNA levels in the inner medulla by ~ 5 fold compared to control levels (Figure 3-2 and 3-3 B). DOCP's main effect was to increase $HK\alpha_2$ mRNA expression in the medulla.

To determine if the changes in $HK\alpha_2$ expression were secondary to DOCP-induced hypokalemia, $HK\alpha_1$ and $HK\alpha_2$ mRNA expression levels were compared in control and DOCP-treated (8 days) mice fed a high K^+ diet (Figure 3-3 C and D, respectively). The DOCP-induced stimulation of $HK\alpha_2$ mRNA expression in the renal medulla was absent in mice fed a high K^+ diet (Figure 3-3 D).These results demonstrate that the stimulation of medullary H^+,K^+-ATPase α subunit mRNA expression with DOCP treatment is dependent on dietary K^+ intake and possibly DOCP-induced hypokalemia.

Since blood [HCO_3^-] was not significantly increased by day 6 after DOCP (Table 3-1), we hypothesized that the increased $HK\alpha_2$ subunit mRNA expression observed by DOCP day 8 would be absent at day 6 after treatment. Figure 3-4 shows relative mRNA expression for $HK\alpha_1$ and $HK\alpha_2$ in cortex, outer medulla, and inner medulla of control and DOCP-treated mice (day 6). Medullary $HK\alpha_1$ mRNA expression was significantly increased ~1.5 fold by day 6 after DOCP treatment (Figure 3-4 A). In contrast, DOCP did not increase medullary $HK\alpha_2$ mRNA expression by this time point and there was actually less cortical expression than in control mice (Figure 3-4B). These results are consistent with our hypothesis that renal $HK\alpha_2$ expression would not be increased by

day 6 after DOCP treatment. Our results did show that DOCP induces $HK\alpha_1$ mRNA expression at earlier time points and suggests that both the $HK\alpha_1$- and $HK\alpha_2$-containing H^+,K^+-ATPases may be involved in the physiological effects of DOCP, just at different times.

Aldosterone Treatment in OMCD1 Cells

The next experiments sought to determine if an *in vitro* collecting duct cell model replicated the effect of chronic mineralocorticoids on $HK\alpha_2$ expression. If so, then this model could be used to study the molecular mechanism(s) by which mineralocorticoids increase H^+,K^+-ATPase α subunit expression and activity. OMCD1 cells, which are an immortal cell line derived from cells in the outer medullary collecting duct, have previously been shown to possess SCH-28080 sensitive H^+ secretion indicative of an H^+,K^+-ATPase [88]. PCR analysis of $HK\alpha_1$ mRNA expression demonstrated no significant difference between OMCD1 cells treated with vehicle (ethanol) or 1μM aldosterone for seven days (Figure 3-5). $HK\alpha_2$ mRNA was undetectable in OMCD1 cells. The lack of $HK\alpha_2$ expression in these cells does not make them a good model to study the effect of mineralocorticoids on renal H^+,K^+-ATPases.

Mineralocorticoid Excess in HKα Null Mice

The final set of experiments considered the physiological function of renal H^+,K^+-ATPases in the response to chronic mineralocorticoid excess and specifically characterized the effect of DOCP treatment on the electrolyte and acid-base homeostasis of $HK\alpha_1^{-/-}$ and $HK\alpha_{1,2}^{-/-}$ mice.

Body weight change and blood chemistries were first compared in untreated WT and knockout mice. No significant change in body weight was observed in untreated mice of any genotype over eight days (Figure 3-6). Blood $[K^+]$ was paradoxically greater

in the $HK\alpha_{1,2}^{-/-}$ compared to WT or the $HK\alpha_1^{-/-}$ mice (Table 3-4). Blood [Cl^-] was less in the $HK\alpha_1^{-/-}$ compared to either the WT or $HK\alpha_{1,2}^{-/-}$ mice. Blood [Na^+] and [HCO_3^-] were similar between the genotypes.

DOCP-induced body weight gain over 8 days was comparable in WT and $HK\alpha_{1,2}^{-/-}$ mice (Figure 3-7 A). In contrast, $HK\alpha_1^{-/-}$ mice exhibited nearly twice the body weight gain of WT mice with DOCP treatment. By day 8 after DOCP treatment, blood [Na^+] was similar between the genotypes (Figure 3-7 B). Although DOCP reduced blood [K^+] ~1 mM in mice from all the genotypes, $HK\alpha_{1,2}^{-/-}$ mice still exhibited greater blood [K^+] than WT or $HK\alpha_1^{-/-}$ mice (Figure 3-7 C). The effect of DOCP to decrease blood [Cl^-] (Figure 3-7 D) and increase blood [HCO_3^-] (Figure 3-7 E) in WT mice was eliminated in $HK\alpha_{1,2}^{-/-}$ mice but not in $HK\alpha_1^{-/-}$ mice.

In order to more fully understand the mechanism for the observed differences in body weight gain and blood electrolytes between WT and the HKα knockout mice, urine volume, H_2O intake, urinary Na^+, and urinary K^+ retention were compared over the time course (8 days) of DOCP treatment. Urine electrolyte (Na^+ or K^+) retention was calculated as dietary intake minus urinary excretion of that electrolyte.

Urine volume doubled by the end of DOCP treatment in both WT and $HK\alpha_{1,2}^{-/-}$ mice (Figure 3-8 A). However, urine volume did not increase in DOCP-treated $HK\alpha_1^{-/-}$ mice. Urine volume was significantly reduced from day 7 to day 8 after DOCP treatment in $HK\alpha_1^{-/-}$ mice. However, H_2O intake was quite similar between the genotypes over most of the time course (Figure 3-8 B). Nevertheless, on DOCP day 8, $HK\alpha_1^{-/-}$ mice exhibited a considerable reduction in H_2O intake that correlates with their decreased urine volume.

Over the course of DOCP treatment, $HK\alpha_{1,2}^{-/-}$ retained significantly less urinary Na^+ than WT or $HK\alpha_1^{-/-}$ mice (Figure 3-8 C). In the comparison of day 8 of DOCP treatment to control urinary Na^+ retention, $HK\alpha_1^{-/-}$ mice exhibited a greater stimulation of urinary Na^+ retention than WT mice (Figure 3-8 D). The greater urinary Na^+ retention of $HK\alpha_1^{-/-}$ mice on DOCP day 8 is consistent with their decreased urine volume on that day. No significant differences in urinary K^+ retention between the genotypes were observed over the time course of DOCP treatment except at day 8 (Figure 3-8 E). At DOCP day 8, urinary K^+, like Na^+, retention was greater in $HK\alpha_1^{-/-}$ mice than either WT or $HK\alpha_{1,2}^{-/-}$ mice (Figure 3-8 F).

Although the mice were pair fed, analysis of stool samples from WT, $HK\alpha_1^{-/-}$, and $HK\alpha_{1,2}^{-/-}$ mice revealed that $HK\alpha_1^{-/-}$ mice excreted 50% more dry stool weight than either the WT or $HK\alpha_{1,2}^{-/-}$ mice on day 8 of DOCP treatment (Figure 3-9 A). Fecal Na^+ excretion significantly decreased in DOCP-treated WT and $HK\alpha_{1,2}^{-/-}$ mice (Figure 3-9 B). In contrast, DOCP-treated $HK\alpha_1^{-/-}$ mice exhibited greater fecal Na^+ excretion than WT or $HK\alpha_{1,2}^{-/-}$ mice. Interestingly, fecal K^+ loss was evident in both $HK\alpha_1^{-/-}$ and $HK\alpha_{1,2}^{-/-}$ mice under control conditions (Figure 3-9 C). Fecal K^+ excretion decreased in WT mice treated with DOCP but increased ~50% in DOCP-treated $HK\alpha_1^{-/-}$ and $HK\alpha_{1,2}^{-/-}$ mice (Figure 3-9 C).

In the context of whole animal physiology, it is important to examine the overall electrolyte balance as the sum of urinary and fecal excretion subtracted from the intake of that electrolyte. Overall Na^+ and K^+ balance were compared under control conditions and on day 8 of DOCP treatment. Na^+ balance was not significantly different between the genotypes under control conditions (Figure 3-10 A). As expected, Na^+ balance was

greater in WT mice with DOCP treatment compared to control conditions. A similar effect was observed in $HK\alpha_1^{-/-}$ mice. In contrast, Na^+ balance was significantly less in DOCP-treated $HK\alpha_{1,2}^{-/-}$ mice than either WT or $HK\alpha_1^{-/-}$ mice. Under control conditions, WT, $HK\alpha_1^{-/-}$ and mice $HK\alpha_{1,2}^{-/-}$ mice had similar K^+ balance (Figure 3-10 B). DOCP-treatment caused $HK\alpha_1^{-/-}$ mice to exhibit greater K^+ balance than WT. $HK\alpha_{1,2}^{-/-}$ mice exhibited lower K^+ balance (~40% less) than WT mice with DOCP treatment (Figure 3-10 B).

Discussion

These studies revealed that the long-acting mineralocorticoid, DOCP, caused hypokalemia and metabolic alkalosis ~ 8 days after administration to mice. DOCP-induced metabolic alkalosis correlated with increased renal medullary $HK\alpha_2$ mRNA expression and a high K^+ diet abrogated this effect. The overall deficit in K^+ retention and resistance to metabolic alkalosis of DOCP-treated $HK\alpha_{1,2}^{-/-}$ mice and the lack of this deficit in $HK\alpha_1^{-/-}$ mice suggests the importance of $HK\alpha_2$-containing H^+,K^+-ATPases to mediate greater K^+ reabsorption and H^+ secretion with mineralocorticoid excess. Notably, the elimination of DOCP-induced urinary Na^+ retention in $HK\alpha_{1,2}^{-/-}$ mice also implies that the renal $HK\alpha_2$-containing H^+,K^+-ATPases are important for mineralocorticoid-induced Na^+ retention.

Previous transcription factor analysis of mouse *Atp12a* ($HK\alpha_2$) promoter detected one potential HRE within 1500 bp of the transcription start site, indicating that at least the $HK\alpha_2$-containing H^+,K^+-ATPases were potential MR targets.[166] In contrast, a putative HRE was not detected in the rabbit *Atp12a* promoter.[228] Figure 3-11 depicts our own analysis of putative HREs in *Atp4a* ($HK\alpha_1$) and *Atp12a* ($HK\alpha_2$) promoters. The criteria for identification of putative HREs included detection by both TESS and TF Search

software programs. Both algorithms detected two putative HRE half sites (75% match) in the *Atp4a* and *Atp12a* promoters and the position, direction, and sequence of these prospective sites are shown in Figure 3-11. The two sites in the *Atp12a* promoter most closely resemble the HRE half site consensus sequence (AGAACA). These sites do not possess a clear, canonical inverted palindrome (AGAACAnnnTGTTCT) that is expected for HREs. Therefore, the HKα subunit genes, *Atp4a* and *Atp12a*, are likely not early, genomic targets of mineralocorticoid action. Consistent with this conclusion, our results have shown that DOCP requires 8 days to induce metabolic alkalosis and an increase in medullary $HK\alpha_2$ mRNA expression in mice.

The effect of long term mineralocorticoid excess to change renal H^+,K^+-ATPase activity has been previously examined.[41] Although no effect of the mineralocorticoid, aldosterone, was observed within that study, H^+,K^+-ATPase activity was measured as SCH-28080 sensitive. This inhibitor primarily targets $HK\alpha_1$-containing H^+,K^+-ATPases and has little, if any, effect on $HK\alpha_2$-containing H^+,K^+-ATPases.[229] Thus, the effect of mineralocorticoids on $HK\alpha_2$-containing H^+,K^+-ATPases was not investigated in that study. Our observations that DOCP treatment dramatically augments $HK\alpha_2$ mRNA expression in the renal medulla of mice in a dietary K^+ dependent manner suggests that mineralocorticoids stimulate $HK\alpha_2$-containing H^+,K^+-ATPases primarily as a secondary response to alterations of blood $[K^+]$. In contrast to *in vivo* studies, chronic mineralocorticoid treatment of *in vitro* cell models would not affect extracellular $[K^+]$. This may be the reason why chronic aldosterone treatment of OMCD1 cells did not affect $HK\alpha_2$ mRNA expression. Overall, these results substantiate the conclusion that

mineralocorticoids secondarily activate $HK\alpha_2$-containing H^+,K^+-ATPases to mediate K^+ reabsorption/conservation.

The increase in renal medullary $HK\alpha_2$ subunit expression in the kidney coincided with an increase in blood [HCO_3^-] in DOCP-treated WT mice. The similar time course of these two events suggests that H^+,K^+-ATPase-mediated H^+ secretion is responsible for a significant portion of the increase in blood [HCO_3^-] with mineralocorticoid excess. Most importantly, in contrast to WT and $HK\alpha_1^{-/-}$ mice, DOCP treatment did not significantly increase blood [HCO_3^-] in $HK\alpha_{1,2}^{-/-}$ mice. These data strongly support the hypothesis that $HK\alpha_2$-containing H^+,K^+-ATPases mediate the development of mineralocorticoid-induced alkalosis.

Excessive body weight gain and urinary Na^+ retention in DOCP-treated $HK\alpha_1^{-/-}$ mice and its elimination in $HK\alpha_{1,2}^{-/-}$ mice suggests that the mineralocorticoid sensitive component of urinary Na^+ and fluid reabsorption depends on the $HK\alpha_2$-containing H^+,K^+-ATPases. Precedent for such a conclusion is supported by evidence from Spicer et al. [219] showing that colonic ENaC activity is dependent on $HK\alpha_2$-containing H^+,K^+-ATPases. In that study, the colons of $HK\alpha_2^{-/-}$ mice exhibited reduced colonic amiloride-sensitive (ENaC-mediated) short circuit current compared to WT mice on a normal and dietary Na^+ restricted diet. Therefore, it is possible that urinary Na^+ loss in DOCP-treated $HK\alpha_{1,2}^{-/-}$ mice results from insufficient mineralocorticoid stimulation of renal ENaC-mediated Na^+ reabsorption.

Also, the excessive urinary K^+ and Na^+ retention observed in DOCP-treated $HK\alpha_1^{-/-}$ mice and its elimination in the $HK\alpha_{1,2}^{-/-}$ mice is consistent with a compensatory up-regulation of $HK\alpha_2$-containing H^+,K^+-ATPases in $HK\alpha_1^{-/-}$ mice. This compensatory

increase would cause greater Na^+ and fluid retention with mineralocorticoid excess. This effect may have deleterious consequences for blood pressure regulation in $HK\alpha_1^{-/-}$ mice.

The results of these studies provide evidence for an important role of the H^+,K^+-ATPases in mineralocorticoid-mediated effects on K^+, acid-base, and Na^+ balance. Future investigation into the mechanism(s) by which the renal H^+,K^+-ATPases contribute to Na^+ and fluid balance promises to shed important light on the pathogenesis of mineralocorticoid hypertension.

Table 3-1. Body weight change (%) in control and DOCP-treated WT mice

	Day 0	Day 2	Day 4	Day 6	Day 8
Control (N=7)	0 ± 0	1.2 ± 0.68	1.1 ± 1.5	3.2 ± 1.4	3.0 ± 1.8
DOCP (N=7)	0 ± 0	0.1 ± 1.20	2.0 ± 1.2	5.4 ± 1.4 [a,b]	6.1 ± 1.2 [a,b]

Data were analyzed by two-way ANOVA with repeated measures. [a] denotes P<0.05 versus Day 2 and [b] versus Day 4 within the same treatment group.

Table 3-2. Blood analysis of DOCP treatment in WT mice

	Control (N=13-14)	Day 2 (N=3-4)	Day 4 (N=4)	Day 6 (N=3)	Day 8 (N=3)
$[Na^+]$ (mM)	148.0 ± 0.41	150.0 ± 1.30	153.0 ± 1.80 [a]	153.0 ± 0.80 [a]	150.0 ± 0.41
$[K^+]$ (mM)	3.9 ± 0.08	3.5 ± 0.12	3.5 ± 0.17	2.9 ± 0.21 [a]	2.8 ± 0.07 [a,b]
$[Cl^-]$ (mM)	118.0 ± 0.51	120.0 ± 1.80	116.0 ± 0.95	117.0 ± 0.35	111.0 ± 0.82 [a,b,c,d]
$[HCO_3^-]$ (mM)	18.0 ± 0.51	19.0 ± 0.87	20.0 ± 1.20	20.0 ± 0.53	23.0 ± 2.00 [a]

Data were analyzed by one-way ANOVA. Day indicates number of days after DOCP treatment. [a] denotes P<0.05 versus Control, [b] versus Day 2, [c] versus Day 4 and [d] versus Day 6.

Table 3-3. Physiological response to high K^+ (5%) diet and DOCP (day 8) in WT mice

	Control (N=4)	DOCP (N=4)
Body weight change (%)	-2.0 ± 0.42	-0.9 ± 1.38
Blood $[Na^+]$ (mM)	149.0 ± 0.99	151.0 ± 0.88
Blood $[K^+]$ (mM)	4.3 ± 0.06	4.3 ± 0.18
Blood $[Cl^-]$ (mM)	119.0 ± 0.45	121.0 ± 1.30
Blood $[HCO_3^-]$ (mM)	17.3 ± 0.64	18.2 ± 1.01

Data were analyzed by unpaired Student's *t*-test.

Table 3-4. Differences in blood chemistry of WT and HKα null mice on a normal diet

	WT (N=13-14)	$HK\alpha_1^{-/-}$ (N=5)	$HK\alpha_{1,2}^{-/-}$ (N=9)
Blood $[Na^+]$ (mM)	148.0 ± 0.41	149.0 ± 1.1	148.0 ± 0.58
Blood $[K^+]$ (mM)	3.9 ± 0.08	3.9 ± 0.1	4.4 ± 0.17 †
Blood $[Cl^-]$ (mM)	118.0 ± 0.51	114.0 ± 1.3 †	116.0 ± 0.91
Blood $[HCO_3^-]$ (mM)	18.0 ± 0.51	21.0 ± 1.2	19.0 ± 0.69

Data were analyzed by one-way ANOVA. † denotes P<0.05 versus WT.

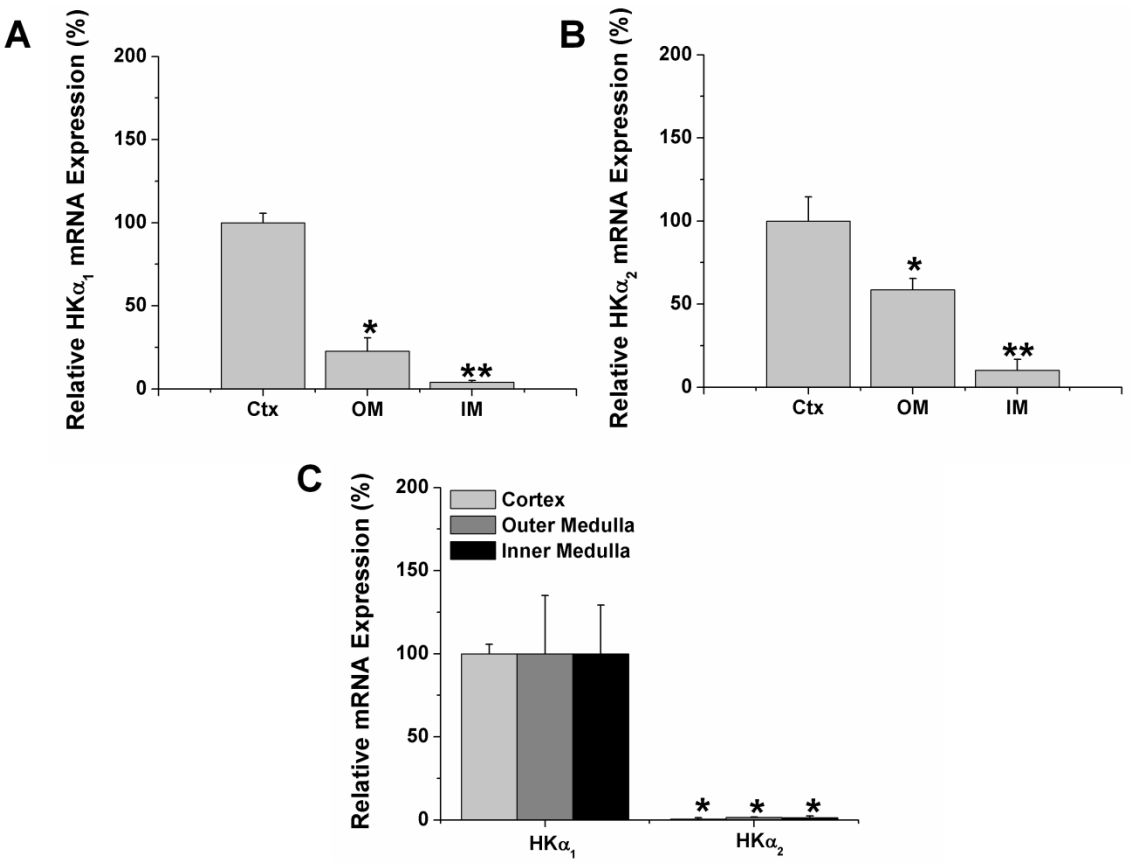

Figure 3-1. Relative mRNA expression of $HK\alpha_1$ and $HK\alpha_2$ differs in mouse kidney. Real time PCR was performed to quantify relative mRNA expression for A) $HK\alpha_1$ and B) $HK\alpha_2$ in cortex, outer medulla, and inner medulla of mice on a normal diet. C) $HK\alpha_2$ expression was compared to $HK\alpha_1$ expression in each kidney segment. Expression was set relative to β-actin. Fold changes ($2^{-\Delta\Delta Ct}$) in expression were calculated and set to %, with cortical (A and B) or $HK\alpha_1$ (C) expression set at 100%. Data are presented as mean ± SEM and analyzed by one-way ANOVA.* $P<0.05$ compared to cortex or $HK\alpha_1$ and ** compared to outer medulla; N=6.

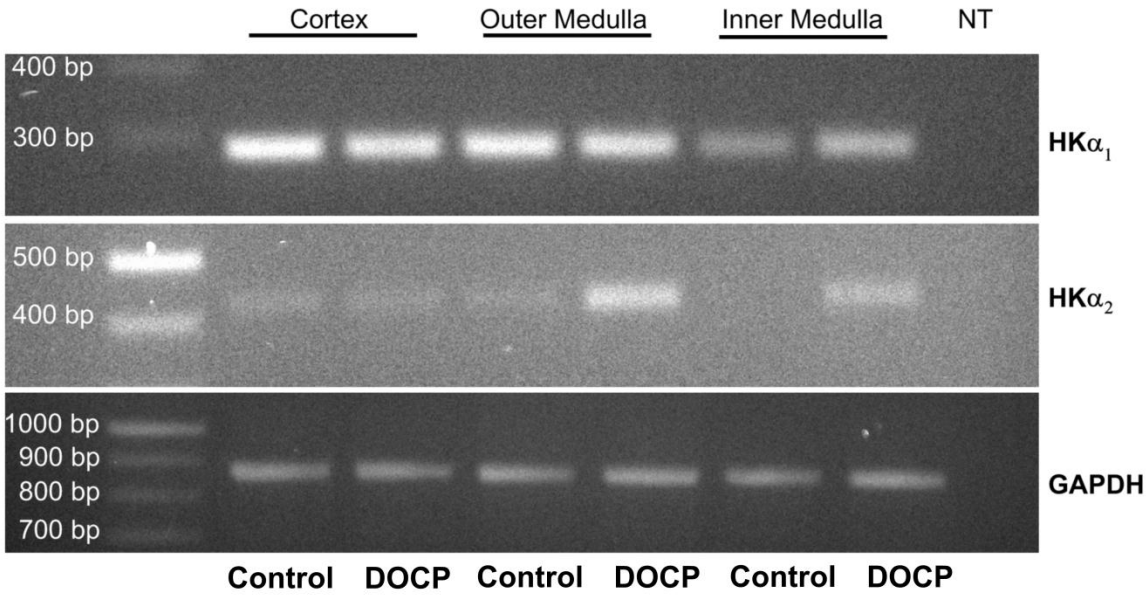

Figure 3-2. DOCP stimulated medullary HKα subunit mRNA expression in mice. Reverse transcriptase PCR (37 cycles) was used to amplify cDNA transcripts of $HK\alpha_1$ (282 bp) and $HK\alpha_2$ (471 bp) subunits in cortex, outer medulla, and inner medulla of control and DOCP-treated mice. PCR amplification of GAPDH (871 bp; 30 cycles) was used as loading control.

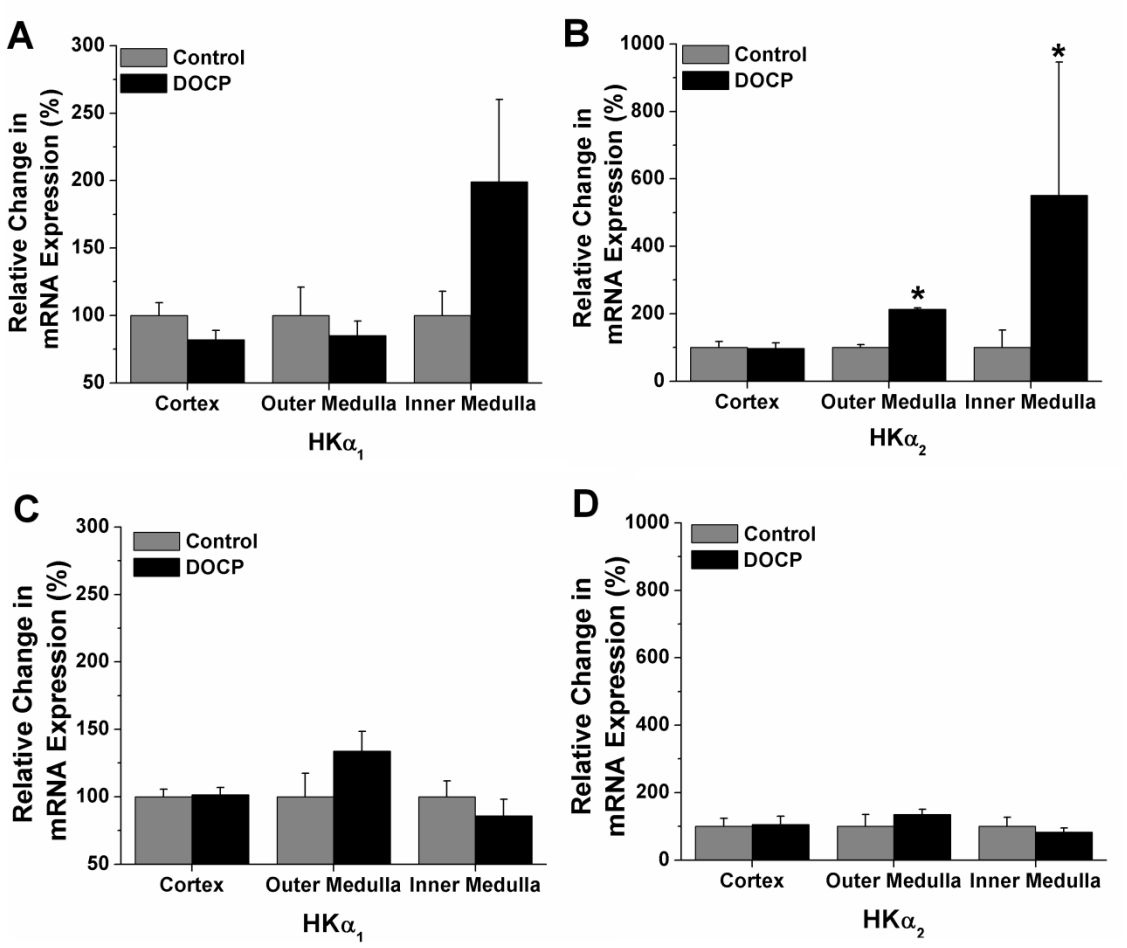

Figure 3-3. DOCP induced medullary HKα_2 expression in a K^+ dependent manner. Real time PCR was performed to quantify relative mRNA expression for A) HKα_1 and B) HKα_2 in cortex, outer medulla, and inner medulla of control mice and those treated with DOCP for eight days on a normal diet. Relative mRNA expression was also determined for C) HKα_1 and D) HKα_2 in cortex, outer medulla, and inner medulla of control and DOCP-treated mice on a high K^+ (5%) diet. Expression was set relative to β-actin. Fold changes ($2^{-\Delta\Delta Ct}$) in expression were calculated and set to %, with control set at 100%. Data are presented as mean ± SEM and expression with DOCP treatment was compared to control levels by Student's *t*-test. * $P<0.05$ compared to control; N=7-10 for normal diet and N=4 for high K^+ diet.

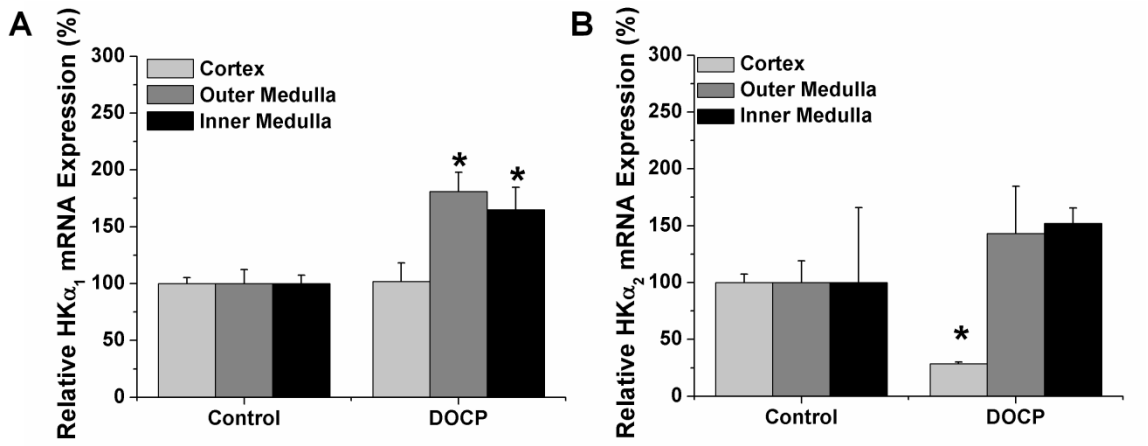

Figure 3-4. The effect of DOCP to alter HKα subunit mRNA expression is time-dependent. Real time PCR was performed to quantify relative mRNA expression for A) $HK\alpha_1$ and B) $HK\alpha_2$ in cortex, outer medulla, and inner medulla of control and DOCP-treated (day 6) mice fed a normal diet. Expression was set relative to β-actin. Fold changes ($2^{-\Delta\Delta Ct}$) in expression were calculated and set to %, with control set at 100%. Data are presented as mean ± SEM and expression with DOCP treatment was compared to control levels by Student's *t*-test. * $P<0.05$ compared to control; N=4.

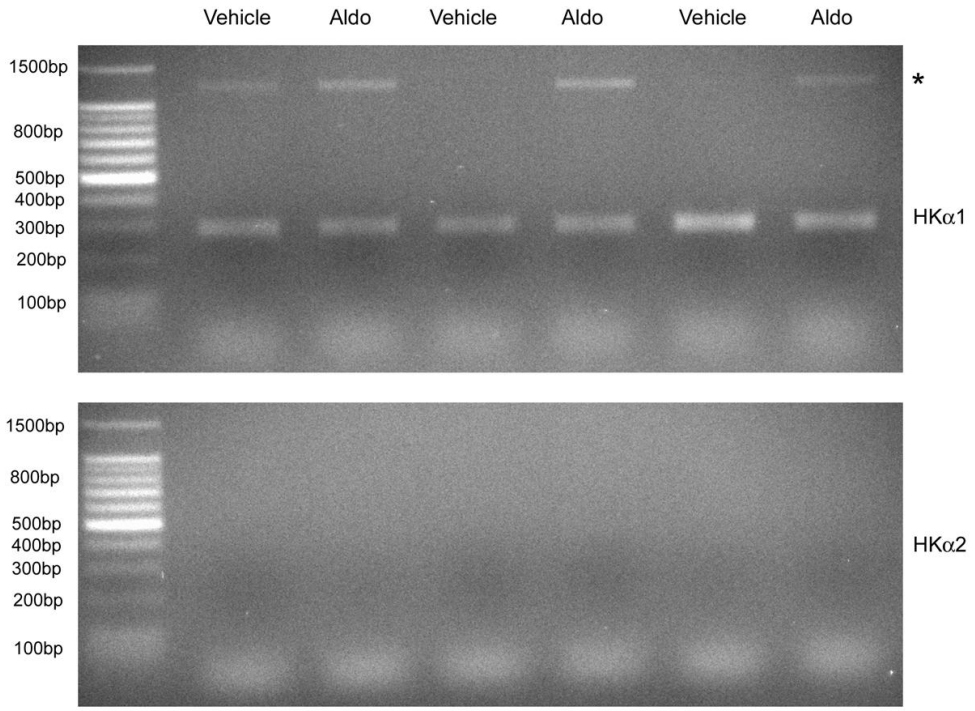

Figure 3-5. Chronic aldosterone treatment did not affect HKα subunit expression in OMCD1 cells. Reverse transcriptase PCR was used to amplify cDNA transcripts of $HK\alpha_1$ (282 bp) and $HK\alpha_2$ (471 bp) subunits in OMCD1 cells treated with vehicle (ethanol) or aldosterone (Aldo, 1µM) daily for 7 days. * designates genomic amplification.

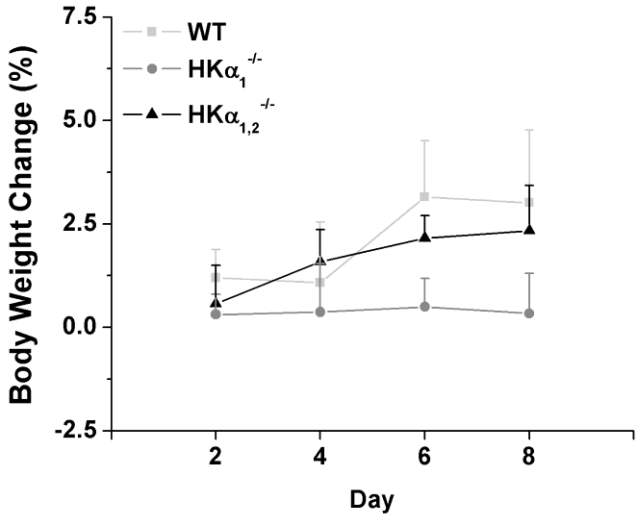

Figure 3-6. WT, $HK\alpha_1^{-/-}$, and $HK\alpha_{1,2}^{-/-}$ mice had similar body weight gain over eight days on a normal diet. Body weight change (%) is shown as the difference from starting body weight (day zero). Data are shown as mean ± SEM and were analyzed by one-way repeated measure ANOVA. N=5-7.

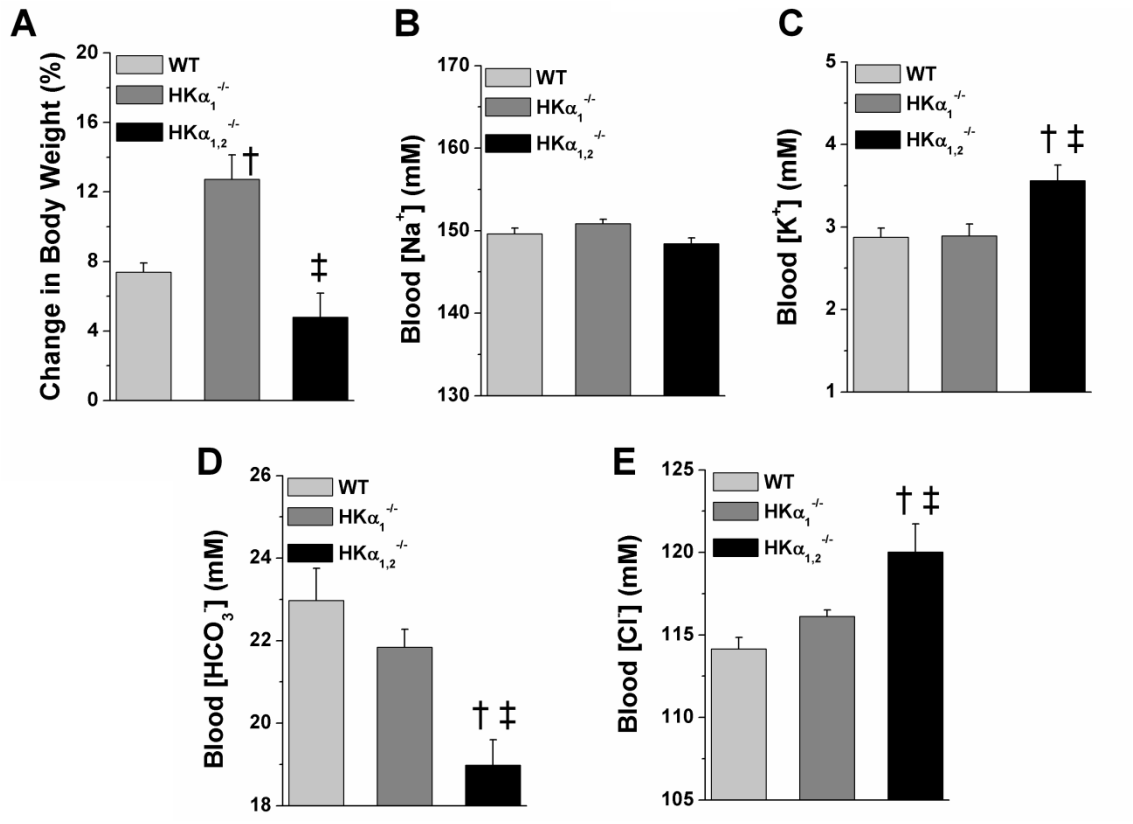

Figure 3-7. Body weight and blood chemistries differ in DOCP-treated WT, $HK\alpha_1^{-/-}$ and $HK\alpha_{1,2}^{-/-}$ mice. All data shown are from the eighth day of DOCP treatment. A) Body weight change (%) is shown as the percent change in body weight from day zero. Arterial blood samples were collected from the aorta and B) blood $[Na^+]$, C) $[K^+]$, D) $[HCO_3^-]$ and E) $[Cl^-]$,were measured on a clinical blood gas analyzer. Data are presented as mean ± SEM and were analyzed by one-way ANOVA followed by post-hoc Student-Newman-Keuls test. † $P<0.05$ compared to WT and ‡ compared to $HK\alpha_1^{-/-}$ mice. N=10-11 WT and N=5 $HK\alpha_1^{-/-}$ and $HK\alpha_{1,2}^{-/-}$ mice.

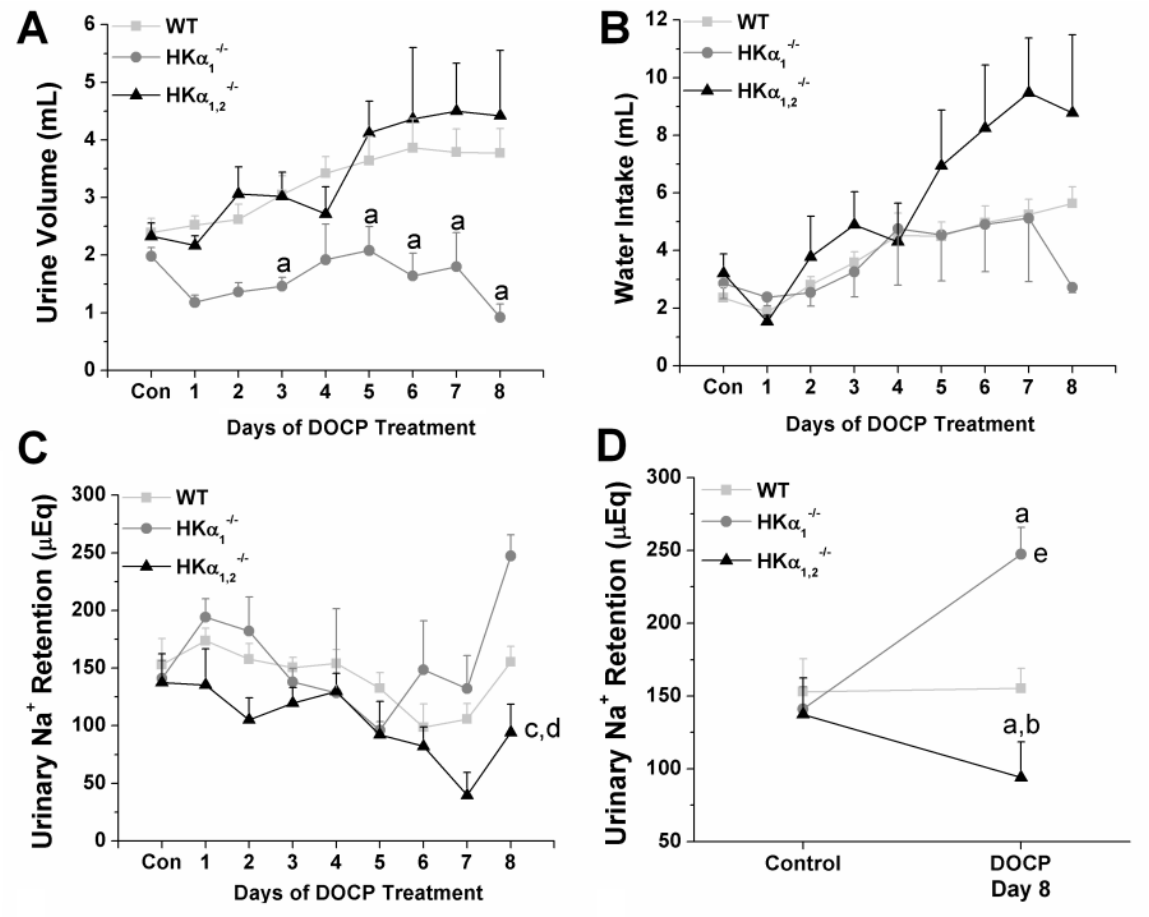

Figure 3-8. DOCP treatment differentially altered urinary Na^+ and K^+ retention in WT and HKα null mice. A) Urinary volume, B) H_2O intake, and C-D) urinary Na^+ and E-F) K^+ retention were measured in WT, $HK\alpha_1^{-/-}$ and $HK\alpha_{1,2}^{-/-}$ mice from the day preceding treatment (Con) and over an eight day period of DOCP treatment. Urinary electrolyte retention (µEq) was calculated as the urinary excretion per day subtracted from dietary intake on that day. All data were analyzed by a two-way repeated measure ANOVA with post hoc Student-Newman-Keuls test and are shown as mean ± SEM. [a] denotes $P<0.05$ versus WT and [b] versus $HK\alpha_1^{-/-}$ mice on the same day. [c] denotes $P<0.05$ versus WT and [d] versus $HK\alpha_1^{-/-}$ mice over the entire time course. [e] denotes $P<0.05$ versus control. WT, N=10; $HK\alpha_1^{-/-}$, N=5; $HK\alpha_{1,2}^{-/-}$, N=5.

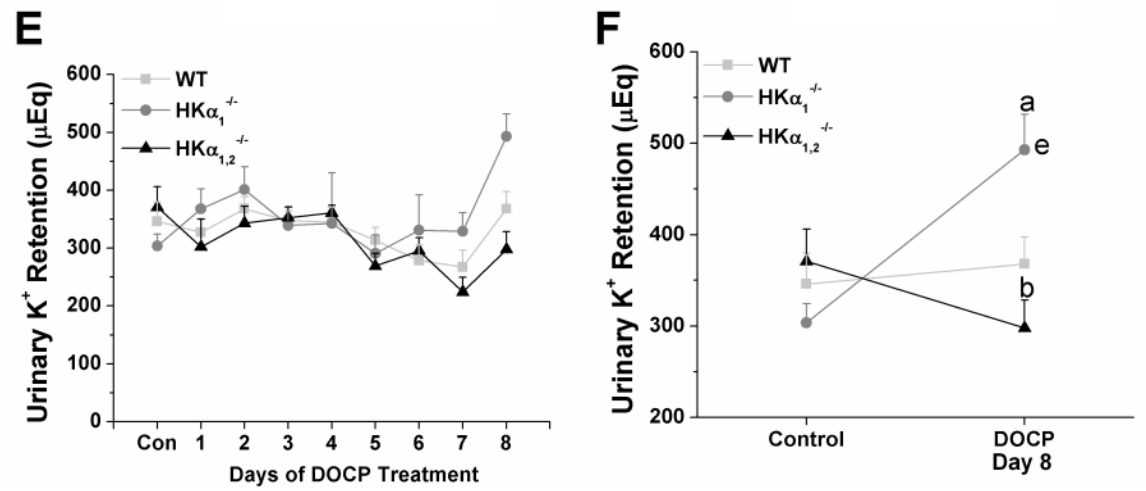

Figure 3-8. Continued

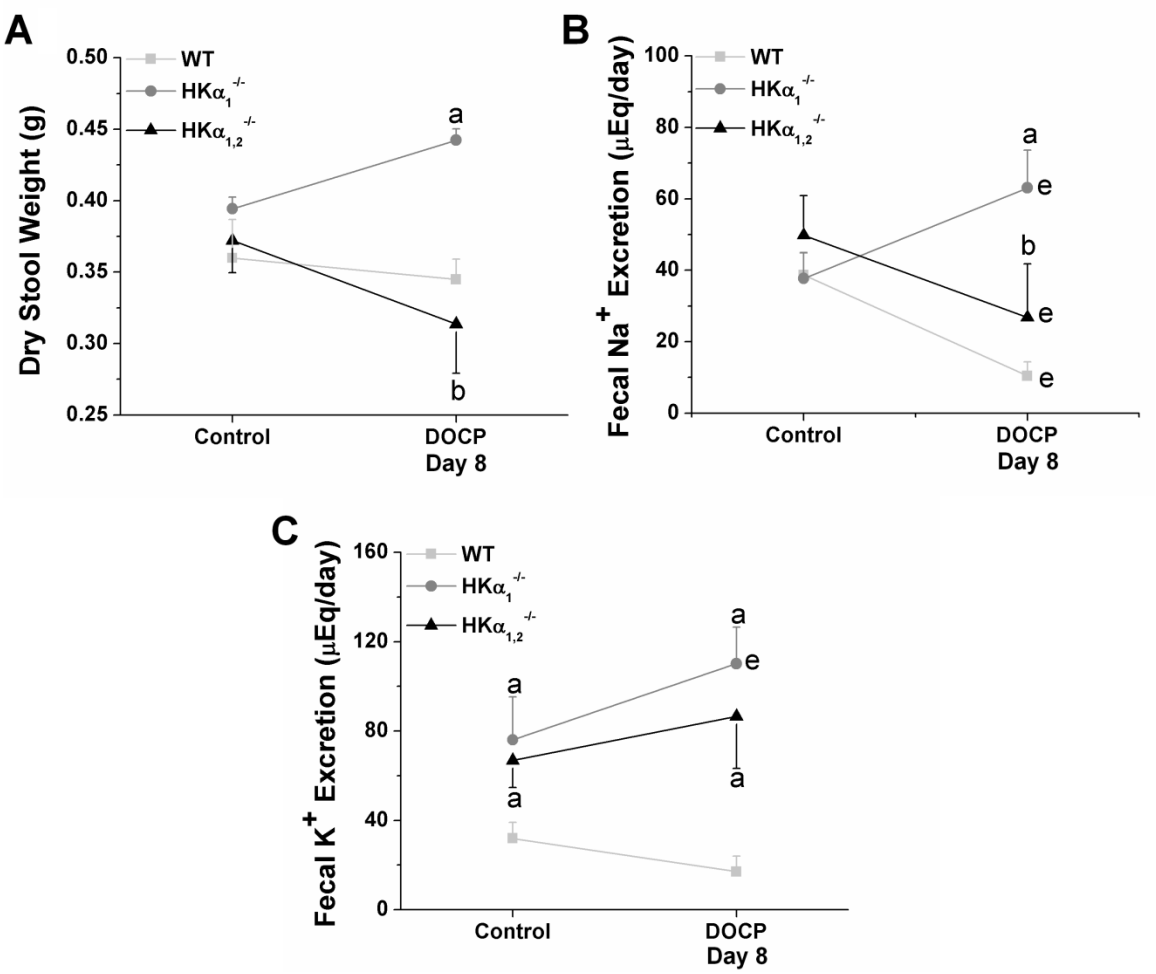

Figure 3-9. Control and DOCP-treated WT and HKα null mice exhibited altered fecal electrolyte excretion. A) Fecal output, B) Na^+, and C) K^+ excretion were measured in WT, $HK\alpha_1^{-/-}$, and $HK\alpha_{1,2}^{-/-}$ mice on the day preceding treatment (control) and on day eight of DOCP treatment. Data are shown as mean ± SEM. and were analyzed by two-way repeated measure ANOVA with post hoc Student-Newman-Keuls test. [a] denotes $P<0.05$ versus WT and [b] versus $HK\alpha_1^{-/-}$ mice on the same day. [e] denotes $P<0.05$ versus control in the same genotype. WT, N=11; $HK\alpha_1^{-/-}$, N=4; $HK\alpha_{1,2}^{-/-}$, N=5-6.

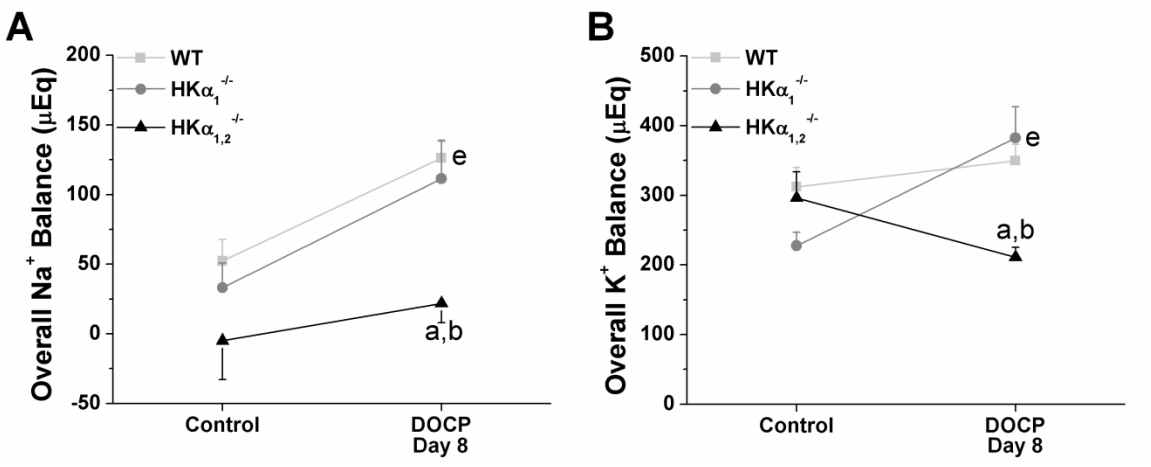

Figure 3-10. HKα null mice display disturbances in overall electrolyte balance with DOCP treatment. Overall A) Na^+ and B) K^+ balance (µEq) are shown for WT, $HK\alpha_1^{-/-}$, and $HK\alpha_{1,2}^{-/-}$ mice on the day preceding treatment (control) and on day eight of DOCP treatment. Overall electrolyte balance was calculated as the sum of urinary and fecal excretion subtracted from dietary intake. Data are shown as mean ± SEM and were analyzed by two-way repeated measure ANOVA with post hoc Student-Newman-Keuls test or one-way repeated measure ANOVA with post-hoc Tukey test. [a] denotes $P<0.05$ versus WT and [b] versus $HK\alpha_1^{-/-}$ mice on the same day. [e] denotes $P<0.05$ versus control in the same genotype.. WT, N=10; $HK\alpha_1^{-/-}$, N=4; $HK\alpha_{1,2}^{-/-}$, N=5.

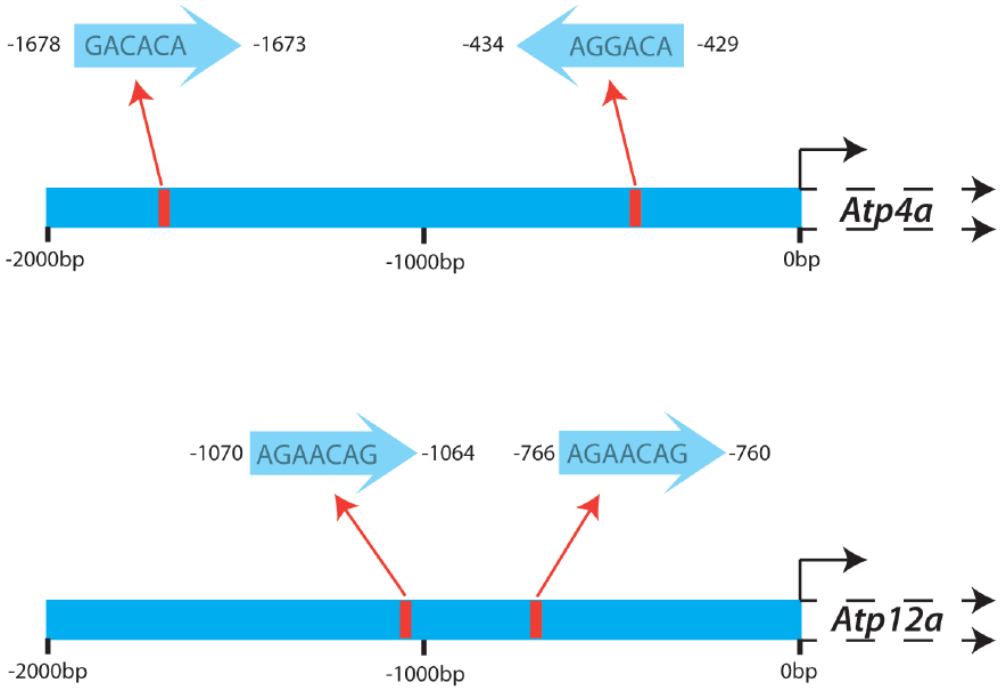

Figure 3-11. Putative HRE half sites are present in *Atp4a* and *Atp12a* promoters. Two separate transcription factor binding algorithms (TESS and TF Search) were used to detect prospective HRE half sites in the *Atp4a* and *Atp12a* promoters. Zero bp indicates the transcription start site. Blue arrows represent potential binding direction.

CHAPTER 4
DIETARY POTASSIUM DEPLETION IN HKA NULL MICE

Our previous study demonstrated that the mineralocorticoid, DOCP, chronically stimulates renal $HK\alpha_2$ expression and a high K^+ diet abolishes this effect. Our observations also suggest that $HK\alpha_2$-containing H^+,K^+-ATPases mediate the effects of DOCP to cause metabolic alkalosis and urinary Na^+ retention. Similar to the effect of DOCP, chronic low dietary K^+ intake causes hypokalemia and metabolic alkalosis.[230] Low dietary K^+ is known to stimulate the activity of renal and colonic H^+,K^+-ATPases, suggesting their importance in K^+ conservation during this dietary challenge.[133, 135, 231] $HK\alpha_2$ mRNA and protein expression are specifically and dramatically increased with dietary K^+ depletion in both the kidney and colon. [181, 187, 232, 233] One study has reported that renal cortical $HK\alpha_1$ mRNA expression also increases with dietary K^+ depletion.[190] $HK\alpha_2^{-/-}$ mice exhibit severe hypokalemia with dietary K^+ restriction, indicating that $HK\alpha_2$-containing H^+,K^+-ATPases are physiologically important for K^+ conservation. [218] However, this effect of dietary K^+ depletion in $HK\alpha_2^{-/-}$ mice is a result of fecal, not urinary, K^+ loss.

Chronic low dietary K^+ intake also causes urinary Na^+ retention similar to mineralocorticoids. [221, 234] It is plausible then that the renal H^+,K^+-ATPases are responsible for K^+ depletion-induced urinary Na^+ retention. However, $HK\alpha_2^{-/-}$ mice do not exhibit altered urinary or fecal Na^+ excretion when fed a K^+ depleted diet.[218] Nevertheless, the marked increase in urinary Na^+ retention observed with dietary K^+ depletion may well involve both the $HK\alpha_1$- and $HK\alpha_2$-containing H^+,K^+-ATPases. The single knockout may not be insufficient to elicit a significant renal phenotype.

With dietary K^+ depletion, the increased H^+,K^+-ATPase activity would not only result in K^+ reabsorption but also H^+ secretion. Therefore, the renal H^+,K^+-ATPases may be the mechanism responsible for greater distal nephron H^+ secretion [235] and resultant metabolic alkalosis of dietary K^+ depletion. [230] Renal H^+,K^+-ATPases may also be the mechanism responsible for the exacerbated urinary acidification and dramatic metabolic alkalosis of dietary K^+ restriction combined with mineralocorticoid excess. [236, 237] Nonetheless, $HK\alpha_2^{-/-}$ mice do not display any abnormality in plasma acid-base parameters when fed a low K^+ diet.[218]

Experiments performed in $HK\alpha_2^{-/-}$ mice suggest that renal $HK\alpha_2$-containing H^+,K^+-ATPases are not alone required for urinary K^+ conservation, the development of metabolic alkalosis, or the stimulation of urinary Na^+ retention observed with dietary K^+ depletion. The remaining $HK\alpha_1$ subunit in the $HK\alpha_2^{-/-}$ mice may maintain normal renal K^+, Na^+, and H^+ handling. For that reason, we investigated whether $HK\alpha_1^{-/-}$ or $HK\alpha_{1,2}^{-/-}$ mice displayed dysfunctional urinary K^+, Na^+, and acid-base handling with dietary K^+ depletion. We also examined whether $HK\alpha_1^{-/-}$ or $HK\alpha_{1,2}^{-/-}$ mice displayed altered systemic Na^+, K^+, and acid-base balance with combined dietary K^+ depletion and DOCP treatment.

Results

Dietary K^+ Depletion in HKα Null Mice

Previous studies have demonstrated a dramatic loss of body weight in the dietary K^+ depleted $HK\alpha_2^{-/-}$ mice. [218] If $HK\alpha_1$ partially compensated for loss of $HK\alpha_2$, then $HK\alpha_{1,2}^{-/-}$ mice would be expected to display exacerbated body weight loss with dietary K^+ depletion. Changes in body weight in WT and $HK\alpha_{1,2}^{-/-}$ fed either a normal or K^+ depleted diet were followed for 8 days (Figure 4-1). No significant differences in body

weight change were observed between WT and $HK\alpha_{1,2}^{-/-}$ mice on a normal gel diet for 8 days. Food intake was not significantly different between WT and $HK\alpha_{1,2}^{-/-}$ mice fed the normal gel diet (10.2 ± 0.69 g versus 12.3 ± 0.66 g, respectively). Dietary K^+ depletion caused an ~ 5% loss in body weight in WT mice. Body weight loss was two-fold greater in $HK\alpha_{1,2}^{-/-}$ mice. The differences in body weight loss are comparable to previous observations in $HK\alpha_2^{-/-}$ mice. [218] Decreased food intake did not account for this drop in body weight as WT and $HK\alpha_{1,2}^{-/-}$ mice displayed similar food intake (11.5 ± 0.82 g and 10.9 ± 0.68 g, respectively).

To assess the effect of H^+,K^+-ATPase knockout on K^+ homeostasis, blood $[K^+]$ was measured in WT and $HK\alpha_{1,2}^{-/-}$ mice fed either a normal or K^+ depleted diet for 8 days. Blood $[K^+]$ was similar in WT and $HK\alpha_{1,2}^{-/-}$ mice fed a normal diet (Figure 4-2 A). Although dietary K^+ depletion led to hypokalemia in both WT and the double knockout mice, the reduction in blood $[K^+]$ was an additional 1mM in $HK\alpha_{1,2}^{-/-}$ mice. In a separate experiment, we examined the effect of dietary K^+ depletion on blood $[K^+]$ in $HK\alpha_1^{-/-}$ mice. In contrast to the results from $HK\alpha_{1,2}^{-/-}$ mice, the drop in blood $[K^+]$ in $HK\alpha_1^{-/-}$ mice was not significantly different from that of WT mice (Table 4-1).

We next determined if the reduced blood $[K^+]$ observed in $HK\alpha_{1,2}^{-/-}$ mice resulted from urinary or fecal K^+ loss. Urinary K^+ retention was calculated as daily dietary K^+ intake minus the daily urinary K^+ excretion. Urinary K^+ retention was identical in WT and $HK\alpha_{1,2}^{-/-}$ mice provided a normal diet (Figure 4-2 B). By day 8 of dietary K^+ depletion, both the WT and $HK\alpha_{1,2}^{-/-}$ mice reduced urinary K^+ excretion to almost undetectable levels when measured with ion-sensitive electrodes. Therefore, we also measured urine

[K^+] by flame photometer. Surprisingly, $HK\alpha_{1,2}^{-/-}$ mice exhibited slightly greater urinary K^+ retention than WT mice on day 8 of dietary K^+ depletion (Figure 4-2 C).

Fecal K^+ wasting was quite apparent in $HK\alpha_{1,2}^{-/-}$ mice (Figure 4-2 D). $HK\alpha_{1,2}^{-/-}$ mice excreted nearly 4 times more fecal K^+ than WT mice on a normal diet. Fecal K^+ output decreased with dietary K^+ depletion in both genotypes (Figure 4-2 D) but was still as much as 7 times greater in $HK\alpha_{1,2}^{-/-}$ mice than WT mice by day 8 of K^+ depletion.

To determine whether H^+,K^+-ATPases are required for increased Na^+ and fluid retention with dietary K^+ depletion, urinary Na^+ retention and urine volume were compared between WT and $HK\alpha_{1,2}^{-/-}$ mice on day 8 of a normal or K^+ depleted diet. Urinary Na^+ retention was calculated as dietary Na^+ intake minus urinary Na^+ excretion. Dietary K^+ depletion stimulated urinary Na^+ retention to a similar extent in both WT and $HK\alpha_{1,2}^{-/-}$ mice (Figure 4-3 A). However, urine volume was significantly more in $HK\alpha_{1,2}^{-/-}$ mice than in WT mice fed a normal or K^+ depleted diet (Figure 4-3B).

To determine if $HK\alpha_{1,2}^{-/-}$ mice displayed excess urinary K^+ or Na^+ loss during the earlier stages of dietary K^+ depletion, urine K^+ and Na^+ retention were compared in pair fed WT and $HK\alpha_{1,2}^{-/-}$ mice given a normal diet for 4 days then switched to a K^+ depleted diet for 4 days. Urinary K^+ retention was similar in WT and $HK\alpha_{1,2}^{-/-}$ mice over the time course (Figure 4-4 A). Urinary Na^+ retention was also similar between the genotypes (Figure 4-4 B).

To test the hypothesis that renal H^+,K^+-ATPases mediate K^+ depletion-induced metabolic alkalosis, acid-base homeostasis was compared in WT and $HK\alpha_{1,2}^{-/-}$ mice during dietary K^+ depletion. Blood [HCO_3^-] and net urinary acid excretion were measured in WT and $HK\alpha_{1,2}^{-/-}$ mice fed either a normal or K^+ deplete diet for 8 days.

Blood [HCO_3^-] was similar in WT and $HK\alpha_{1,2}^{-/-}$ mice when fed a normal diet (Figure 4-5 A). Under normal dietary conditions, $HK\alpha_{1,2}^{-/-}$ mice displayed a surprisingly more acidic urine pH than WT mice (Figure 4-5 B). Consistent with urine pH results, $HK\alpha_{1,2}^{-/-}$ mice excreted nearly twice the urinary NH_4^+ and 60 times more urinary titratable acid than WT mice (Figure 4-5 C and D, respectively). Net urinary acid excretion, calculated as the sum of urinary NH_4^+ and titratable acid excretion, was nearly 3-fold greater in $HK\alpha_{1,2}^{-/-}$ mice compared to WT mice fed a normal diet (Figure 4-5 E).

Dietary K^+ depletion did not significantly affect blood [HCO_3^-] in WT or $HK\alpha_{1,2}^{-/-}$ mice (Figure 4-5 A). Urine alkalinized with dietary K^+ depletion in $HK\alpha_{1,2}^{-/-}$ mice but not in WT mice (Figure 4-5 B). Urine NH_4^+ excretion increased and titratable acidity decreased in mice from both genotypes fed a K^+ depleted diet (Figure 4-5 C and D, respectively). However, titratable acidity was still significantly greater in $HK\alpha_{1,2}^{-/-}$ mice compared to WT. Overall, net urinary acid excretion was not significantly different between K^+ depleted WT and double knockout mice (Figure 4-5 E).

To determine if the more acidic urine pH of $HK\alpha_{1,2}^{-/-}$ mice under normal conditions was a result of knockout of $HK\alpha_1$ or $HK\alpha_2$, urine pH was measured in $HK\alpha_1^{-/-}$ mice fed a normal gel diet. Similar to $HK\alpha_{1,2}^{-/-}$ mice, $HK\alpha_1^{-/-}$ mice exhibited a more acidic urine pH than WT mice (Figure 4-6). These data indicate that knockout of $HK\alpha_1$ in mice results in enhanced urine acidification.

Expression of Renal Acid-Base Transporters in HKα Null Mice

The paradoxical augmentation of urinary acid excretion in $HK\alpha_{1,2}^{-/-}$ mice warranted further examination of compensatory changes in acid-base transport in the kidney. Therefore, we examined the mRNA expression levels of several renal acid-base transporters using real time PCR. Expression levels of the majority of acid-base

transporters examined were unaltered in $HK\alpha_{1,2}^{-/-}$ mice compared to WT mice (Table 4-2). However, medullary mRNA expression of AE1 was ~30% greater in $HK\alpha_{1,2}^{-/-}$ mice. Also, cortical expression of NHE3 was roughly 40% less in $HK\alpha_{1,2}^{-/-}$ mice compared to WT.

We assume that increased AE1 expression corresponds to greater AE1-mediated HCO_3^- reabsorption in $HK\alpha_{1,2}^{-/-}$ mice and increased H^+-ATPase activity would be expected to accompany the stimulation of AE1 activity. However, we did not observe significantly increased H^+-ATPase B_1 or a_4 subunit mRNA expression levels in $HK\alpha_{1,2}^{-/-}$ mice (Table 4-2). Stimulation of H^+-ATPase activity appears to primarily occur via post-translational mechanisms, including trafficking to the plasma membrane. Therefore, we also examined plasma membrane protein expression of H^+-ATPase B1/B2 in cortex and medulla from WT, $HK\alpha_1^{-/-}$ and $HK\alpha_{1,2}^{-/-}$ mice fed normal lab chow (Figure 4-7). Although it is only an N of 2, striking qualitative differences between the genotypes were not obvious.

Dietary K^+ Depletion and Mineralocorticoid Excess in HKα Null Mice

The next experiments investigated whether either or both of the renal $HK\alpha_1$- and $HK\alpha_2$-containing H^+,K^+-ATPases were responsible for the exacerbation of metabolic alkalosis with combined dietary K^+ depletion and mineralocorticoid excess. WT, $HK\alpha_1^{-/-}$ and $HK\alpha_{1,2}^{-/-}$ mice were fed a normal gel diet for three days then switched to a K^+ depleted gel diet for eight days. Half the animals in each genotype were also treated with DOCP at the start of the K^+ depleted diet. Body weight and food intake were compared over the entire time course. Total kidney weight and blood chemistries were measured on the last day of the experiment.

Our previous results showed that $HK\alpha_{1,2}^{-/-}$ mice lost more body weight with dietary K^+ depletion than WT mice. Dietary K^+ depletion combined with DOCP treatment caused a substantially greater loss of body weight in $HK\alpha_{1,2}^{-/-}$ mice compared to dietary K^+ depletion alone (Figure 4-8 A). This effect was not observed in WT or $HK\alpha_1^{-/-}$ mice. Despite the body weight loss of $HK\alpha_{1,2}^{-/-}$ mice, food intake was similar in WT and $HK\alpha_{1,2}^{-/-}$ mice on a K^+ depleted diet (Figure 4-8 B). However, DOCP-treated $HK\alpha_1^{-/-}$ mice exhibited significantly greater food intake than DOCP-treated WT mice over the entire time course. Significant renal hypertrophy was observed in $HK\alpha_{1,2}^{-/-}$ mice fed a K^+ depleted diet (Figure 4-8 C). This effect was exacerbated with DOCP treatment.

DOCP treatment and dietary K^+ depletion reduced blood $[K^+]$ an additional 1mM compared to dietary K^+ depletion alone in each genotype (Figure 4-9 A). Eight days of dietary K^+ depletion did not increase blood $[HCO_3^-]$ in mice from any genotype (Figure 4-9 B). However, dietary K^+ depletion and DOCP treatment caused an ~5mM increase in blood $[HCO_3^-]$ in WT mice. Surprisingly, DOCP treatment in K^+ depleted $HK\alpha_{1,2}^{-/-}$ mice caused an even more severe increase in blood $[HCO_3^-]$ of ~15mM. The $HK\alpha_{1,2}^{-/-}$ mice exhibited a reciprocal decrease in blood $[Cl^-]$ (Figure 4-9 C). $HK\alpha_{1,2}^{-/-}$ mice also displayed greater blood $[Na^+]$ than WT or $HK\alpha_1^{-/-}$ mice on a K^+ depleted diet (Figure 4-9 D), indicating fluid volume loss and dehydration. Hematocrit was greater in both $HK\alpha_1^{-/-}$ and $HK\alpha_{1,2}^{-/-}$ mice compared to WT with dietary K^+ depletion alone (Figure 4-9 E), also indicating dehydration.

Discussion

In this study, we investigated the effect of dietary K^+ depletion in WT, $HK\alpha_1^{-/-}$ and $HK\alpha_{1,2}^{-/-}$ mice. Dietary K^+ depletion caused worse hypokalemia in $HK\alpha_{1,2}^{-/-}$ mice than WT or $HK\alpha_1^{-/-}$ mice, indicating that $HK\alpha_2$-containing H^+,K^+-ATPases are required for K^+

conservation. However, significant urinary K^+ loss did not occur in $HK\alpha_{1,2}^{-/-}$ mice. Fecal K^+ loss was apparent in the double knockouts under normal and dietary K^+ depleted conditions, similar to observations in $HK\alpha_2^{-/-}$ mice.[218, 219] The data indicate that only the colonic $HK\alpha_2$-containing H^+,K^+-ATPases are required for K^+ conservation with dietary K^+ depletion. Renal $HK\alpha_2$-containing H^+,K^+-ATPases are also not required for K^+ depletion-induced urinary Na^+ retention. The observation that $HK\alpha_1^{-/-}$ and $HK\alpha_{1,2}^{-/-}$ mice have a more acidic urine pH suggests that knockout of $HK\alpha_1$-containing H^+,K^+-ATPases, either in the kidney or other tissues, affects urinary acid excretion. The mechanism for this is still unclear. In contrast to our expectations, DOCP-treated $HK\alpha_{1,2}^{-/-}$ mice fed a K^+ depleted diet displayed a remarkably severe metabolic alkalosis. The data suggest that renal H^+,K^+-ATPases play completely different roles during mineralocorticoid excess in the presence and absence of dietary K^+. The hypernatremia observed in DOCP-treated $HK\alpha_{1,2}^{-/-}$ mice fed a K^+ depleted diet also suggests that the renal H^+,K^+-ATPases are important in fluid volume homeostasis under this condition.

Considerable evidence has suggested that H^+,K^+-ATPases and, more specifically, $HK\alpha_2$- containing H^+,K^+-ATPases mediate K^+ reabsorption in the collecting duct and the colon.[86, 87] Therefore, we expected that $HK\alpha_{1,2}^{-/-}$ mice would display a more severe hypokalemia than WT or $HK\alpha_1^{-/-}$ mice when fed a K^+ depleted diet. The excessive fecal K^+ wasting of $HK\alpha_{1,2}^{-/-}$ mice indicates that colonic $HK\alpha_2$-containing H^+,K^+-ATPases facilitate K^+ conservation under K^+ depleted conditions. Our observation that urinary K^+ conservation is intact in $HK\alpha_{1,2}^{-/-}$ mice suggests that other mechanisms in the kidney, such as shutdown of K^+ secretion, compensate for the lack of

H^+,K^+-ATPase-mediated K^+ reabsorption or that renal H^+,K^+-ATPases do not contribute to net K^+ reabsorption *in vivo* under normal physiological conditions.

Our previous studies show that mineralocorticoids do not cause urinary Na^+ retention in $HK\alpha_{1,2}^{-/-}$ mice. We hypothesized that the urinary Na^+ retention of dietary K^+ depletion would also be dependent on the renal H^+,K^+-ATPases. However, dietary K^+ depletion-induced Na^+ retention was intact in $HK\alpha_{1,2}^{-/-}$ mice. The differences in the urinary Na retention of $HK\alpha_{1,2}^{-/-}$ mice during mineralocorticoid excess and dietary K^+ depletion are possibly related to differences in mineralocorticoid status and the activation of ENaC-mediated Na^+ reabsorption. In contrast to mineralocorticoid excess which is accepted to stimulate urinary Na^+ reabsorption through ENaC, dietary K^+ depletion-induced urinary Na^+ retention may be independent of ENaC. First, dietary K^+ depletion is known to be low mineralocorticoid state. [238] Second, ENaC subunit plasma membrane protein abundance in the cortical collecting duct has been shown to change in proportion to dietary K^+ intake.[239] In particular, a low K^+ diet decreases plasma membrane abundance of ENaC subunits. Therefore, it is plausible that the low mineralocorticoid state of low dietary K^+ intake shuts down H^+,K^+-ATPase-dependent (ENaC-mediated) Na^+ reabsorption by the collecting duct and dissociates Na^+ retention from the renal H^+,K^+-ATPases.

Contrary to dietary K^+ depletion alone, dietary K^+ depletion combined with DOCP treatment would be expected to increase ENaC expression and activity in the collecting duct. The hypernatremia, greater blood hematocrit, and body weight loss of DOCP-treated $HK\alpha_{1,2}^{-/-}$ mice fed a K^+ depleted diet indicates an inability to retain Na^+ or

H_2O. Whether this relates to altered ENaC activity and urinary Na^+ or H_2O retention needs to be addressed.

The striking metabolic alkalosis observed in $HK\alpha_{1,2}^{-/-}$ mice fed a K^+ depleted diet and treated with DOCP is yet unexplained. Whether this effect stems from a gastrointestinal or renal H^+ loss in the $HK\alpha_{1,2}^{-/-}$ mice should be investigated. The metabolic alkalosis possibly results from inactivation of pendrin-mediated Cl^- reabsorption and HCO_3^- secretion. [121, 122] Additional experiments are needed to clarify the involvement of renal H^+,K^+-ATPases in the effects of dietary K^+ depletion with mineralocorticoid excess.

Many other acid secreting mechanisms are present in the nephron and collecting duct (reviewed by Wagner et al. [36]) that may compensate for knockout of renal H^+,K^+-ATPases. Our examination of mRNA expression levels for several acid-base transporters in kidneys from $HK\alpha_{1,2}^{-/-}$ mice revealed the anion exchanger 1 (AE1) as the only likely candidate. However, the change in expression of this transporter (30%) was not dramatic. Excessive activity of medullary AE1 in conjunction with an apical H^+ secretion mechanism could help explain, at least in part, the more acidic urine of $HK\alpha_1$ null mice. One study has shown that outer medullary collecting ducts of $HK\alpha_1^{-/-}$ mice possessed greater H^+-ATPase-mediated H^+ secretion and apical polarity of this transporter than WT mice. [240] Using immunogold localization, we have not observed increased H^+-ATPase localization to the apical plasma membrane of ICs in $HK\alpha_1^{-/-}$ compared to WT mice fed a normal diet (Verlander et al. Unpublished observations).

Nevertheless, one expects compensatory stimulation of the H^+-ATPase in $HK\alpha_1$ null mice to only maintain normal urinary acidification. The greater net urinary acid

excretion observed in $HK\alpha_1$ null mice is surprising. The potential of reduced gastric acid secretion in the $HK\alpha_1$ null mice to affect urinary acid excretion cannot be ignored. Pancreatic HCO_3^- secretion buffers gastric acid secretion in response to an acidic environment (for a review of gastrointestinal acid-base transporters see reference [241]). However, acid-independent release of pancreatic HCO_3^- can occur in response to gastrin-releasing peptide. [242] Interestingly, $HK\alpha_1^{-/-}$ mice displayed significantly elevated levels of gastric and serum gastrin [213], suggesting that gastrin-releasing peptide levels maybe elevated. Increased levels of gastrin-releasing peptide in $HK\alpha_1^{-/-}$ mice, if present, would be expected to cause excessive pancreatic HCO_3^- secretion with subsequent stool HCO_3^- loss. This net alkali deficit would lead to metabolic acidosis. However, there are other renal mechanisms for excretion of the remaining acid load. Therefore, this may be one mechanism for the acidic urine of $HK\alpha_1^{-/-}$ mice.

In conclusion, the role of the renal H^+,K^+-ATPases in urinary K^+ conservation and acidification with dietary K^+ depletion remains unclear. Tissue-specific knockout mice are needed to more fully understand the role of the renal H^+,K^+-ATPases independent from the role of the gastrointestinal H^+,K^+-ATPases. This is especially important to decipher the role of renal H^+,K^+-ATPases in urinary acid excretion under normal and K^+ depleted dietary conditions.

Table 4-1. Blood chemistries for WT and $HK\alpha_1^{-/-}$ mice on a K^+ depleted diet.

	WT (N=4)	$HK\alpha_1^{-/-}$ (N=4)	
$[Na^+]$, mM	147.0 ± 0.48	148.0 ± 0.47	
$[K^+]$, mM	3.9 ± 0.10	3.8 ± 0.18	
$[Cl^-]$, mM	114.0 ± 0.96	109.0 ± 0.89	†
Calculated $[HCO_3^-]$, mM	19.7 ± 0.95	22.1 ± 0.74	

Data are shown for day 8 of the diet and were analyzed by Student's *t*-test. † denotes P<0.05 versus WT.

Table 4-2. Quantitative analysis of renal acid – base transporter mRNA expression profile in WT and $HK\alpha_{1,2}^{-/-}$ mice fed a normal diet.

Gene	Common name	Function	Tissue			
			Cortex		Medulla	
			WT (N=6)	$HK\alpha_{1,2}^{-/-}$ (N=8)	WT (N=6)	$HK\alpha_{1,2}^{-/-}$ (N=8)
Atp6v0a4	H^+-ATPase a4	H^+ secretion	1.0 ± 0.07	1.20 ± 0.07	1.0 ± 0.17	1.00 ± 0.13
Atp6v1b1	H^+-ATPase B1	H^+ secretion	1.0 ± 0.21	0.76 ± 0.10	1.0 ± 0.23	1.30 ± 0.11
Slc4a1	AE1	Cl^-/HCO_3^- exchange	1.0 ± 0.22	1.10 ± 0.30	1.0 ± 0.06	1.30 ± 0.12 †
Slc26a4	Pendrin	Cl^-/HCO_3^- exchange	1.0 ± 0.08	0.73 ± 0.10	NT	NT
Rhbg	Rhbg	NH_3 transport	1.0 ± 0.16	0.69 ± 0.12	1.0 ± 0.09	0.94 ± 0.09
Rhcg	Rhcg	NH_3 transport	1.0 ± 0.07	0.81 ± 0.07	1.0 ± 0.09	0.95 ± 0.05
Slc9a2	NHE2	Na^+/H^+ exchange	1.0 ± 0.10	0.93 ± 0.11	1.0 ± 0.15	1.00 ± 0.14
Slc9a3	NHE3	Na^+/H^+ exchange	1.0 ± 0.11	0.62 ± 0.08 †	1.0 ± 0.12	0.70 ± 0.12

Data were analyzed by Student's *t*-test. † denotes P<0.05 versus WT. NT means not tested.

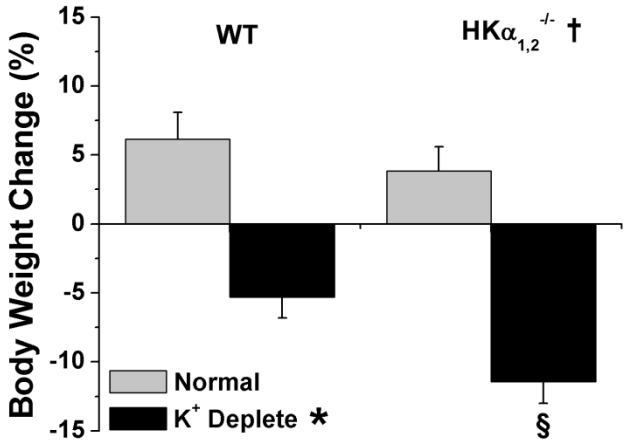

Figure 4-1. $HK\alpha_{1,2}^{-/-}$ mice lost substantial body weight with dietary K^+ depletion. Body weight change (%) is shown as the percent change from day 0 to day 8. Data are presented as mean ± SEM and were analyzed by two-way ANOVA followed by a post hoc Student-Newman-Keuls test, if appropriate. * denotes $P<0.05$ versus normal diet, † versus WT, and § versus WT on same diet. N=6-8.

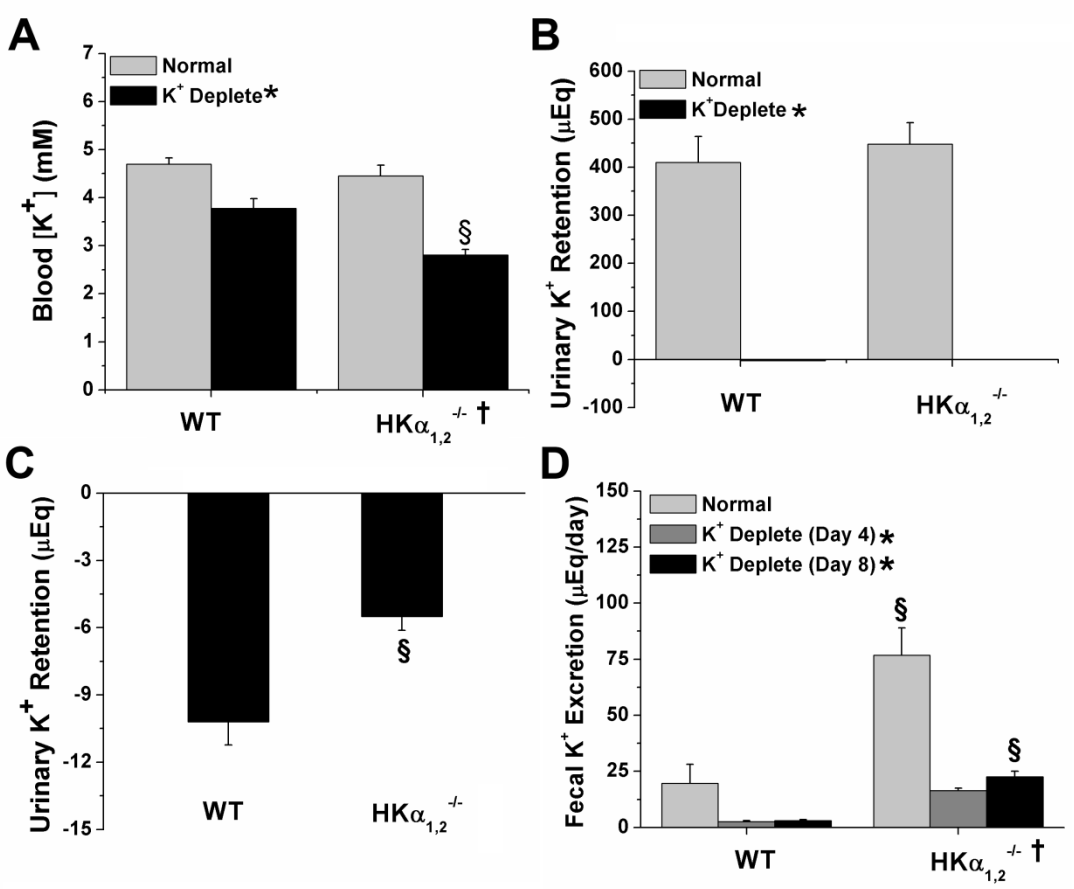

Figure 4-2. Dietary K^+ depletion caused excessive fecal (not urinary) K^+ excretion in $HK\alpha_{1,2}^{-/-}$ mice. A) Blood [K^+] is shown for WT and $HK\alpha_{1,2}^{-/-}$ mice fed a normal or K^+ depleted diet ad libitum for 8 days. B) Urinary K^+ retention (day 8) is shown and was calculated as the daily K^+ intake minus daily urinary K^+ excretion. C) Urinary K^+ retention on day 8 of a K^+ depleted diet was measured by flame photometer also. D) Fecal K^+ excretion (µEq / g stool) is shown for day 4 of the normal diet and day 4 and 8 of the K^+ depleted diet. Data are presented as mean ± SEM and were analyzed by two-way ANOVA followed by a post hoc Student-Newman-Keuls test, if appropriate. * denotes $P<0.05$ versus normal diet, † versus WT, and § versus WT on same diet. N=6-8

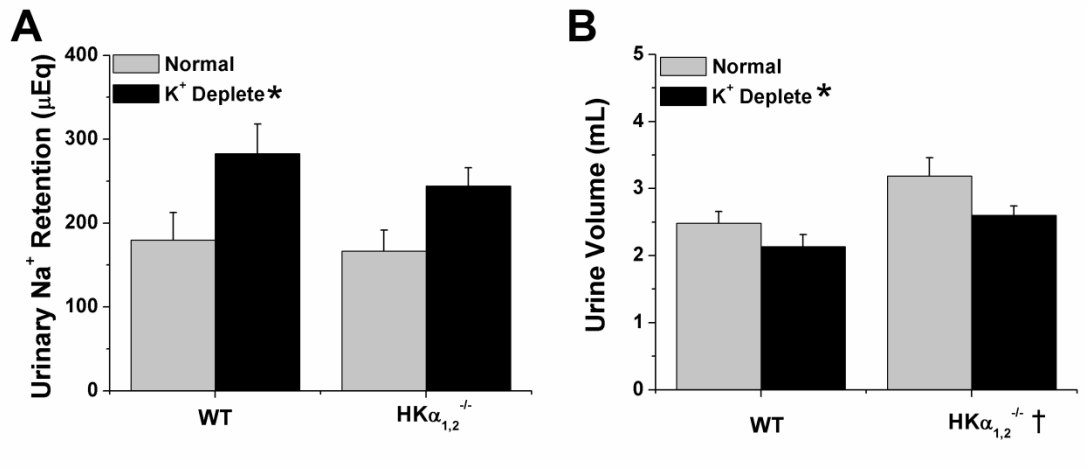

Figure 4-3. Dietary K^+ depletion caused urinary Na^+ retention in WT and $HK\alpha_{1,2}^{-/-}$ mice. A) Urinary Na^+ retention (day 8) and B) urine volume are shown for WT and $HK\alpha_{1,2}^{-/-}$ mice fed a normal or K^+ depleted gel diet ad libitum for 8 days. Urinary Na^+ retention was calculated as the daily Na^+ intake minus daily urinary Na^+ excretion. Data are presented as mean ± SEM and were analyzed by two-way ANOVA followed by a post hoc Student-Newman-Keuls test, if appropriate. * denotes $P<0.05$ versus normal diet and † versus WT. N=6-8

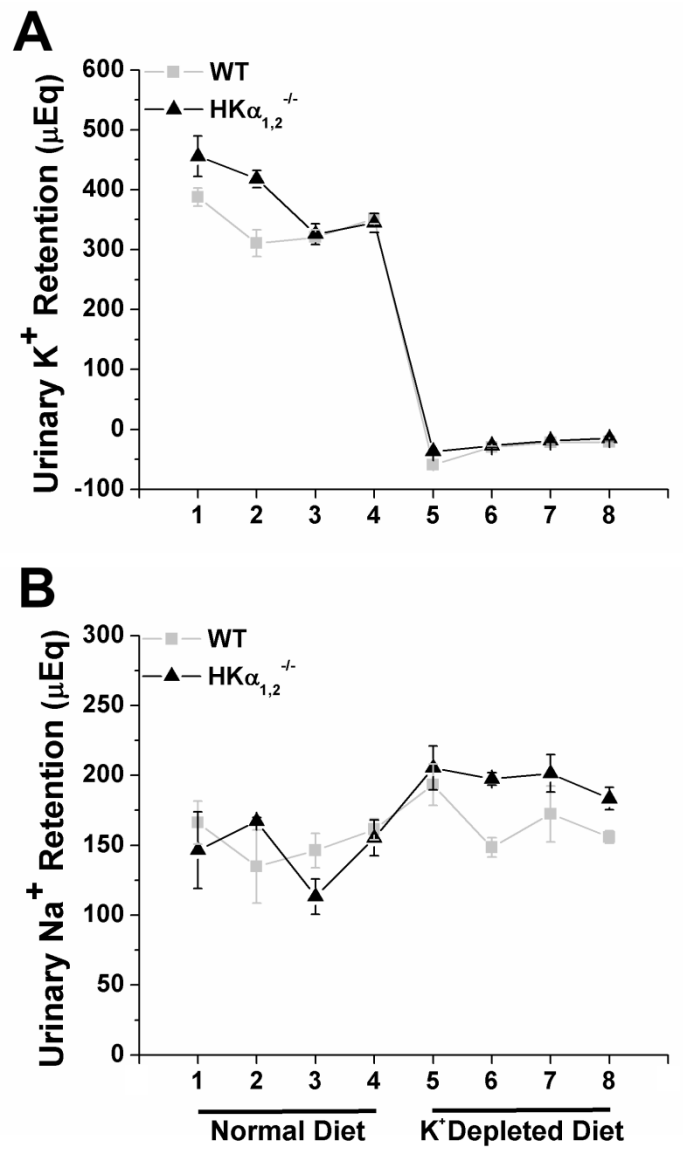

Figure 4-4. $HK\alpha_{1,2}^{-/-}$ mice do not lose urinary K^+ or Na^+ at an earlier time point on a K^+ depleted diet. A) Urinary K^+ retention and B) Na^+ retention are shown in pair fed WT and $HK\alpha_{1,2}^{-/-}$ mice who were given a normal diet for 4 days then switched to a K^+ depleted diet for 4 days. Data are shown as mean ± SEM and were analyzed by two-way repeated measure ANOVA. N=4-5.

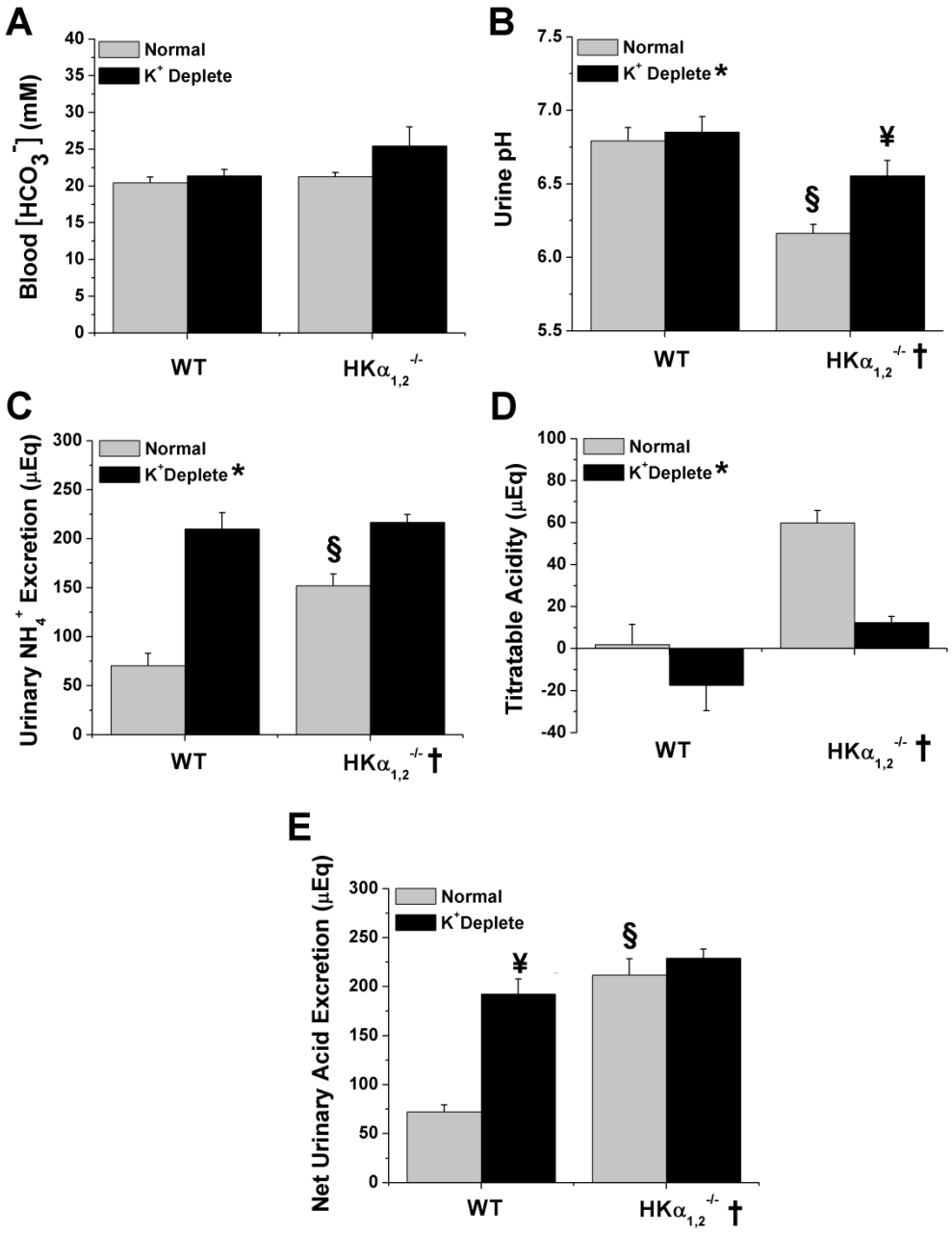

Figure 4-5. Urinary acid excretion is abnormal in $HK\alpha_{1,2}^{-/-}$ mice. A) Blood [HCO_3^-] (calculated), B) urine pH, C) NH_4^+ excretion, D) titratable acidity, and E) net acid excretion (day 8) were assessed in WT and $HK\alpha_{1,2}^{-/-}$ mice fed a normal or K^+ deplete gel diet ad libitum for 8 days. Data are presented as mean ± SEM and were analyzed by two-way ANOVA followed by a post hoc Student-Newman-Keuls or Tukey test, if appropriate. * denotes $P<0.05$ versus normal diet, † versus WT, ¥ versus normal diet in same genotype, and § versus WT on the same diet. N=6-8.

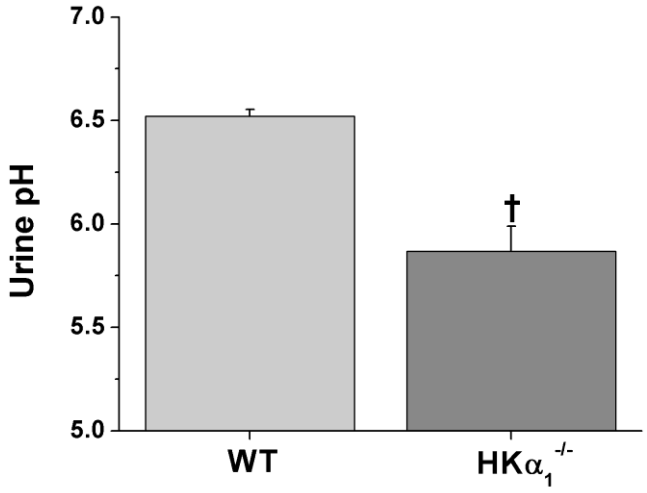

Figure 4-6. $HK\alpha_1^{-/-}$ mice exhibit more acidic urine than WT mice. Urine pH was measured in WT and $HK\alpha_1^{-/-}$ mice fed a normal gel diet for 4 days. Data are presented as mean ± SEM and were analyzed by Student's *t*-test. † denotes P<0.05 versus WT. N=3

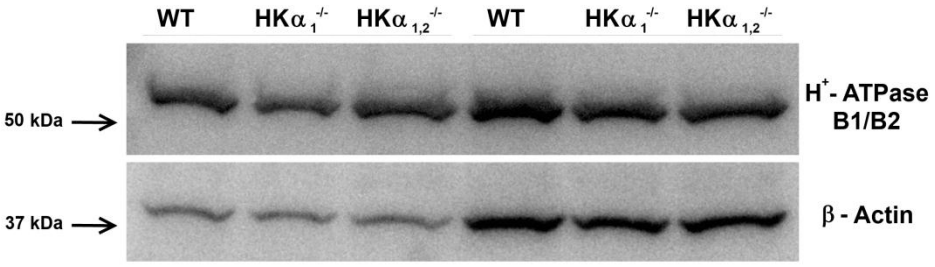

Figure 4-7. H^+-ATPase plasma membrane protein expression does not appear altered in $HK\alpha_1^{-/-}$ or $HK\alpha_{1,2}^{-/-}$ mice. Levels of H^+-ATPase B1/B2 (~55kDa) protein were detected by Western blot analysis of plasma membrane protein fractions (25-50µg) from renal medulla of WT and $HK\alpha_{1,2}^{-/-}$ mice. β-actin protein (~42kDa) levels served as a loading control. N=2.

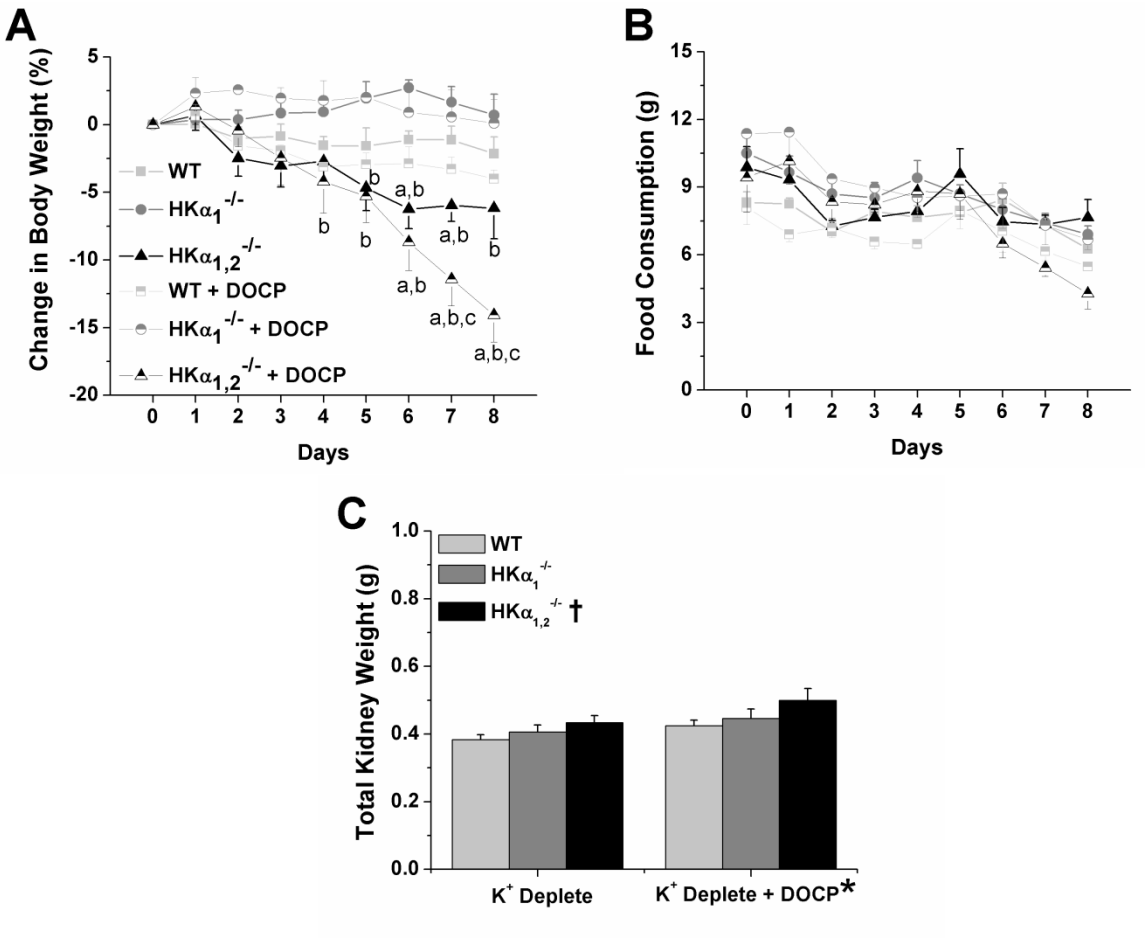

Figure 4-8. Dietary K^+ depletion with DOCP treatment caused body weight loss and renal hypertrophy in $HK\alpha_{1,2}^{-/-}$ mice. A) Body weight (% change from day 0), B) food consumption, and C) kidney weight are shown for WT, $HK\alpha_1^{-/-}$, and $HK\alpha_{1,2}^{-/-}$ mice fed a K^+ depleted diet for 8 days with or without DOCP treatment at day zero. Data are shown as mean ± SEM and were analyzed by two-way ANOVA with or without repeated measures followed by post-hoc Holm-Sidak test, where appropriate. [a] denotes $P<0.05$ versus WT, [b] versus $HK\alpha_1^{-/-}$ mice and [e] versus K^+ depleted diet on the same day. † denotes $P<0.05$ versus WT and * versus K^+ depleted diet. N=3-4.

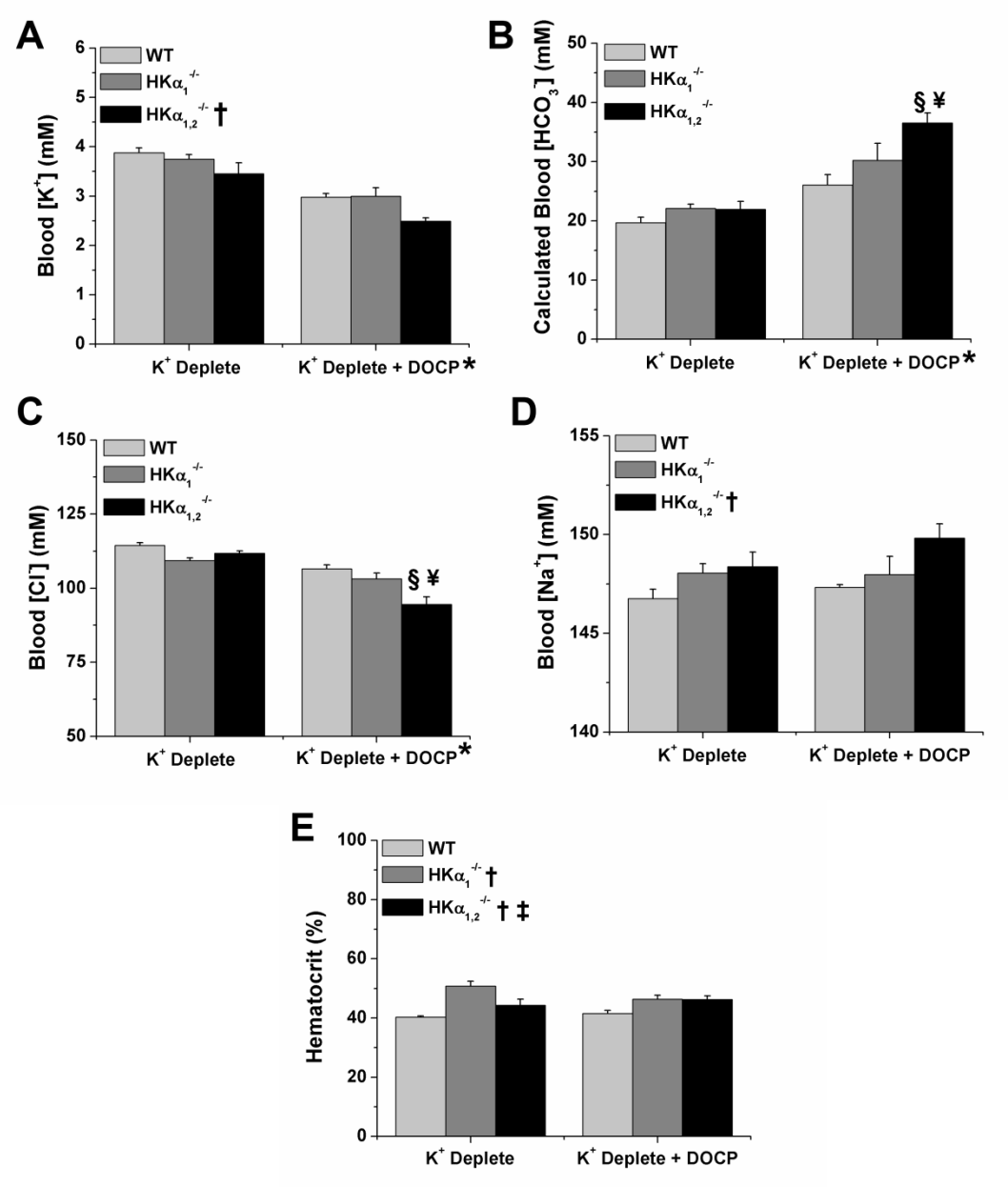

Figure 4-9. Combined dietary K^+ depletion and DOCP treatment caused metabolic alkalosis and hypernatremia in $HK\alpha_{1,2}^{-/-}$ mice. A) Blood [K^+], B) [HCO_3^-] (calculated), C) [Cl^-], D) [Na^+], and E) hematocrit were compared in WT, $HK\alpha_1^{-/-}$ and $HK\alpha_{1,2}^{-/-}$ mice fed a K^+ depleted diet for 8 days. Half of the mice were also treated with DOCP. Data are shown as mean ± SEM and were analyzed by two-way ANOVA followed by post-hoc Holm-Sidak test, where appropriate. † denotes $P<0.05$ versus WT and ‡ versus $HK\alpha_1^{-/-}$ mice regardless of treatment. § denotes $P<0.05$ versus WT and ¥ versus $HK\alpha_1^{-/-}$ within the same treatment group. N=3-4.

CHAPTER 5
MECHANISMS OF H^+,K^+-ATPASE-MEDIATED NA^+ TRANSPORT

Our previous results revealed that mineralocorticoid-induced urinary Na^+ retention requires the presence of H^+,K^+-ATPases. In contrast, renal H^+,K^+-ATPases are not required for dietary K^+ depletion-induced Na^+ retention. Several lines of evidence indicate a similar association between Na^+ transport and renal or colonic H^+,K^+-ATPases. A low Na^+ diet, which induces secondary hyperaldosteronism, has been shown to double ouabain-sensitive H^+,K^+-ATPase-mediated H^+ secretion in rat ICs after ~ two weeks.[191] The ouabain sensitivity suggests activation of $HK\alpha_2$-containing H^+,K^+-ATPases. In this same study, Silver and colleagues also examined H^+,K^+-ATPase activity in collecting ducts from adrenalectomized rats replaced with aldosterone levels similar to Na^+ depleted rats. H^+,K^+-ATPase-mediated H^+ secretion in ICs was not increased by aldosterone loading alone. Those results suggest that low dietary Na^+ stimulates renal $HK\alpha_2$-containing H^+,K^+-ATPases independently of mineralocorticoids. Another study examining$HK\alpha_2$ protein expression in the colon and kidney of Na^+ depleted rats reported that dietary Na^+ depletion stimulated $HK\alpha_2$ protein expression only within the distal colon and not in the kidney. [192] The latter study demonstrates that dietary Na^+ restriction increases renal $HK\alpha_2$-containing H^+,K^+-ATPase activity independently of changes in expression.

The physiological response of $HK\alpha_2^{-/-}$ mice to dietary Na^+ restriction has been investigated. [219] Under dietary Na^+ restricted conditions, $HK\alpha_2^{-/-}$ mice exhibited greater fecal K^+ and Na^+ loss than WT mice. αENaC mRNA expression, detected by Northern blot, appeared decreased in both the colon and kidney of Na^+ restricted $HK\alpha_2^{-/-}$ mice compared to WT mice. It was also found that $HK\alpha_2^{-/-}$ mice fed either a normal or Na^+

restricted diet exhibited significantly reduced amiloride-sensitive, electrogenic Na^+ current within the colon compared to WT mice. Spicer and colleagues speculated that colonic H^+,K^+-ATPase-mediated K^+ recycling was required for ENaC-mediated Na^+ reabsorption. Their model proposed that K^+ secretion via apical K^+ channels and K^+ recycling and H^+ secretion via H^+,K^+-ATPases maintain electrochemical gradients necessary for electrogenic Na^+ reabsorption through ENaC and the Na^+,K^+-ATPase.

In that same study, no significant differences in urinary Na^+ excretion were observed between Na^+ restricted WT and $HK\alpha_2^{-/-}$ mice.[219] However, renal ENaC activity was not examined. Interestingly, urinary K^+ excretion was reduced in Na^+ restricted $HK\alpha_2^{-/-}$ mice compared to WT, suggesting activation of other K^+ reabsorptive mechanisms. It is possible that the unaltered renal Na^+ conservation of $HK\alpha_2^{-/-}$ mice results from coupling of the remaining $HK\alpha_1$-containing H^+,K^+-ATPase and ENaC.

For our study, we hypothesized that $HK\alpha_{1,2}^{-/-}$ mice would display reduced renal ENaC expression and exhibit significant urinary Na^+ loss with dietary Na^+ depletion due to the reduction in ENaC-mediated Na^+ reabsorption. Therefore, we examined renal ENaC mRNA and protein expression in WT and $HK\alpha_{1,2}^{-/-}$ mice under normal conditions. We next compared the physiological response of WT and $HK\alpha_{1,2}^{-/-}$ mice to dietary Na^+ depletion. Since we previously observed that $HK\alpha_{1,2}^{-/-}$ mice consume slightly more food than WT mice under normal conditions, we also hypothesized the $HK\alpha_{1,2}^{-/-}$ mice lack enough of some nutrient like Na^+ in their diet. Therefore, we more closely examined food and H_2O intake in $HK\alpha_{1,2}^{-/-}$ mice. We also measured urinary aldosterone excretion in WT and $HK\alpha_{1,2}^{-/-}$ mice fed ad libitum and pair fed to WT mice (food restriction).

Results

ENaC Subunit Expression in HKα Null Mice

Real time PCR was performed to determine relative mRNA expression of α -, β -, and γENaC in renal cortex and medulla from male WT and HK$\alpha_{1,2}^{-/-}$ mice on a normal gel diet. mRNA expression of α -, β -, and γENaC subunits were not significantly different in the cortex and medulla of HK$\alpha_{1,2}^{-/-}$ mice compared to WT mice (Figure 5-1). Using samples from the same mice used in the mRNA experiment, ENaC total protein expression was also determined in renal medulla of WT and HK$\alpha_{1,2}^{-/-}$ mice by Western blot analysis. A representative Western blot is shown in Figure 5-2 A. Using antibodies from Carolyn Ecelbarger, a band was detected at the expected size for full length α- and γENaC protein (~85kDa). Medullary αENaC protein expression was clearly reduced in HK$\alpha_{1,2}^{-/-}$ mice compared to WT. Band densitometry revealed that HK$\alpha_{1,2}^{-/-}$ mice had ~45% less αENaC protein expression than WT mice (Figure 5-2 B).

Dietary Na^+ Depletion in HKα Null Mice

In the next set of experiments, we investigated the physiological responses of WT and HK$\alpha_{1,2}^{-/-}$ mice to dietary Na^+ depletion. We hypothesized that dietary Na^+ depletion would cause fluid volume loss and urinary Na^+ wasting in HK$\alpha_{1,2}^{-/-}$ mice. Body weight and blood chemistries were measured in WT and HK$\alpha_{1,2}^{-/-}$ mice pair fed a Na^+ depleted gel diet for one week. WT and HK$\alpha_{1,2}^{-/-}$ mice did not display significant differences in body weight gain by day 7 of dietary Na^+ depletion (Figure 5-3 A). Interestingly, Na^+ depleted HK$\alpha_{1,2}^{-/-}$ mice displayed greater blood hematocrit than WT mice (Figure 5-3 B), suggesting volume depletion in the double knockout mice. Blood [Na^+] and [K^+] were similar between WT (151 ± 0.97 mM and 5.1 ± 0.091 mM, respectively) and HK$\alpha_{1,2}^{-/-}$ mice (151 ± 0.43 mM and 5.3 ± 0.30 mM, respectively). Technical difficulties with urine

collection throughout this experiment precludes the assessment of urinary Na^+ and K^+ excretion in WT and $HK\alpha_{1,2}^{-/-}$ mice over the time course of dietary Na^+ depletion.

Food Intake and Urinary Aldosterone Levels in HKα null mice

Our previous studies showed that $HK\alpha_{1,2}^{-/-}$ mice have a tendency to consume more food than WT when fed ad libitum. Therefore, we measured food and H_2O intake in WT and $HK\alpha_{1,2}^{-/-}$ mice fed a normal gel diet ad libitum for one week. Urine volume and osmolality were also measured in WT and $HK\alpha_{1,2}^{-/-}$ mice. On an ad libitum diet, $HK\alpha_{1,2}^{-/-}$ mice consumed significantly more food per body weight (g) than WT mice (Figure 5-4 A). H_2O intake was not significantly different between WT and $HK\alpha_{1,2}^{-/-}$ mice (Figure 5-4 B). However, the double knockouts excreted a greater urine volume than WT mice (Figure 5-4 C). Since the double knockouts consume more gel food than WT mice, this probably results from greater H_2O intake through the gel food. Urine osmolality was the same between the two genotypes (Figure 5-4 D), indicating no difference in urine concentrating ability.

We also examined the ability of WT and $HK\alpha_{1,2}^{-/-}$ mice to maintain normal body weight under ad libitum and pair fed (food/Na^+ restricted) conditions. WT and $HK\alpha_{1,2}^{-/-}$ mice were pair fed a normal gel diet or fed ad libitum with free access to H_2O for one week. Feeding $HK\alpha_{1,2}^{-/-}$ mice the same amount of food as WT mice caused a considerable loss of body weight in the knockout mice, suggesting fluid volume loss (Figure 5-5). In contrast, both WT and $HK\alpha_{1,2}^{-/-}$ mice gained a similar amount of body weight when fed ad libitum (Figure 5-5).

Dietary Na^+ deficiency is known to increase plasma and urinary aldosterone levels.[243] Therefore, we expected greater urinary aldosterone levels in $HK\alpha_{1,2}^{-/-}$ mice pair fed to WT mice due to a restriction in dietary Na^+ intake. We measured urinary

aldosterone levels in male WT and HK$\alpha_{1,2}^{-/-}$ mice fed ad libitum and in HK$\alpha_{1,2}^{-/-}$ mice pair fed to WT mice. Urinary aldosterone excretion was similar between the genotypes during ad libitum intake (Figure 5-6 A). However, pair feeding caused a pronounced increase in urinary aldosterone in HK$\alpha_{1,2}^{-/-}$ mice. Although not significant, pair fed female HK$\alpha_{1,2}^{-/-}$ mice also exhibited a tendency for increased urinary aldosterone excretion compared to either WT or HK$\alpha_{1}^{-/-}$ mice (Figure 5-7 B). More studies are needed to determine if both male and female HK$\alpha_{1,2}^{-/-}$ mice respond similarly to dietary Na^+ restriction.

Discussion

In this study, we investigated the mechanism and further defined the role of renal H^+,K^+-ATPases in urinary Na^+ conservation. Total protein expression of αENaC was considerably reduced in the renal medulla of HK$\alpha_{1,2}^{-/-}$ mice, suggesting that renal H^+,K^+-ATPases are required for normal ENaC expression. Dietary Na^+ depletion caused increased blood hematocrit in HK$\alpha_{1,2}^{-/-}$ mice, indicating fluid volume loss. Restricting food intake of HK$\alpha_{1,2}^{-/-}$ mice caused loss of body weight and greatly increased urinary aldosterone excretion in the double knockouts as well. Taken together, our results further signify that renal H^+,K^+-ATPases play an essential part in urinary Na^+ conservation, at least in part through a mechanism involving ENaC.

The decreased total protein abundance of αENaC in the medulla of HK$\alpha_{1,2}^{-/-}$ mice would be expected to provide less reserve for ENaC translocation to the plasma membrane during states of Na^+ deprivation. Our data suggest that HK$\alpha_{1,2}^{-/-}$ mice consume more food in order to increase dietary Na^+ consumption and maintain salt balance. This hypothesis will need to be confirmed. However, the body weight loss and

increased urinary aldosterone excretion of food restricted $HK\alpha_{1,2}^{-/-}$ mice is consistent with this hypothesis.

The reduced protein expression of αENaC in the medulla of $HK\alpha_{1,2}^{-/-}$ mice may represent a mechanism for the urinary Na^+ loss observed in DOCP-treated $HK\alpha_{1,2}^{-/-}$ mice. It is possible that fewer ENaC channels are available for apical plasma membrane insertion and activation during DOCP treatment in the $HK\alpha_{1,2}^{-/-}$ mice. Several lines of evidence also suggest that both the $HK\alpha_1$- and $HK\alpha_2$-containing H^+,K^+-ATPases directly reabsorb Na^+ on the K^+ binding site.[148, 156-158] Therefore, the disruption of direct Na^+ reabsorption by the renal H^+,K^+-ATPases in $HK\alpha_{1,2}^{-/-}$ mice may also be a mechanism for the observed urinary Na^+ loss in these knockouts. The lack of a similar phenotype in $HK\alpha_1^{-/-}$ mice also implies that the requirement of renal H^+,K^+-ATPases for Na^+ reabsorption is specific to $HK\alpha_2$-containing H^+,K^+-ATPases. The unavailability of specific $HK\alpha_2$-containing H^+,K^+-ATPase inhibitors has hindered investigation into direct $HK\alpha_2$-mediated Na^+ reabsorption. However, the most immediate studies should focus on determining whether knockout of $HK\alpha_2$-containing H^+,K^+-ATPases produces a similar urinary Na^+ handling defect as in the $HK\alpha_{1,2}^{-/-}$ mice. From that point, the mechanism, be it direct or indirect, can be more fully studied.

$HK\alpha_{1,2}^{-/-}$ mice displayed reduced ability to maintain Na^+ balance during DOCP treatment and dietary Na^+ restriction. Whether these effects in the $HK\alpha_{1,2}^{-/-}$ mice are related to reduced ENaC-mediated Na^+ reabsorption or elimination of direct H^+,K^+-ATPase-mediated Na^+ reabsorption in the connecting segment and renal collecting duct remains to be determined. Nonetheless, the results of these studies and

our previous ones support the hypothesis that renal H^+,K^+-ATPases (probably $HK\alpha_2$-containing) are required to maintain Na^+ balance.

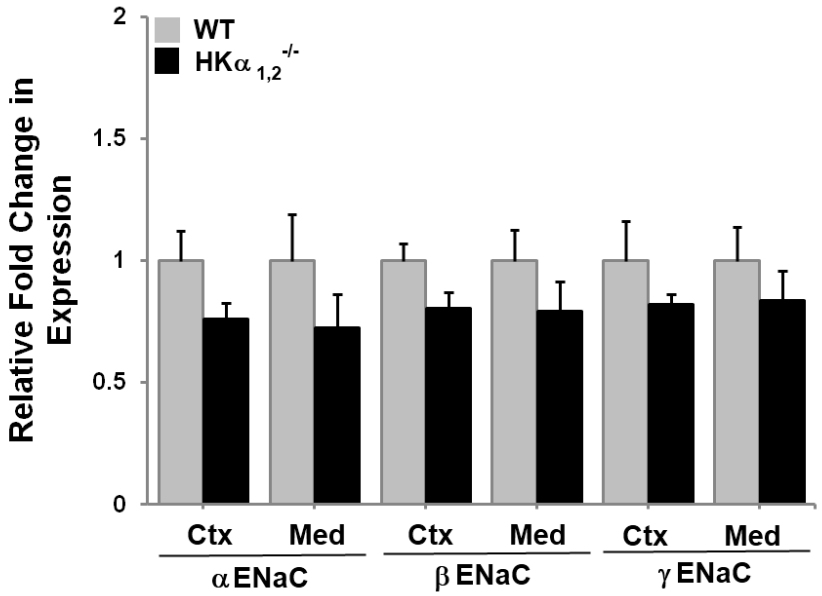

Figure 5-1. ENaC subunit mRNA expression is similar in WT and HK$\alpha_{1,2}^{-/-}$ mice. Real time PCR was used to assess α-, β-, and γ-ENaC mRNA expression in kidney cortex (Ctx) and medulla (Med) from WT and HK$\alpha_{1,2}^{-/-}$ mice fed a normal diet. Expression was set relative to β-actin. Fold changes ($2^{-\Delta\Delta Ct}$) in expression were calculated, with WT set at 1. Data are presented as mean ± SEM and analyzed by Student's *t*-test. N=6-8.

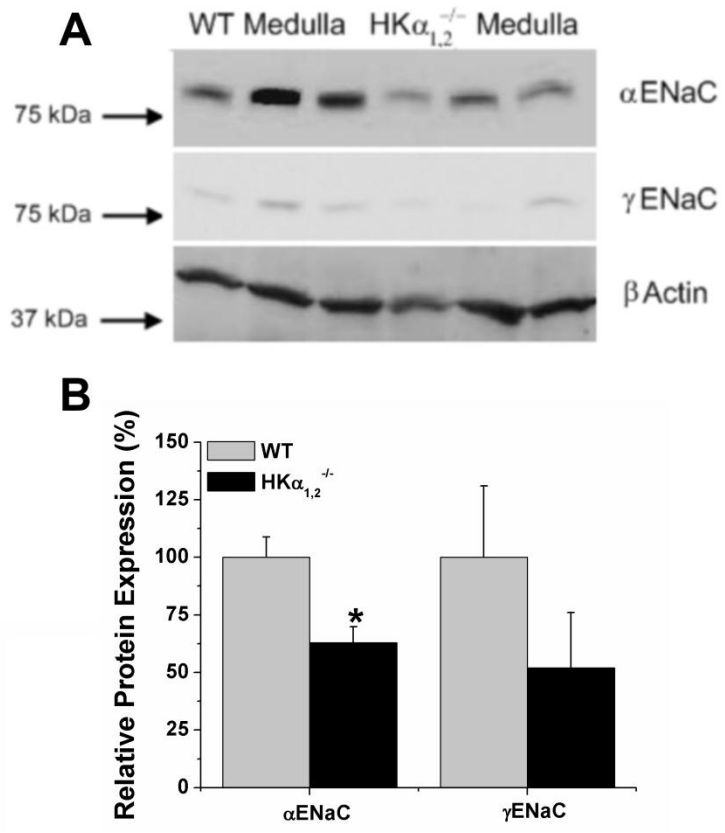

Figure 5-2. Medullary αENaC protein expression is reduced in $HK\alpha_{1,2}^{-/-}$ mice. Western blot analysis was used to assess α- and γENaC protein expression in total protein fractions from renal medulla of WT and $HK\alpha_{1,2}^{-/-}$ mice fed a normal gel diet ad libitum. A) A representative blot is shown for α- and γENaC protein (~85kDa) expression with β-actin (~42kDa) used a loading control. B) Densitometry analysis of blots for α- and γENaC protein expression, corrected for β-actin levels, with WT expression set to 100%. Data are shown as mean ± SEM and were analyzed by Student's *t*-test. † denotes $P<0.05$ versus WT. N=5 for αENaC and N=3 for γENaC.

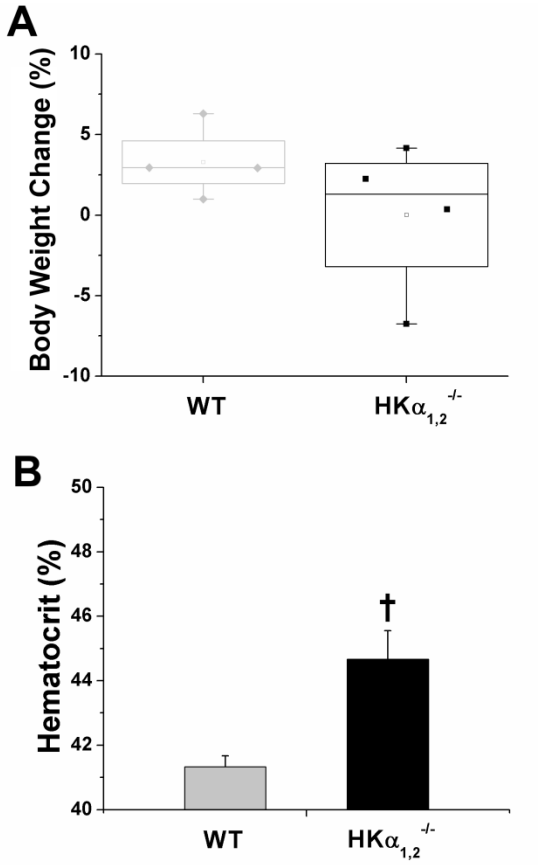

Figure 5-3. Dietary Na^+ depletion increased blood hematocrit in $HK\alpha_{1,2}^{-/-}$ mice. A) Body weight, shown as percent change from day 0 to day 7, and B) blood hematocrit (%, day 7) were compared in WT and $HK\alpha_{1,2}^{-/-}$ mice pair fed a Na^+ depleted gel diet for 7 days. Data for body weight are shown in box chart with individual data points shown. Data are shown as mean ± SEM for hematocrit. All data were analyzed by Student's *t*-test. † denotes $P<0.05$ versus WT. N=4.

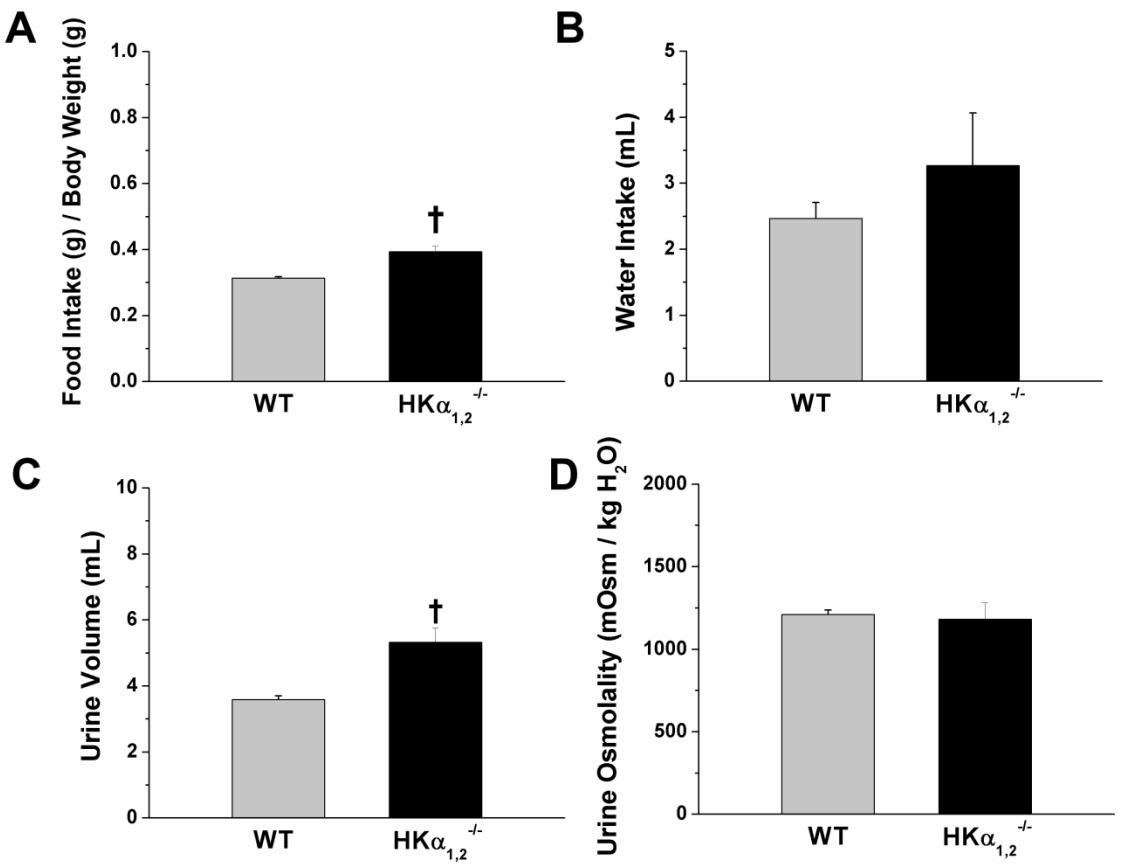

Figure 5-4. $HK\alpha_{1,2}^{-/-}$ mice display altered appetite, H_2O intake, and urine volume on a normal diet. A) Food consumption, B) H_2O intake, C) urine volume, and D) urine osmolality were measured in WT and $HK\alpha_{1,2}^{-/-}$ mice fed a normal gel diet ad libitum for one week. Data are an average of 3 days (day 5 to 7) shown as mean ± SEM and were analyzed by Student's *t*-test. † denotes $P<0.05$ versus WT. N=3.

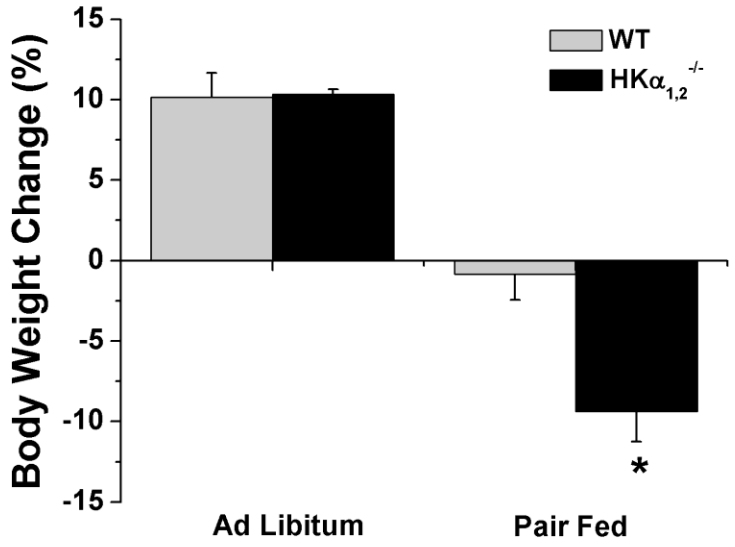

Figure 5-5. $HK\alpha_{1,2}^{-/-}$ mice lost considerable body weight when pair fed. Body weight, shown as percent change from day 0, was measured in WT and $HK\alpha_{1,2}^{-/-}$ mice fed ad libitum or pair fed a normal gel diet for one week. Data are shown as mean ± SEM and were analyzed by Student's *t*-test. * denotes $P<0.05$ versus WT. N=4.

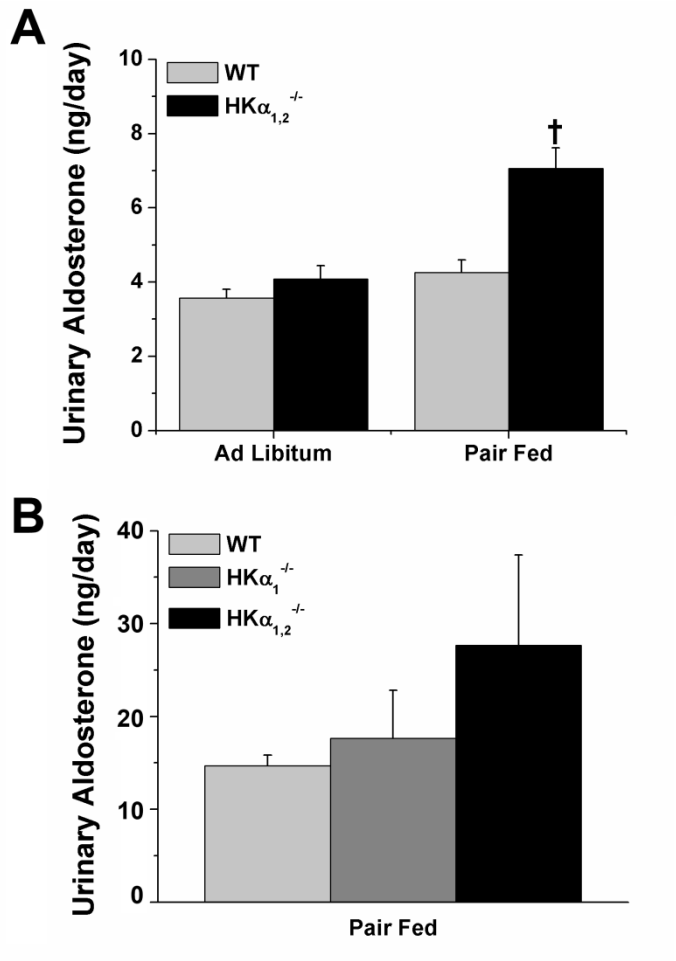

Figure 5-6. Food restriction (pair feeding) caused $HK\alpha_{1,2}^{-/-}$ mice to exhibit augmented urinary aldosterone excretion. A) Urine aldosterone, shown as ng excreted per day, was measured in male WT and $HK\alpha_{1,2}^{-/-}$ mice fed ad libitum or pair fed a normal gel diet. B) Urine aldosterone levels were also measured in female WT, $HK\alpha_{1}^{-/-}$, and $HK\alpha_{1,2}^{-/-}$ mice pair fed a normal gel diet. Data are shown as mean ± SEM and were analyzed by Student's *t*-test or one-way ANOVA with post hoc Tukey test. † denotes $P<0.05$ versus WT on the same diet. N=3-4.

CHAPTER 6
CONCLUSIONS AND FUTURE DIRECTIONS

Our studies establish the importance of renal H^+,K^+-ATPases to mineralocorticoid- and Na^+ depletion-induced Na^+ retention in addition to their formerly recognized K^+ reabsorptive and H^+ secretory action. Conclusions and future directions will be discussed concerning the study of the renal H^+,K^+-ATPases' involvement in Na^+, K^+, and acid-base homeostasis. Hypotheses will be made concerning vasopressin and molecular regulation of renal H^+,K^+-ATPases. Finally, the prospective functions of H^+,K^+-ATPases outside the kidney will be discussed.

H^+,K^+-ATPase-mediated Na^+ Retention

The most remarkable observation within our studies is the influence of renal H^+,K^+-ATPases on renal Na^+ handling. Specifically, our results demonstrate that renal H^+,K^+-ATPases are essential for mineralocorticoid-induced urinary Na^+ retention. Since DOCP-treated $HK\alpha_{1,2}^{-/-}$ mice displayed significant urinary Na^+ loss compared to WT and $HK\alpha_1^{-/-}$ mice, it is probable that renal $HK\alpha_2$-containing H^+,K^+-ATPases are the isoform important to mineralocorticoid-induced urinary Na^+ retention. The mechanism(s) responsible for coupling of Na^+ reabsorption to the H^+,K^+-ATPases remains unknown. Coupling to ENaC-dependent Na^+ reabsorption appears particularly promising. This section discusses and proposes investigation into prospective H^+,K^+-ATPase-requiring Na^+ reabsorptive mechanisms and conditions. This section also discusses the plausible role of H^+,K^+-ATPases in blood pressure regulation.

Potential Mechanism(s) of H^+,K^+-ATPase-mediated Na^+ Transport

In future experiments, it will first be necessary to determine whether both $HK\alpha_1$-and $HK\alpha_2$-containing H^+,K^+-ATPases or $HK\alpha_2$-containing H^+,K^+-ATPases alone

are required for mineralocorticoid-induced urinary Na^+ retention and to maintain Na^+ balance with dietary Na^+ restriction. Examination of the physiological response of $HK\alpha_2^{-/-}$ mice to DOCP treatment and dietary Na^+ depletion should answer this question.

Two lines of evidence indicate that H^+,K^+-ATPases are important for ENaC-mediated Na^+ reabsorption. 1) Other investigators have observed a reduction in colonic ENaC activity in $HK\alpha_2^{-/-}$ mice.[219] 2) We found that medullary αENaC subunit protein expression is dramatically reduced in $HK\alpha_{1,2}^{-/-}$ mice. In the colon, ENaC and $HK\alpha_2$-containing H^+,K^+-ATPases reside in the same cell type. However, in the collecting duct, ENaC and H^+,K^+-ATPases are primarily present in the neighboring PCs and ICs, respectively.[90, 185, 244] The location of ENaC and H^+,K^+-ATPases in separate cell types suggests an extracellular mechanism for altered ENaC expression in kidneys from $HK\alpha_{1,2}^{-/-}$ mice. Although $HK\alpha_2$-containing H^+,K^+-ATPases primarily localize to ICs, studies have shown apical plasma membrane localization in PCs.[90, 185] The expression of ENaC and $HK\alpha_2$-containing H^+,K^+-ATPases in the same cell type implies that either an intracellular or autocrine mechanism of reduced ENaC protein expression may also exist in $HK\alpha_{1,2}^{-/-}$ mice. Indeed, both paracrine and autocrine mechanisms may be involved.

Although the signaling mechanisms have not been identified, recent studies have demonstrated that extracellular [HCO_3^-] can stimulate ENaC protein expression and activity.[121] Those studies showed that pendrin null mice displayed more acidic urine than WT and had reduced renal ENaC expression.[122] Acetazolamide, which increases HCO_3^- delivery to the collecting duct, corrected ENaC expression and activity in pendrin null mice.[121] An analogous mechanism may be present in $HK\alpha_{1,2}^{-/-}$ mice. Similar to

pendrin null mice, $HK\alpha_{1,2}^{-/-}$ mice exhibited more acidic urine than WT mice in our studies. An equivalent examination of ENaC expression and ENaC-mediated (amiloride sensitive) Na^+ reabsorption in $HK\alpha_{1,2}^{-/-}$ mice under normal conditions and in response to acetazolamide should be performed.

However, urine acidity is unlikely to be the primary basis for decreased ENaC expression in $HK\alpha_{1,2}^{-/-}$ mice because a similar urine acidity is observed in $HK\alpha_1^{-/-}$ mice. In distinction to $HK\alpha_{1,2}^{-/-}$ mice, $HK\alpha_1^{-/-}$ mice exhibited exacerbated Na^+ retention with mineralocorticoid excess, suggesting that ENaC function would be intact in the single knockouts.

The discussion above is speculative. Experiments are first needed to determine whether and under what conditions (such as mineralocorticoid excess) ENaC activity is reduced in collecting ducts from $HK\alpha_{1,2}^{-/-}$ mice. The next objectives should involve investigation of whether ENaC requires $HK\alpha_1$- or $HK\alpha_2$-containing H^+,K^+-ATPases by examination of ENaC activity in collecting ducts from single HKα knockouts. Finally, it should be determined if the lack of mineralocorticoid-induced Na^+ retention in $HK\alpha_{1,2}^{-/-}$ mice results from reduced ENaC activity, expression, and plasma membrane localization. The results of these proposed experiments will address the question of whether ENaC represents the mechanism for H^+,K^+-ATPase-mediated Na^+ retention.

It is possible that renal $HK\alpha_2$-containing H^+,K^+-ATPases are required for the Na^+-retaining effects of other hormonal and dietary conditions of increased Na^+ retention. In support of this hypothesis, chronic (two weeks) dietary NaCl restriction, a diet known to stimulate ENaC expression and Na^+ reabsorptive activity, also activates SCH-28080 sensitive H^+,K^+-ATPase-mediated H^+ secretion in ICs.[191] In addition, our

own data demonstrating that $HK\alpha_{1,2}^{-/-}$ mice show signs of fluid loss with dietary Na^+ depletion support the hypothesis that conditions of enhanced ENaC-mediated urinary Na^+ retention required augmented H^+,K^+-ATPase activity. Examination of urinary Na^+ excretion and ENaC activity in collecting ducts from Na^+ restricted $HK\alpha_1^{-/-}$, $HK\alpha_2^{-/-}$, and $HK\alpha_{1,2}^{-/-}$ mice is necessary to fully resolve the function of renal H^+,K^+-ATPases in urinary Na^+ retention during dietary Na^+ depletion.

If it is found that reduced ENaC-mediated Na^+ reabsorption is not the mechanism for urinary Na^+ loss in $HK\alpha_{1,2}^{-/-}$ mice subjected to DOCP or dietary Na^+ depletion, then other studies are needed to determine whether H^+,K^+-ATPases directly reabsorb Na^+. H^+,K^+-ATPase-mediated Na^+ reabsorption could be measured as amiloride- and hydrochlorothiazide-insensitive Na^+ flux. This relative H^+,K^+-ATPase-mediated Na^+ flux should be measured and compared in collecting ducts from WT and HKα null mice under normal, mineralocorticoid-stimulated, and Na^+ deplete conditions. If direct Na^+ transport occurs via H^+,K^+-ATPases, one would expect amiloride- and hydrochlorothiazide-insensitive Na^+ flux to increase with DOCP and dietary Na^+ deplete conditions in collecting ducts from WT mice and that this activity would be absent in $HK\alpha_{1,2}^{-/-}$ mice under any condition. Finally, measurement of amiloride- and hydrochlorothiazide-insensitive Na^+ flux in HKα single null mice should allow for determination of the H^+,K^+-ATPase isoform responsible for direct Na^+ reabsorption.

Blood Pressure Phenotypes in HKα Null Mice

Based on the reduced renal medullary ENaC abundance in $HK\alpha_{1,2}^{-/-}$ mice and potential for reduction in ENaC-mediated Na^+ retention, one might expect the double knockouts to exhibit lower blood pressure than WT mice under normal conditions. Recently completed experiments performed by Jeanette Lynch in our laboratory

compared blood pressure phenotypes in male WT, $HK\alpha_1^{-/-}$ and $HK\alpha_{1,2}^{-/-}$ mice under normal conditions. Despite less medullary αENaC protein expression, $HK\alpha_{1,2}^{-/-}$ mice showed similar blood pressure as WT and $HK\alpha_1^{-/-}$ mice (WT, 115 ± 2.2 mmHg; $HK\alpha_1^{-/-}$, 112 ± 3.3 mmHg; $HK\alpha_{1,2}^{-/-}$, 114 ± 3.0 mmHg). Under normal conditions, urinary Na^+ retention, like blood pressure, is also similar in the three genotypes. These results may suggest similar ENaC activity in WT, $HK\alpha_1^{-/-}$ and $HK\alpha_{1,2}^{-/-}$ mice under normal conditions.

Although blood pressure is normal in $HK\alpha_{1,2}^{-/-}$ mice under normal conditions, the differences in urinary Na^+ excretion observed in DOCP-treated knockout mice suggests blood pressure differences may exist with DOCP treatment. We found that DOCP induced greater urinary Na^+ retention in $HK\alpha_1^{-/-}$ mice and less urinary Na^+ retention in $HK\alpha_{1,2}^{-/-}$ mice. These two results would be expected to cause a greater increase in blood pressure in $HK\alpha_1^{-/-}$ mice and smaller increase in blood pressure in $HK\alpha_{1,2}^{-/-}$ mice relative to WT mice. Preliminary examination of the blood pressure response of WT, $HK\alpha_1^{-/-}$, and $HK\alpha_{1,2}^{-/-}$ mice to DOCP treatment has not demonstrated significant phenotypic differences. However, DOCP only increased blood pressure slightly (<10mmHg). The mild increase in blood pressure of DOCP-treated mice may reflect the fact that our background mouse strain, C57BL/6J, is somewhat resistant to desoxycorticosterone-mediated hypertension.[245] Also, the hypertensive actions of desoxycorticosterone-induced renal Na^+ retention have classically been studied under conditions of high dietary Na^+ intake, which was not used in our studies

Characterization of the role of renal H^+,K^+-ATPases in blood pressure regulation requires a more thorough examination of blood pressure responses in HKα null mice, particularly in response to increased or decreased dietary Na^+ intake and also in the

absence or presence of mineralocorticoid excess. These experiments may need to be performed in a different, more desoxycorticosterone-sensitive, background mouse strain.

H^+,K^+-ATPase-mediated K^+ Retention and Recycling

This section discusses observed and proposed roles of renal H^+,K^+-ATPases in K^+ homeostasis. To our knowledge, our studies are the first to demonstrate that HKα null mice exhibit insufficient renal K^+ retention. However, there are stark differences between the response of HKα null mice to mineralocorticoids and dietary K^+ depletion. Since both conditions cause hypokalemia, the results indicate that renal H^+,K^+-ATPases do not respond only to decreased plasma $[K^+]$. Our studies also imply that $HK\alpha_2$-containing H^+,K^+-ATPases primarily facilitate K^+ recycling in the collecting duct. This has been suggested for H^+,K^+-ATPases present in other tissues. Finally, our observation that female, not male, $HK\alpha_{1,2}^{-/-}$ mice have greater blood $[K^+]$ than WT mice under normal conditions indicate that H^+,K^+-ATPases regulate K^+ homeostasis in a sex-dependent manner.

Role of H^+,K^+-ATPases in Mineralocorticoid and Dietary K^+-dependent Control of K^+ Homeostasis

With the use of HKα null mice, we showed that mineralocorticoids activate renal $HK\alpha_2$-containing H^+,K^+-ATPases limiting urinary K^+ loss. Interestingly, our results suggest that loss of $HK\alpha_1$ up-regulates mineralocorticoid-induced K^+ reabsorption through $HK\alpha_2$-containing H^+,K^+-ATPases since the excessive urinary K^+ retention observed in DOCP-treated $HK\alpha_1^{-/-}$ mice is absent in $HK\alpha_{1,2}^{-/-}$ mice. Examination of H^+,K^+-ATPase-mediated K^+ flux in collecting ducts from DOCP-treated WT and $HK\alpha_1^{-/-}$

mice should clarify whether $HK\alpha_2$-containing H^+,K^+-ATPases are indeed the mechanism for greater K^+ retention in $HK\alpha_1^{-/-}$ mice.

Our results also indicate that mineralocorticoids induce $HK\alpha_2$-containing H^+,K^+-ATPases in a K^+ dependent manner. High dietary K^+ intake prevents the effect of mineralocorticoids to decrease plasma $[K^+]$ and to stimulate medullary $HK\alpha_2$ subunit expression. Experiments are necessary 1) to examine whether the effects of a high K^+ diet indeed correspond to inhibition of mineralocorticoid-induced H^+,K^+-ATPase K^+ reabsorption in the collecting duct; and 2) whether $HK\alpha_{1,2}^{-/-}$ mice, fed a high K^+ diet, no longer exhibit greater urinary K^+ loss than WT mice with mineralocorticoid excess.

In contrast to the role of renal H^+,K^+-ATPases during mineralocorticoid excess, neither the renal $HK\alpha_1$- nor $HK\alpha_2$-containing H^+,K^+-ATPases appear to be required for maximal urinary K^+ conservation during dietary K^+ depletion. However, as evidenced by fecal K^+ loss in both $HK\alpha_2^{-/-}$ and $HK\alpha_{1,2}^{-/-}$ mice, the colonic $HK\alpha_2$-containing H^+,K^+-ATPases do mediate significant K^+ reabsorption during K^+ depletion. Importantly, the absence of H^+,K^+-ATPases in the gastrointestinal system complicates interpretation of these data because mice null for $HK\alpha_1$ or $HK\alpha_2$ exhibit excessive fecal K^+ loss even under normal circumstances. In effect, the knockout mice are likely primed for urinary K^+ conservation, probably through other transporters proximal to the collecting duct. Ultimately, the generation and study of kidney-specific knockouts for HKα subunits is desirable for understanding the role of renal H^+,K^+-ATPases in urinary K^+ reabsorption.

K^+ Recycling by H^+,K^+-ATPases

The magnitude of urinary K^+ loss in DOCP-treated $HK\alpha_{1,2}^{-/-}$ mice was small, especially compared to the magnitude of urinary Na^+ loss. This relatively mild phenotype and the lack of renal K^+ loss in K^+ depleted $HK\alpha_{1,2}^{-/-}$ mice suggests that the

primary function of renal HKα_2-containing H^+,K^+-ATPases is not K^+ reabsorption. Evidence from the kidney [12] and stomach [246] indicate that H^+,K^+-ATPases in coordination with an apical K^+ channel can function to recycle K^+. Coimmunoprecipitation and immunolocalization experiments are needed to identify potential K^+ channels associated with renal HKα_2-containing H^+,K^+-ATPases. Finally, studies should address whether K^+ recycling through the associated K^+ channel is indeed the primary function of HKα_2-containing H^+,K^+-ATPases. Specifically, H^+,K^+-ATPase-mediated H^+ secretion in ICs of the collecting duct should be measured in the presence and absence of pharmacological blockade of the identified K^+ channel using both WT and HK$\alpha_2^{-/-}$ mice.

This mode of K^+ recycling has been proposed as the reason why HKα_2-containing H^+,K^+-ATPases are required for ENaC-mediated Na^+ reabsorption in the colon.[219] A model for this coordinated transport mechanism within the kidney is shown in Figure 6-1. Specifically, this model proposes that H^+,K^+-ATPase-mediated K^+ recycling provides the driving force (efflux of K^+ from PCs) to facilitate electrogenic Na^+ reabsorption through ENaC. Investigation of ENaC-mediated Na^+ flux in collecting ducts from WT and HK$\alpha_2^{-/-}$ mice in the presence and absence of inhibitors for the associated K^+ channel should address whether this proposed model is indeed accurate.

Role of H^+,K^+-ATPases in Sex Hormone Control of K^+ Homeostasis

Until recently, sex hormones have not been recognized to have significant influence on K^+ homeostasis. New evidence from Crambert and colleagues shows that low dietary K^+ increased adrenal progesterone production. [206] The study also showed that progesterone causes urinary K^+ retention. The mechanism appears to be through activation of renal HKα_2-containing H^+,K^+-ATPases. Our studies showed that female

$HK\alpha_{1,2}^{-/-}$ mice, in contrast to males, display a slight hyperkalemia compared to WT and $HK\alpha_1^{-/-}$ mice. The results indicate that $HK\alpha_2$-containing H^+,K^+-ATPases, present in the kidney or other tissues, play a yet undetermined part in the effect of sex hormones on K^+ homeostasis. A very informative experiment may be to assess plasma $[K^+]$ and K^+ excretion in response to ovariectomy and adrenalectomy in female WT and $HK\alpha_{1,2}^{-/-}$ mice. The proposed studies will address whether sex hormones produce the slight hyperkalemia present in female $HK\alpha_{1,2}^{-/-}$ mice.

Experiments should also be conducted to understand the regulation of renal K^+ handling by other sex hormones and the potential involvement of renal H^+,K^+-ATPases. Specifically, urinary K^+ excretion could be examined in males, females, and ovariectomized females in response to progesterone, estrogen, and testosterone. Also, the effects of these hormones and pregnancy on H^+,K^+-ATPase-mediated K^+ flux and HKα subunit expression in the collecting duct could be studied. The results of these studies should clarify whether progesterone is the only sex hormone that modifies K^+ homeostasis. It should also address whether other sex hormones and pregnancy influence K^+ reabsorption through renal $HK\alpha_2$-containing H^+,K^+-ATPases.

H^+,K^+-ATPase-mediated H^+ Secretion

The importance of H^+,K^+-ATPases in the regulation of acid-base homeostasis has been debated for many years. Nevertheless, our studies show for the first time that $HK\alpha_2$-containing H^+,K^+-ATPases mediate the majority of mineralocorticoid-induced metabolic alkalosis. The role of H^+,K^+-ATPases to affect acid-base balance during normal and dietary K^+ depleted conditions is not clear. The following section will summarize and propose studies concerning the importance of H^+,K^+-ATPases in the kidney and gastrointestinal system to acid-base homeostasis.

Effects of Mineralocorticoids and Dietary K^+ Depletion on Acid-Base Balance

Our data showing that DOCP treatment did not cause increased plasma [HCO_3^-] in $HK\alpha_{1,2}^{-/-}$ mice indicate that $HK\alpha_2$-containing H^+,K^+-ATPases mediate all of the effect of mineralocorticoids to cause metabolic alkalosis. Nevertheless, our studies did not address whether the metabolic alkalosis results from renal or colonic $HK\alpha_2$-containing H^+,K^+-ATPases. Increased medullary $HK\alpha_2$ mRNA expression in DOCP-treated mice suggests a renal mechanism. An important contribution of the colonic $HK\alpha_2$-containing H^+,K^+-ATPase cannot be ignored. Whether the renal, colonic, or both $HK\alpha_2$-containing H^+,K^+-ATPases facilitate mineralocorticoid- induced H^+ secretion and the resultant metabolic alkalosis needs to be investigated. Measurements of urinary acid excretion and colonic H^+,K^+-ATPase-mediated H^+ secretion in DOCP-treated WT and $HK\alpha_2^{-/-}$ mice should address this question.

In our studies, we did not observe increased plasma [HCO_3^-] in WT mice after eight days on a K^+ depleted diet. Similar results have been observed in mice and dogs.[206, 218, 237] It is possible that a longer period of dietary K^+ depletion is needed to achieve metabolic alkalosis in mice. Whether this relates to stimulation of H^+,K^+-ATPase-mediated H^+ secretion in the kidney or colon could be studied using HKα null mice. However, it is unlikely that loss of colonic H^+,K^+-ATPase-mediated H^+ secretion significantly affects acid-base balance because neither $HK\alpha_2^{-/-}$ [218] nor $HK\alpha_{1,2}^{-/-}$ mice exhibited disturbances in blood [HCO_3^-] despite excessive fecal K^+ loss on a normal and K^+ depleted diet. Overall, we conclude that, despite their activation, renal and colonic H^+,K^+-ATPases do not significantly affect acid-base homeostasis during low dietary K^+ intake alone.

Gastrointestinal Effects on Urinary Acid Excretion

One completely surprising observation in our studies is that mice null for $HK\alpha_1$ exhibit more acidic urine than WT mice. These results are surprising because $HK\alpha_1$-containing H^+,K^+-ATPases are supposed to reside on the apical membrane of both the gastric mucosa and ICs of the collecting duct where they would secrete H^+.[185, 247] One expects the loss of these H^+ secreting transporters in the kidney to cause urine alkalinization, not acidification. Compensatory stimulation of other H^+ secretion mechanisms in the kidneys of $HK\alpha_1$ null mice may represent one potential mechanism for the greater urinary acidification observed in these knockout mice. However, this compensation should only maintain normal net urine acid excretion in the knockouts, not stimulate more acid excretion than WT mice.

It has always been assumed that loss of gastric acid secretion would not affect acid-base balance because the secreted acid later stimulates pancreatic HCO_3^- secretion for its neutralization.[248] However, evidence indicates that the gastric peptide hormone, gastrin-releasing peptide, can activate pancreatic HCO_3^- secretion in the absence of gastric acid.[242] Gastrin-releasing peptide stimulates gastric acid secretion and is the hormone responsible for the release of gastrin in the stomach.[248] The fact that $HK\alpha_1^{-/-}$ mice exhibit dramatically augmented levels of circulating and gastric gastrin suggests that gastrin – releasing peptide levels are also increased in these knockout mice.[213] First, serum and gastric levels of gastrin-releasing peptide could be compared in WT and $HK\alpha_1^{-/-}$ mice. If greater in the knockouts, then pancreatic HCO_3^- secretion could be measured. It will also need to be determined whether inhibition of pancreatic HCO_3^- secretion corrects net urine acid excretion in $HK\alpha_1^{-/-}$ mice. Really, tissue-specific

HKα knockout mice are needed to define the separate roles of H^+,K^+-ATPases in the gastrointestinal system and the kidney to affect acid-base homeostasis.

Dietary Acid-Dependent Regulation of Renal H^+,K^+-ATPases

Several lines of evidence suggest that dietary acid loading stimulates renal H^+,K^+-ATPase-mediated H^+ secretion. [100, 193, 197, 198] Dietary acid loading stimulates the expression of $HK\alpha_1$ and $HK\alpha_2$ mRNA expression in a time-dependent manner.[100] Studies are needed to assess the role of each separate renal H^+,K^+-ATPase isoform in the acid secretory response to dietary acid loading. In a preliminary study, we found that urine pH decreased in WT mice fed a 0.28 M NH_4Cl loaded diet for 6 days (Figure 6-2). A similar effect was not observed in $HK\alpha_1^{-/-}$ mice. These preliminary data suggest that renal $HK\alpha_1$-containing H^+,K^+-ATPases participate in the dietary acid-induced urinary acidification.

However, significant metabolic acidosis was not observed in NH_4Cl loaded WT mice. Also, no differences in blood [HCO_3^-] (19.9 ± 1.3 mM in WT versus 20.5 ± 0.082 mM in $HK\alpha_1^{-/-}$ mice, N=3) were observed between NH_4Cl loaded WT and $HK\alpha_1^{-/-}$ mice. Future studies need to use an acid loading model that produces significant acidosis. This will be essential to understanding the role of renal H^+,K^+-ATPases in the response to dietary acid challenges. HCl acid loading produces metabolic acidosis in mice. [128] The time-dependent renal and systemic response of kidney specific $HK\alpha_1^{-/-}$ and $HK\alpha_2^{-/-}$ mice to HCl acid loading should be investigated. The results of these proposed studies will more completely define the function of renal H^+,K^+-ATPases in dietary acid elimination and acid-base homeostasis.

MicroRNA Regulation of H^+,K^+-ATPases

New evidence indicates that microRNA regulation of gene expression is quite important to normal kidney function and pathophysiology.[249] Much investigation of microRNAs in the kidney has focused on cancer. However, a recent study has shown that miR-192 regulates WNK1, an important modulator of distal tubular NCC.[250] This report suggests that microRNAs are important regulatory mechanisms of electrolyte transport.

MicroRNAs bind to the 3' UTR of a target gene's mRNA transcript and either cause mRNA degradation or inhibit translation through a variety of mechanisms.[249] Our own observation that renal $HK\alpha_2$ mRNA expression is quite low or even undetectable at times sparked examination of potential microRNA binding sites within the 3' UTR of $HK\alpha_2$ mRNA using an online software program called TargetScanMouse (www.targetscan.org). The program algorithm detected a potential mmu-miR-505 binding site conserved within other species, including human, rat, and rabbit (Figure 6-3). However, analysis of miR-505 expression in the cortex and medulla of mouse kidney revealed very low expression of this microRNA (Ct greater than or equal to 36). These data suggest that microRNAs are probably not a primary mechanism to control $HK\alpha_2$ expression. With the discovery of more microRNAs and better understanding of microRNA mechanisms, it may be important to reevaluate microRNA regulation of $HK\alpha_2$ mRNA expression.

Interaction between Vasopressin and Renal H^+,K^+-ATPases

One of the most striking observations of our studies was the dramatic decline in urine volume of DOCP-treated $HK\alpha_1^{-/-}$ mice. Two other lines of data suggest involvement of H^+,K^+-ATPases in H_2O balance. 1) $HK\alpha_{1,2}^{-/-}$ mice exhibited polyuria

under normal conditions. 2) $HK\alpha_{1,2}^{-/-}$ mice displayed hypernatremia with combined dietary K^+ depletion and DOCP treatment. Indeed, the anti-diuretic hormone, vasopressin has been shown to activate HCO_3^- reabsorption (or H^+ secretion) and alter acid-base transporter expression in the collecting duct.[251, 252] Other studies have shown that vasopressin increases ATPase activity of the H^+-ATPase through V1R-dependent mechanism.[39] In the same study, vasopressin was not shown to stimulate vanadate-sensitive H^+,K^+-ATPase activity. However, the presence of ouabain to inhibit the Na^+,K^+-ATPase makes the data difficult to interpret because $HK\alpha_2$-containing H^+,K^+-ATPases are also sensitive to ouabain.

In future studies, H^+,K^+-ATPase-mediated H^+ secretion could be measured in ICs of control and vasopressin-treated collecting ducts from WT and HKα null mice. V1R and V2R antagonists could be used to define the mechanism of vasopressin action. It is quite possible that the response of H^+,K^+-ATPases to vasopressin is more delayed than that of H^+-ATPases. H^+-ATPases respond earlier to mineralocorticoid stimulation than H^+,K^+-ATPases.[39] Studies should be conducted to examine time-dependent changes in acid-base homeostasis of vasopressin-treated mice. These changes could then be correlated to renal HKα subunit expression and activity in the collecting duct. More experiments are needed to clarify whether the $HK\alpha_1$- or $HK\alpha_2$-containing H^+,K^+-ATPases participate in vasopressin-stimulated H^+ secretion in ICs.

Our own preliminary evidence is consistent with an interaction between vasopressin and H^+,K^+-ATPases. We found that urine osmolality and vasopressin levels were greater in $HK\alpha_1^{-/-}$ mice than either WT or $HK\alpha_{1,2}^{-/-}$ mice (Figure 6-4). To completely understand whether vasopressin-induced H_2O reabsorption requires renal

H^+,K^+-ATPases, separate measurements of the renal response of HKα null mice to vasopressin and H_2O deprivation are required.

Function of H^+,K^+-ATPases in Other Organ Systems

H^+,K^+-ATPases localize to several different tissues in addition to the kidney. In the stomach, the H^+,K^+-ATPase is most well known for its role in gastric acid secretion, and, in the colon, for its roles in K^+ reabsorption. However, the function of H^+,K^+-ATPases within other organ systems remains mostly unresolved. Based on our own observations and the literature, two areas of particular interest include the role of gastric H^+,K^+-ATPases in obesity and $K^=$ reabsorption and the role of $HK\alpha_1$-containing H^+,K^+-ATPases in bone resorption.

Role of Gastric H^+,K^+-ATPases in Obesity and K^+ Reabsorption

Relatively recent evidence has demonstrated that the gastric mucosa releases a peptide hormone named ghrelin which in addition to activation of gastric acid secretion also regulates energy balance.[253] Through its effects on the hypothalamic neuropeptide Y system, ghrelin stimulates food intake and gastric emptying and can contribute to certain obesity phenotypes.

This connection between food intake and gastric acid secretion may be quite important for our own studies since we have observed greater food consumption in $HK\alpha_{1,2}^{-/-}$ than WT mice. Also, longitudinal assessment of body weight change in male and female WT and $HK\alpha_1^{-/-}$ mice from age 7 to 16 weeks has shown that $HK\alpha_1^{-/-}$ mice gain weight at a faster rate than WT mice (Figure 6-5). Our previous data and the preliminary data described herein suggest that knockout of gastric acid secretion results in slight hyperphagia and obesity. We hypothesize that $HK\alpha_1$ null mice will exhibit greater gastric ghrelin production as a compensatory mechanism to activate gastric acid

secretion. This excess ghrelin may cause an orexigenic and obesity phenotype in the knockout mice. To study this, food intake, fat versus lean mean ratio, and ghrelin levels need to be compared in WT and $HK\alpha_1^{-/-}$ mice.

Either way, the observation that $HK\alpha_1^{-/-}$ mice are obese and exhibit excess adiposity, as determined by our own visual inspection, is concerning with respect to long-term use of proton pump inhibitors in human patients. Our results convey the importance of studying whether chronic proton pump inhibitor therapy increases gastric ghrelin secretion.

One interesting observation of our studies is that $HK\alpha_1^{-/-}$ mice, similar to $HK\alpha_2^{-/-}$ [218] and $HK\alpha_{1,2}^{-/-}$ mice, exhibit significant fecal K^+ loss under normal conditions. Traditionally, the stomach has not been recognized as an important site for K^+ reabsorption. The gastric H^+,K^+-ATPases and apical K^+ channels have principally been thought to participate in K^+ recycling to achieve a large H^+ gradient contributing to a very low luminal pH. However, our data suggest that gastric $HK\alpha_1$-containing H^+,K^+-ATPases also participate in net K^+ reabsorption. Measurement of luminal K^+ content in the small intestine of WT and $HK\alpha_1^{-/-}$ mice should answer whether the phenotype of $HK\alpha_1^{-/-}$ mice reflects reduced gastric K^+ reabsorption.

In our studies, we also observed that both $HK\alpha_1^{-/-}$ and $HK\alpha_{1,2}^{-/-}$ mice display significant gastric hypertrophy compared to WT mice under K^+ depleted conditions (Figure 6-6). To our surprise, the $HK\alpha_{1,2}^{-/-}$ mice exhibited an even more severe gastric hypertrophy than $HK\alpha_1^{-/-}$ mice. As determined by Northern blot, $HK\alpha_2$ mRNA expression has not previously been detected in the stomach.[161] However, under normal conditions and with the aid of a much more sensitive method (real time PCR), $HK\alpha_2$ mRNA

expression is also scarcely detectable in the kidney. Future studies should determine whether and under what conditions the stomach expresses $HK\alpha_2$. The presence of $HK\alpha_2$ in the stomach may explain the greater gastric hypertrophy of $HK\alpha_{1,2}^{-/-}$ mice.

Role of H^+,K^+-ATPases in Bone Resorption and Ca^{2+} Homeostasis

Several lines of evidence suggest that $HK\alpha_1$-containing H^+,K^+-ATPases are present in bone and more specifically, osteoclasts. The H^+,K^+-ATPases may be involved in the acidification required for osteoclast-mediated bone resorption. Some of the earliest evidence for H^+,K^+-ATPases in bone showed that omeprazole, a gastric H^+,K^+-ATPase inhibitor, can inhibit bone resorption in an *in vitro* cell model of osteoclasts.[254] Later, physicians began to recognize that long term proton pump inhibitor therapy in humans produced a greater risk of hip fracture and decreased Ca^{2+} absorption by the gut.[255, 256] New studies have now shown that omeprazole inhibits bone resorption in Ca^{2+} phosphate cement in an *in vivo* model.[257] These studies all suggest that H^+,K^+-ATPases are present in osteoclasts and mediate osteoclast-induced acidification and resorption of bone.

Nevertheless, a definitive examination of H^+,K^+-ATPase subunit expression and activity within osteoclasts has not been performed. Our own preliminary assessment of HKα subunit mRNA expression by real time PCR in femoral bone homogenates from WT mice demonstrated a very low expression level of $HK\alpha_1$ (Ct equal to 35). However, measurement of $HK\alpha_1$ expression in isolated osteoclasts is needed to fully confirm localization to osteoclasts. These experiments are in progress in collaboration with Shannon Holliday (University of Florida). In future experiments, H^+,K^+-ATPase-mediated H^+ secretion should be measured in isolated osteoclasts from WT and $HK\alpha_1^{-/-}$ mice and bone density measurements should be compared between the two genotypes. These

studies will address whether $HK\alpha_1$-containing H^+,K^+-ATPases are required for appropriate bone resorption.

The proposed studies in $HK\alpha_1^{-/-}$ mice may be complicated by the requirement of gastric acid secretion for gut Ca^{2+} absorption. In fact, it has been observed that omeprazole decreases gut Ca^{2+} absorption in human paitients.[255] In a preliminary study, we observed that urinary Ca^{2+} excretion was considerably less in $HK\alpha_{1,2}^{-/-}$ than WT mice (Figure 6-7). Taken together, these data suggest either that gastric H^+,K^+-ATPases are required for Ca^{2+} absorption or that loss of osteoclast H^+,K^+-ATPase-mediated bone resorption affects Ca^{2+} balance. Tissue-specific knockout mice of $HK\alpha_1$ in the bone, if present, and stomach will be a useful tool to determine if disrupted Ca^{2+} excretion in $HK\alpha_1$ null mice results from a bone or gastric mechanism.

Final Conclusions

Our studies support further exploration of the mechanisms by which renal H^+,K^+-ATPases modulate Na^+ balance and of their potential involvement in blood pressure control. The role of sex hormones to regulate H^+,K^+-ATPase-mediated K^+ transport is another area of particular interest. Finally, it appears that H^+,K^+-ATPases may play hereto unforeseen but important parts in vasopressin-mediated H_2O reabsorption, obesity, and bone resorption. Much investigation is needed to understand the full importance of H^+,K^+-ATPases to renal physiology and in other tissues throughout the body.

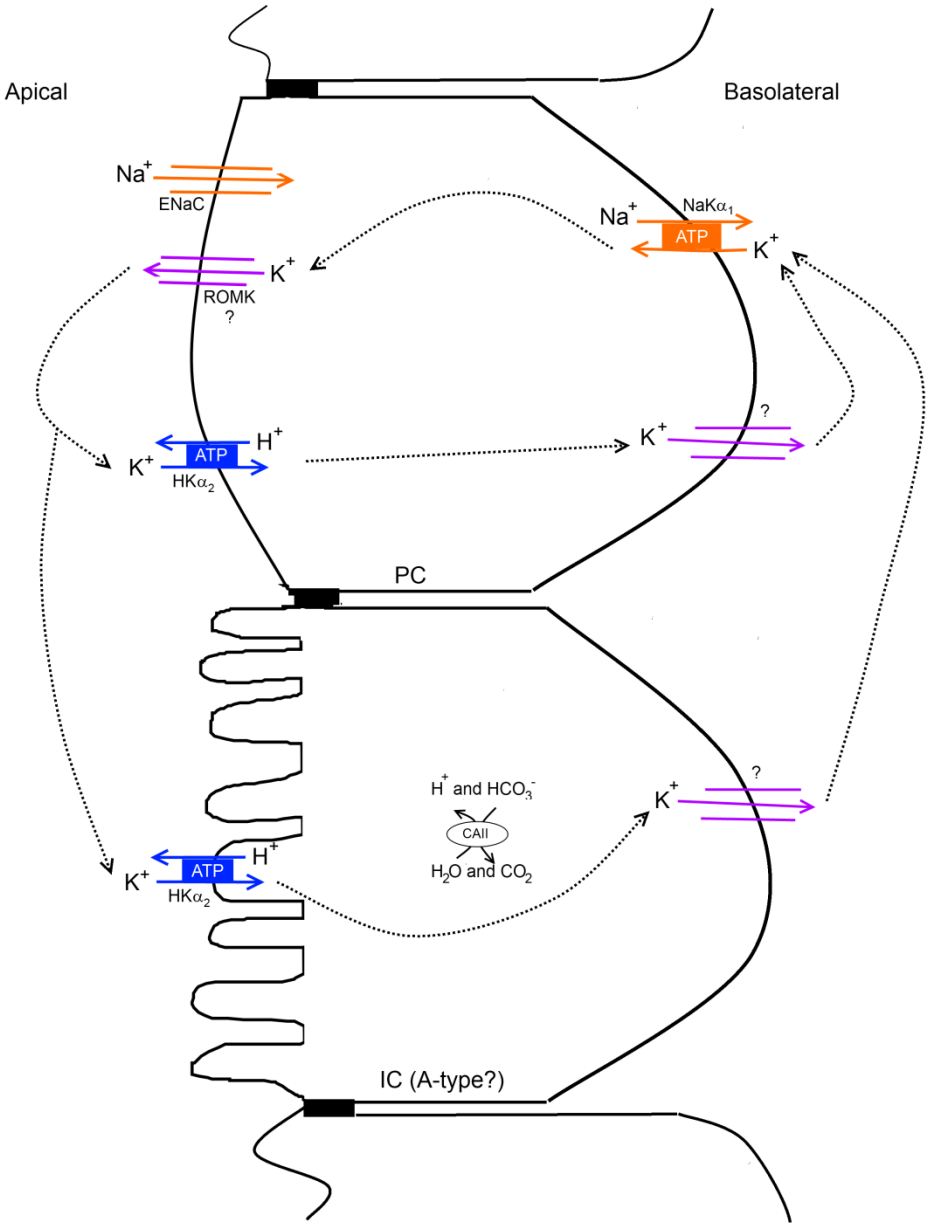

Figure 6-1. Proposed model of coupled ENaC-mediated Na^+ reabsorption and H^+,K^+-ATPase-mediated K^+ recycling in the collecting duct. In PCs, K^+ secretion is, in part, dependent on electrogenic Na^+ reabsorption through ENaC. $HK\alpha_2$-containing H^+,K^+-ATPases in PCs or ICs reabsorb the secreted K^+. The reabsorbed K^+ exits the basolateral membrane of these cells via unknown K^+ channels or cotransporters. The basolateral Na^+,K^+-ATPase of PCs uses the recycled K^+ to reabsorb intracellular Na^+ and maintain electrogenic Na^+ reabsorption through ENaC.

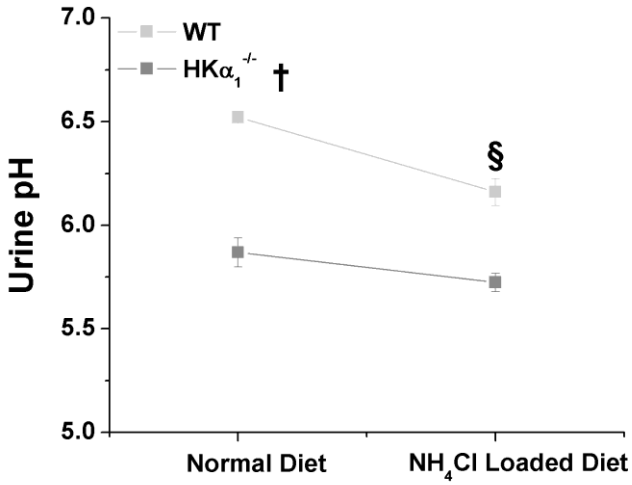

Figure 6-2. An acid-loaded diet did not further acidify urine from $HK\alpha_1^{-/-}$ mice. Urine pH was measured in WT and $HK\alpha_1^{-/-}$ mice pair fed a normal gel diet then switched to a 0.28M NH_4Cl- loaded diet for 6 days. Data are shown as mean ± SEM and were analyzed by two-way repeated measure ANOVA. † denotes $P<0.05$ versus WT. § denotes $P<0.05$ versus normal diet in same genotype. N=3.

tttgtggctgtcccgcatgccattttgatttgggtgtatgacgagatgcggaagttgttcatcaggctctaccctgg
aagctggtgggacaagaacatgtattat**taa**gaccatgtcactcacaggtctcccagcgggatatcagagatgttct
tcttcatgtctggctactcctcaggagatctctgcacaatgtgaacactaccgaaccccatacgagagagacttttc
tacagaaaactgtgtgaagcatacttagcttttgtattttaaagattgagatttaactgtttatatagaattttcat
ctctatgtctgcctccttatttttaaattatgtgaagttcagatgtcagcacagggaagaatatatttatacgtatat
caaggtcactgtgttaaataccttgtgtgtccaaggagtgtgctggggtctgccttaagctaggctgtgattcctc
aggcctcactttcttaccctcacagagacccagcagacccccctaaatccaccaaatgaacttttgtttgctggagt
ttaacctcaagcaaagagtaccaagtgacttaagtgctaatatttatttctaggaaaacattgccgagccctcgcca
gcaatcattgtatgtcagtcatgttttgtgttgtaatcgttagatgtattcatgtgtggcatgtatga**ctatgttga**
caggtccagtgaggccttgtttttaagtaaaagatgttttctat

Figure 6-3. Mmu-miR-505 potentially targets at a distal site in the 3' UTR of the mouse *Atp12a* ($HK\alpha_2$) gene. TargetScanMouse (www.targetscan.org) was used to identify conserved microRNA binding sites in the 3' untranslated region of *Atp12a*. The transcription stop site is shown in red lettering and the putative binding site for mmu-miR-505 is shown in blue lettering.

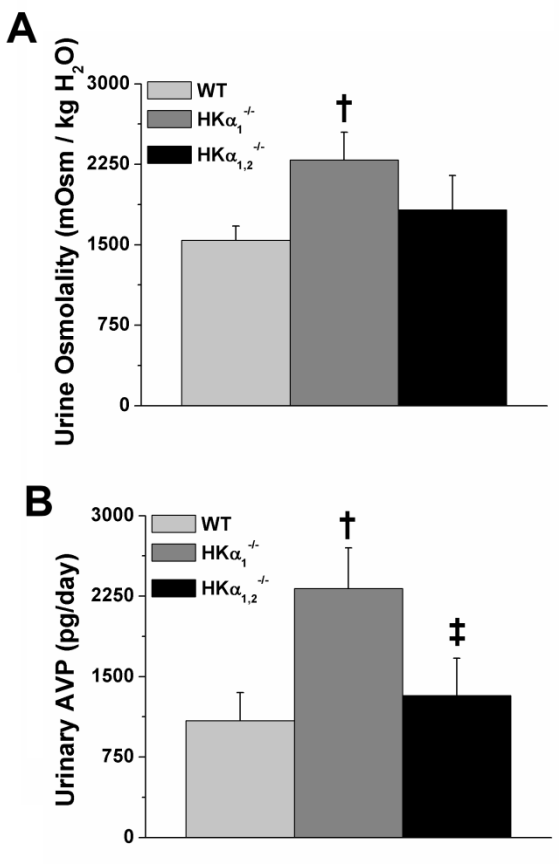

Figure 6-4. $HK\alpha_1^{-/-}$ mice exhibit more concentrated urine and enhanced vasopressin excretion. A) Urine osmolality and B) AVP levels were measured in urine samples from female WT, $HK\alpha_1^{-/-}$, and $HK\alpha_{1,2}^{-/-}$ mice pair fed a normal gel diet. Data are shown as mean ± SEM and were analyzed by one-way ANOVA with post hoc Holm-Sidak test. † denotes $P<0.05$ versus WT and ‡ versus $HK\alpha_1^{-/-}$ mice. N=3-8.

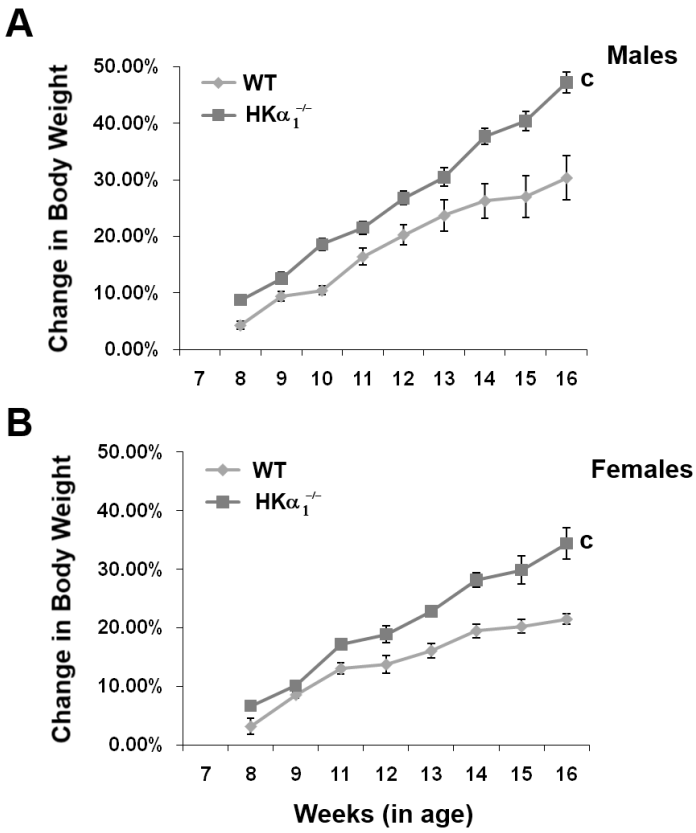

Figure 6-5. $HK\alpha_1^{-/-}$ gain significantly more weight than WT over eight weeks. Body weight, shown as % change from the age of 7 weeks, was measured each week over eight weeks in A) male and B) female WT and $HK\alpha_1^{-/-}$ mice. Data are shown as mean ± SEM and were analyzed by two-way repeated measure ANOVA. ^{c} denotes $P<0.05$ versus WT over the time course. N=5-8.

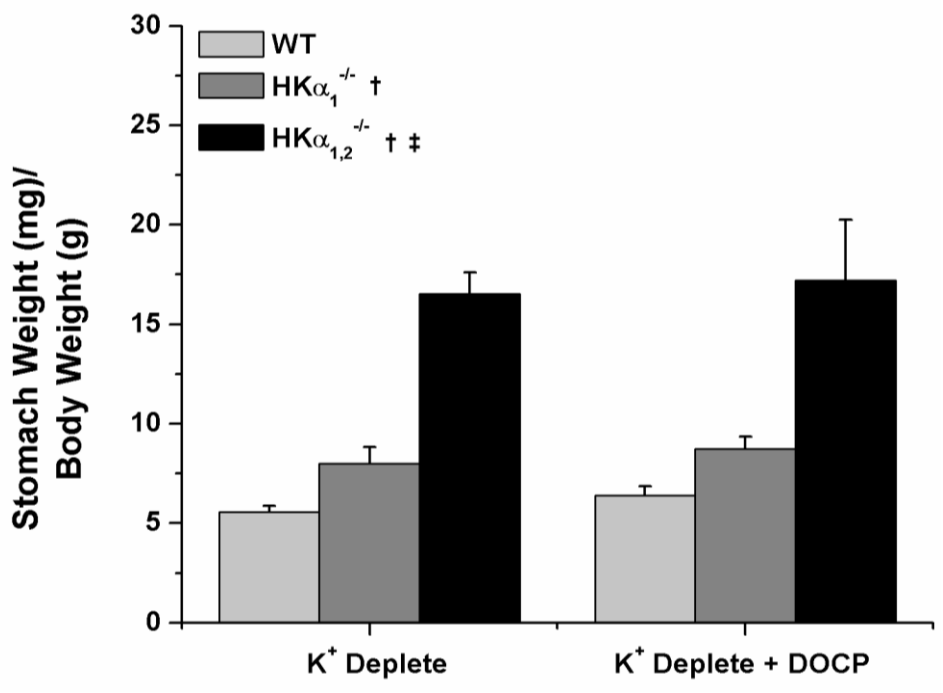

Figure 6-6. $HK\alpha_{1,2}^{-/-}$ mice exhibited more severe gastric hypertrophy than $HK\alpha_1^{-/-}$ mice. Stomach weights were measured in WT, $HK\alpha_1^{-/-}$, and $HK\alpha_{1,2}^{-/-}$ mice that were fed a K^+ depleted diet for 8 days. One half the mice were also treated with DOCP. Data are shown as mean ± SEM and were analyzed by two-way ANOVA with or without repeated measures followed by post-hoc Holm-Sidak test, where appropriate. † denotes $P<0.05$ versus WT and ‡ versus $HK\alpha_1^{-/-}$ mice regardless of DOCP treatment. N=3-4.

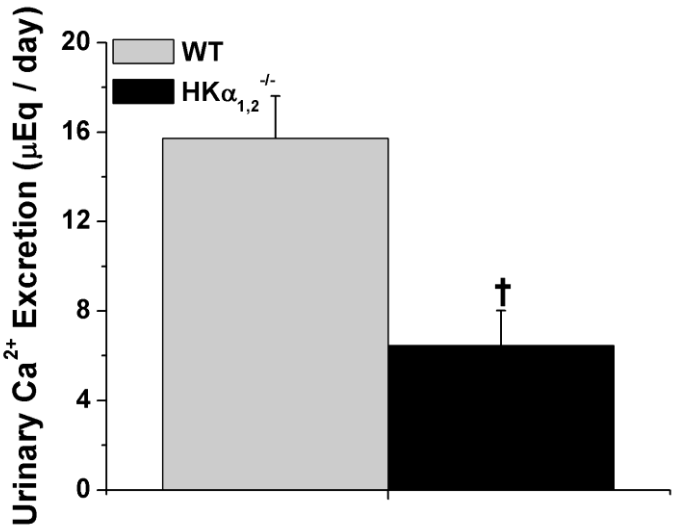

Figure 6-7. $HK\alpha_{1,2}^{-/-}$ mice excrete less urinary Ca^{2+} than WT mice. Urine $[Ca^{2+}]$ was measured in WT and $HK\alpha_{1,2}^{-/-}$ mice pair fed a normal gel diet. Data are shown as mean ± SEM and were analyzed by Student's *t*-test. † denotes $P<0.05$ versus WT. N=4.

LIST OF REFERENCES

1. Giebisch G, Windhager E: Organization of the Urinary System. In: *Medical Physiology,* 2nd ed. edited by Boron WF, Boulpaep EL, Philadelphia, PA, Saunders Elsevier, 2009, pp 749-766

2. Giebisch G, Windhager E: Glomerular Filtration and Renal Blood Flow. In: *Medical Physiology,* 2nd ed. edited by Boron WF, Boulpaep EL, Philadelphia, PA, Saunders Elsevier, 2009, pp 767-781

3. Meneton P, Ichikawa I, Inagami T, Schnermann J: Renal physiology of the mouse. *Am J Physiol Renal Physiol,* 278**:** F339-51, 2000

4. Aronson PS, Boron WF, Boulpaep EL: Transport of Solutes and Water. In: *Medical Physiology,* 2nd ed. edited by Boron WF, Boulpaep EL, Philadelphia, PA, Saunders Elsevier, 2009, pp 106-146

5. Giebisch G, Windhager E: Transport of Sodium and Chloride. In: *Medical Physiology,* 2nd ed. edited by Boron WF, Boulpaep EL, Philadelphia, PA, Saunders Elsevier, 2009, pp 782-796

6. Giebisch G, Krapf R, Wagner C: Renal and extrarenal regulation of potassium. *Kidney Int,* 72**:** 397-410, 2007

7. Wingo CS: Cortical collecting tubule potassium secretion: effect of amiloride, ouabain, and luminal sodium concentration. *Kidney Int,* 27**:** 886-91, 1985

8. Wingo CS: Potassium secretion by the cortical collecting tubule: effect of C1 gradients and ouabain. *Am J Physiol,* 256**:** F306-13, 1989

9. Rieg T, Vallon V, Sausbier M, Sausbier U, Kaissling B, Ruth P, Osswald H: The role of the BK channel in potassium homeostasis and flow-induced renal potassium excretion. *Kidney Int,* 72**:** 566-73, 2007

10. Pluznick JL, Wei P, Grimm PR, Sansom SC: BK-{beta}1 subunit: immunolocalization in the mammalian connecting tubule and its role in the kaliuretic response to volume expansion. *Am J Physiol Renal Physiol,* 288**:** F846-54, 2005

11. Zhou X, Lynch IJ, Xia SL, Wingo CS: Activation of H^+-K^+-ATPase by CO(2) requires a basolateral Ba^{2+}-sensitive pathway during K restriction. *Am J Physiol Renal Physiol,* 279**:** F153-60, 2000

12. Zhou X, Wingo CS: Stimulation of total CO2 flux by 10% CO2 in rabbit CCD: role of an apical Sch-28080- and Ba-sensitive mechanism. *Am J Physiol,* 267**:** F114-20, 1994

13. Giebisch G, Windhager E: Transport of Potassium. In: *Medical Physiology,* 2nd ed. edited by Boron WF, Boulpaep EL, Philadelphia, PA, Saunders Elsevier, 2009, pp 821-834

14. Giebisch G, Windhager E: Transport of Acids and Bases. In: *Medical Physiology,* 2nd ed. edited by Boron WF, Boulpaep EL, Philadelphia, PA, Saunders Elsevier, 2009, pp 851-865

15. Weiner ID, Verlander JW: Role of NH_3 and NH_4^+ transporters in renal acid-base transport. *Am J Physiol Renal Physiol,* 300**:** F11-23, 2011

16. Wall SM: Recent advances in our understanding of intercalated cells. *Curr Opin Nephrol Hypertens,* 14**:** 480-4, 2005

17. Giebisch G, Windhager E: Integration of Salt and Water Balance. In: *Medical Physiology,* 2nd ed. edited by Boron WF, Boulpaep EL, Philadelphia, PA, Saunders Elsevier, 2009, pp 866-880

18. Spat A: Glomerulosa cell--a unique sensor of extracellular K^+ concentration. *Mol Cell Endocrinol,* 217**:** 23-6, 2004

19. Williams GH: Aldosterone biosynthesis, regulation, and classical mechanism of action. *Heart Fail Rev,* 10**:** 7-13, 2005

20. Kim GH, Masilamani S, Turner R, Mitchell C, Wade JB, Knepper MA: The thiazide-sensitive Na-Cl cotransporter is an aldosterone-induced protein. *Proc Natl Acad Sci U S A,* 95**:** 14552-7, 1998

21. Eaton DC, Malik B, Saxena NC, Al-Khalili OK, Yue G: Mechanisms of aldosterone's action on epithelial Na^+ transport. *J Membr Biol,* 184**:** 313-9, 2001

22. Good DW, George T, Watts BA, 3rd: Nongenomic regulation by aldosterone of the epithelial NHE3 Na^+/H^+ exchanger. *Am J Physiol Cell Physiol,* 290**:** C757-63, 2006

23. Drumm K, Kress TR, Gassner B, Krug AW, Gekle M: Aldosterone stimulates activity and surface expression of NHE3 in human primary proximal tubule epithelial cells (RPTEC). *Cell Physiol Biochem,* 17**:** 21-8, 2006

24. Krug AW, Papavassiliou F, Hopfer U, Ullrich KJ, Gekle M: Aldosterone stimulates surface expression of NHE3 in renal proximal brush borders. *Pflugers Arch,* 446**:** 492-6, 2003

25. Boscaro M, Ronconi V, Turchi F, Giacchetti G: Diagnosis and management of primary aldosteronism. *Curr Opin Endocrinol Diabetes Obes,* 15**:** 332-8, 2008

26. Fuller PJ, Young MJ: Mechanisms of mineralocorticoid action. *Hypertension,* 46**:** 1227-35, 2005

27. Khanna A, Kurtzman NA: Metabolic alkalosis. *J Nephrol,* 19 Suppl 9**:** S86-96, 2006

28. Field MJ, Stanton BA, Giebisch GH: Differential acute effects of aldosterone, dexamethasone, and hyperkalemia on distal tubular potassium secretion in the rat kidney. *J Clin Invest,* 74**:** 1792-802, 1984

29. Wingo CS: Effect of ouabain on K secretion in cortical collecting tubules from adrenalectomized rabbits. *Am J Physiol,* 247**:** F588-95, 1984

30. Sorensen MV, Matos JE, Sausbier M, Sausbier U, Ruth P, Praetorius HA, Leipziger J: Aldosterone increases KCa1.1 (BK) channel-mediated colonic K^+ secretion. *J Physiol,* 586**:** 4251-64, 2008

31. Greenlee M, Wingo CS, McDonough AA, Youn JH, Kone BC: Narrative review: evolving concepts in potassium homeostasis and hypokalemia. *Ann Intern Med,* 150**:** 619-25, 2009

32. Wingo CS, Kokko JP, Jacobson HR: Effects of in vitro aldosterone on the rabbit cortical collecting tubule. *Kidney Int,* 28**:** 51-7, 1985

33. Rabinowitz L: Aldosterone and potassium homeostasis. *Kidney Int,* 49**:** 1738-42, 1996

34. Frindt G, Palmer LG: K^+ secretion in the rat kidney: Na^+ channel-dependent and -independent mechanisms. *Am J Physiol Renal Physiol,* 297**:** F389-96, 2009

35. Welbourne TC, Francoeur D: Influence of aldosterone on renal ammonia production. *Am J Physiol,* 233**:** E56-60, 1977

36. Wagner CA, Devuyst O, Bourgeois S, Mohebbi N: Regulated acid-base transport in the collecting duct. *Pflugers Arch,* 458**:** 137-56, 2009

37. Dubrovsky AH, Nair RC, Byers MK, Levine DZ: Renal net acid excretion in the adrenalectomized rat. *Kidney Int,* 19**:** 516-28, 1981

38. Winter C, Schulz N, Giebisch G, Geibel JP, Wagner CA: Nongenomic stimulation of vacuolar H^+-ATPases in intercalated renal tubule cells by aldosterone. *Proc Natl Acad Sci U S A,* 101**:** 2636-41, 2004

39. Dos Santos PM, Freitas FP, Mendes J, Tararthuch AL, Fernandez R: Differential regulation of H^+-ATPases in MDCK-C11 cells by aldosterone and vasopressin. *Can J Physiol Pharmacol,* 87**:** 653-65, 2009

40. Gekle M, Silbernagl S, Oberleithner H: The mineralocorticoid aldosterone activates a proton conductance in cultured kidney cells. *Am J Physiol,* 273**:** C1673-8, 1997

41. Eiam-Ong S, Kurtzman NA, Sabatini S: Regulation of collecting tubule adenosine triphosphatases by aldosterone and potassium. *J Clin Invest,* 91**:** 2385-92, 1993

42. Barrett EJ: Organization of Endocrine Control. In: *Medical Physiology,* 2nd ed. edited by Boron WF, Boulpaep EL, Philadelphia, PA, Saunders Elsevier, 2009, pp 1011-1027

43. Giebisch G, Windhager E: Urine Concentration and Dilution. In: *Medical Physiology,* 2nd ed. edited by Boron WF, Boulpaep EL, Philadelphia, PA, Saunders Elsevier, 2009, pp 835-850

44. Noda Y, Sohara E, Ohta E, Sasaki S: Aquaporins in kidney pathophysiology. *Nat Rev Nephrol,* 6**:** 168-78, 2010

45. Bugaj V, Pochynyuk O, Stockand JD: Activation of the epithelial Na^+ channel in the collecting duct by vasopressin contributes to water reabsorption. *Am J Physiol Renal Physiol,* 297**:** F1411-8, 2009

46. Kohan DE: The renal medullary endothelin system in control of sodium and water excretion and systemic blood pressure. *Curr Opin Nephrol Hypertens,* 15**:** 34-40, 2006

47. Kohan DE: Endothelin, hypertension and chronic kidney disease: new insights. *Curr Opin Nephrol Hypertens,* 19**:** 134-9, 2010

48. Davenport AP, Kuc RE, Maguire JJ, Harland SP: ETA receptors predominate in the human vasculature and mediate constriction. *J Cardiovasc Pharmacol,* 26 Suppl 3**:** S265-7, 1995

49. Bugaj V, Pochynyuk O, Mironova E, Vandewalle A, Medina JL, Stockand JD: Regulation of the epithelial Na^+ channel by endothelin-1 in rat collecting duct. *Am J Physiol Renal Physiol,* 295**:** F1063-70, 2008

50. Nakano D, Pollock JS, Pollock DM: Renal medullary ETB receptors produce diuresis and natriuresis via NOS1. *Am J Physiol Renal Physiol,* 294**:** F1205-11, 2008

51. Wesson DE: Endothelin role in kidney acidification. *Semin Nephrol,* 26**:** 393-8, 2006

52. Wesson DE: Regulation of kidney acid excretion by endothelins. *Kidney Int,* 70**:** 2066-73, 2006

53. Laghmani K, Preisig PA, Alpern RJ: The role of endothelin in proximal tubule proton secretion and the adaptation to a chronic metabolic acidosis. *J Nephrol,* 15 Suppl 5**:** S75-87, 2002

54. Laghmani K, Preisig PA, Moe OW, Yanagisawa M, Alpern RJ: Endothelin-1/endothelin-B receptor-mediated increases in NHE3 activity in chronic metabolic acidosis. *J Clin Invest,* 107**:** 1563-9, 2001

55. Laghmani K, Sakamoto A, Yanagisawa M, Preisig PA, Alpern RJ: A consensus sequence in the endothelin-B receptor second intracellular loop is required for NHE3 activation by endothelin-1. *Am J Physiol Renal Physiol,* 288**:** F732-9, 2005

56. Khanna A, Simoni J, Hacker C, Duran MJ, Wesson DE: Increased endothelin activity mediates augmented distal nephron acidification induced by dietary protein. *Trans Am Clin Climatol Assoc,* 116**:** 239-56; discussion 257-8, 2005

57. Teng-umnuay P, Verlander JW, Yuan W, Tisher CC, Madsen KM: Identification of distinct subpopulations of intercalated cells in the mouse collecting duct. *J Am Soc Nephrol,* 7**:** 260-74, 1996

58. Gormley K, Dong Y, Sagnella GA: Regulation of the epithelial sodium channel by accessory proteins. *Biochem J,* 371**:** 1-14, 2003

59. Frindt G, Ergonul Z, Palmer LG: Na channel expression and activity in the medullary collecting duct of rat kidney. *Am J Physiol Renal Physiol,* 292**:** F1190-6, 2007

60. Chen SY, Bhargava A, Mastroberardino L, Meijer OC, Wang J, Buse P, Firestone GL, Verrey F, Pearce D: Epithelial sodium channel regulated by aldosterone-induced protein sgk. *Proc Natl Acad Sci U S A,* 96**:** 2514-9, 1999

61. Verrey F, Schaerer E, Zoerkler P, Paccolat MP, Geering K, Kraehenbuhl JP, Rossier BC: Regulation by aldosterone of Na^+,K^+-ATPase mRNAs, protein synthesis, and sodium transport in cultured kidney cells. *J Cell Biol,* 104**:** 1231-7, 1987

62. Verrey F, Summa V, Heitzmann D, Mordasini D, Vandewalle A, Feraille E, Zecevic M: Short-term aldosterone action on Na,K-ATPase surface expression: role of aldosterone-induced SGK1? *Ann N Y Acad Sci,* 986**:** 554-61, 2003

63. Spindler B, Mastroberardino L, Custer M, Verrey F: Characterization of early aldosterone-induced RNAs identified in A6 kidney epithelia. *Pflugers Arch,* 434**:** 323-31, 1997

64. Stow LR, Gumz ML, Lynch IJ, Greenlee MM, Rudin A, Cain BD, Wingo CS: Aldosterone modulates steroid receptor binding to the endothelin-1 gene (edn1). *J Biol Chem,* 284**:** 30087-96, 2009

65. Pochynyuk O, Bugaj V, Stockand JD: Physiologic regulation of the epithelial sodium channel by phosphatidylinositides. *Curr Opin Nephrol Hypertens,* 17**:** 533-40, 2008

66. Rubera I, Loffing J, Palmer LG, Frindt G, Fowler-Jaeger N, Sauter D, Carroll T, McMahon A, Hummler E, Rossier BC: Collecting duct-specific gene inactivation of alphaENaC in the mouse kidney does not impair sodium and potassium balance. *J Clin Invest,* 112**:** 554-65, 2003

67. Pradervand S, Barker PM, Wang Q, Ernst SA, Beermann F, Grubb BR, Burnier M, Schmidt A, Bindels RJ, Gatzy JT, Rossier BC, Hummler E: Salt restriction induces pseudohypoaldosteronism type 1 in mice expressing low levels of the beta-subunit of the amiloride-sensitive epithelial sodium channel. *Proc Natl Acad Sci U S A,* 96**:** 1732-7, 1999

68. Christensen BM, Perrier R, Wang Q, Zuber AM, Maillard M, Mordasini D, Malsure S, Ronzaud C, Stehle JC, Rossier BC, Hummler E: Sodium and potassium balance depends on alphaENaC expression in connecting tubule. *J Am Soc Nephrol,* 21**:** 1942-51, 2010

69. Leviel F, Hubner CA, Houillier P, Morla L, El Moghrabi S, Brideau G, Hatim H, Parker MD, Kurth I, Kougioumtzes A, Sinning A, Pech V, Riemondy KA, Miller RL, Hummler E, Shull GE, Aronson PS, Doucet A, Wall SM, Chambrey R, Eladari D: The Na^+-dependent chloride-bicarbonate exchanger SLC4A8 mediates an electroneutral Na^+ reabsorption process in the renal cortical collecting ducts of mice. *J Clin Invest,* 120**:** 1627-35, 2010

70. Bouley R, Lu HA, Nunes P, Da Silva N, McLaughlin M, Chen Y, Brown D: Calcitonin has a vasopressin-like effect on aquaporin-2 trafficking and urinary concentration. *J Am Soc Nephrol,* 22**:** 59-72, 2011

71. Terada Y, Tomita K, Nonoguchi H, Yang T, Marumo F: Different localization and regulation of two types of vasopressin receptor messenger RNA in microdissected rat nephron segments using reverse transcription polymerase chain reaction. *J Clin Invest,* 92**:** 2339-45, 1993

72. Carmosino M, Brooks HL, Cai Q, Davis LS, Opalenik S, Hao C, Breyer MD: Axial heterogeneity of vasopressin-receptor subtypes along the human and mouse collecting duct. *Am J Physiol Renal Physiol,* 292**:** F351-60, 2007

73. Memetimin H, Izumi Y, Nakayama Y, Kohda Y, Inoue H, Nonoguchi H, Tomita K: Low pH stimulates vasopressin V2 receptor promoter activity and enhances downregulation induced by V1a receptor stimulation. *Am J Physiol Renal Physiol,* 297**:** F620-8, 2009

74. Amlal H, Krane CM, Chen Q, Soleimani M: Early polyuria and urinary concentrating defect in potassium deprivation. *Am J Physiol Renal Physiol,* 279**:** F655-63, 2000

75. Ma T, Song Y, Yang B, Gillespie A, Carlson EJ, Epstein CJ, Verkman AS: Nephrogenic diabetes insipidus in mice lacking aquaporin-3 water channels. *Proc Natl Acad Sci U S A,* 97**:** 4386-91, 2000

76. Chou CL, Ma T, Yang B, Knepper MA, Verkman AS: Fourfold reduction of water permeability in inner medullary collecting duct of aquaporin-4 knockout mice. *Am J Physiol,* 274**:** C549-54, 1998

77. Wang WH, Giebisch G: Regulation of potassium (K) handling in the renal collecting duct. *Pflugers Arch,* 458**:** 157-68, 2009

78. Frindt G, Palmer LG: Ca-activated K channels in apical membrane of mammalian CCT, and their role in K secretion. *Am J Physiol,* 252**:** F458-67, 1987

79. Frindt G, Palmer LG: Low-conductance K channels in apical membrane of rat cortical collecting tubule. *Am J Physiol,* 256**:** F143-51, 1989

80. Frindt G, Palmer LG: Apical potassium channels in the rat connecting tubule. *Am J Physiol Renal Physiol,* 287**:** F1030-7, 2004

81. Mennitt PA, Wade JB, Ecelbarger CA, Palmer LG, Frindt G: Localization of ROMK channels in the rat kidney. *J Am Soc Nephrol,* 8**:** 1823-30, 1997

82. Pacha J, Frindt G, Sackin H, Palmer LG: Apical maxi K channels in intercalated cells of CCT. *Am J Physiol,* 261**:** F696-705, 1991

83. Najjar F, Zhou H, Morimoto T, Bruns JB, Li HS, Liu W, Kleyman TR, Satlin LM: Dietary K^+ regulates apical membrane expression of maxi-K channels in rabbit cortical collecting duct. *Am J Physiol Renal Physiol,* 289**:** F922-32, 2005

84. Woda CB, Bragin A, Kleyman TR, Satlin LM: Flow-dependent K^+ secretion in the cortical collecting duct is mediated by a maxi-K channel. *Am J Physiol Renal Physiol,* 280**:** F786-93, 2001

85. Wingo CS: Reversible chloride-dependent potassium flux across the rabbit cortical collecting tubule. *Am J Physiol,* 256**:** F697-704, 1989

86. Greenlee MM, Lynch IJ, Gumz ML, Cain BD, Wingo CS: The renal H,K-ATPases. *Curr Opin Nephrol Hypertens*, 2010

87. Gumz ML, Lynch IJ, Greenlee MM, Cain BD, Wingo CS: The renal H^+-K^+-ATPases: physiology, regulation, and structure. *Am J Physiol Renal Physiol,* 298**:** F12-21, 2010

88. Lynch IJ, Greenlee MM, Gumz ML, Rudin A, Xia SL, Wingo CS: Heterogeneity of H-K-ATPase-mediated acid secretion along the mouse collecting duct. *Am J Physiol Renal Physiol,* 298**:** F408-15, 2010

89. Lynch IJ, Rudin A, Xia SL, Stow LR, Shull GE, Weiner ID, Cain BD, Wingo CS: Impaired acid secretion in cortical collecting duct intercalated cells from H-K-ATPase-deficient mice: role of HKalpha isoforms. *Am J Physiol Renal Physiol,* 294**:** F621-7, 2008

90. Verlander JW, Moudy RM, Campbell WG, Cain BD, Wingo CS: Immunohistochemical localization of H-K-ATPase alpha(2c)-subunit in rabbit kidney. *Am J Physiol Renal Physiol,* 281**:** F357-65, 2001

91. Huang CL, Kuo E: Mechanisms of disease: WNK-ing at the mechanism of salt-sensitive hypertension. *Nat Clin Pract Nephrol,* 3**:** 623-30, 2007

92. Lazrak A, Liu Z, Huang CL: Antagonistic regulation of ROMK by long and kidney-specific WNK1 isoforms. *Proc Natl Acad Sci U S A,* 103**:** 1615-20, 2006

93. Palmer LG, Frindt G: Aldosterone and potassium secretion by the cortical collecting duct. *Kidney Int,* 57**:** 1324-8, 2000

94. Fodstad H, Gonzalez-Rodriguez E, Bron S, Gaeggeler H, Guisan B, Rossier BC, Horisberger JD: Effects of mineralocorticoid and K^+ concentration on K^+ secretion and ROMK channel expression in a mouse cortical collecting duct cell line. *Am J Physiol Renal Physiol,* 296**:** F966-75, 2009

95. Wingo CS, Seldin DW, Kokko JP, Jacobson HR: Dietary modulation of active potassium secretion in the cortical collecting tubule of adrenalectomized rabbits. *J Clin Invest,* 70**:** 579-86, 1982

96. Babilonia E, Li D, Wang Z, Sun P, Lin DH, Jin Y, Wang WH: Mitogen-activated protein kinases inhibit the ROMK (Kir 1.1)-like small conductance K channels in the cortical collecting duct. *J Am Soc Nephrol,* 17**:** 2687-96, 2006

97. Li D, Wang Z, Sun P, Jin Y, Lin DH, Hebert SC, Giebisch G, Wang WH: Inhibition of MAPK stimulates the Ca^{2+} -dependent big-conductance K channels in cortical collecting duct. *Proc Natl Acad Sci U S A,* 103**:** 19569-74, 2006

98. Schulz N, Dave MH, Stehberger PA, Chau T, Wagner CA: Differential localization of vacuolar H^+-ATPases containing a1, a2, a3, or a4 (ATP6V0A1-4) subunit isoforms along the nephron. *Cell Physiol Biochem,* 20**:** 109-20, 2007

99. Smith AN, Skaug J, Choate KA, Nayir A, Bakkaloglu A, Ozen S, Hulton SA, Sanjad SA, Al-Sabban EA, Lifton RP, Scherer SW, Karet FE: Mutations in ATP6N1B, encoding a new kidney vacuolar proton pump 116-kD subunit, cause recessive distal renal tubular acidosis with preserved hearing. *Nat Genet,* 26**:** 71-5, 2000

100. Cheval L, Morla L, Elalouf JM, Doucet A: Kidney collecting duct acid-base "regulon". *Physiol Genomics,* 27**:** 271-81, 2006

101. Fejes-Toth G, Naray-Fejes-Toth A: Effect of acid/base balance on H-ATPase 31 kD subunit mRNA levels in collecting duct cells. *Kidney Int,* 48**:** 1420-6, 1995

102. Narbaitz R, Murugesan S, Levine DZ: K depletion and NH_4Cl acidosis increase apical insertion of studded membrane in type A intercalated cells. *Am J Physiol,* 270**:** F649-56, 1996

103. Purkerson JM, Tsuruoka S, Suter DZ, Nakamori A, Schwartz GJ: Adaptation to metabolic acidosis and its recovery are associated with changes in anion exchanger distribution and expression in the cortical collecting duct. *Kidney Int,* 78**:** 993-1005, 2010

104. Tsuruoka S, Schwartz GJ: Metabolic acidosis stimulates H^+ secretion in the rabbit outer medullary collecting duct (inner stripe) of the kidney. *J Clin Invest,* 99**:** 1420-31, 1997

105. Verlander JW, Madsen KM, Cannon JK, Tisher CC: Activation of acid-secreting intercalated cells in rabbit collecting duct with ammonium chloride loading. *Am J Physiol,* 266**:** F633-45, 1994

106. Sabolic I, Brown D, Gluck SL, Alper SL: Regulation of AE1 anion exchanger and H^+-ATPase in rat cortex by acute metabolic acidosis and alkalosis. *Kidney Int,* 51**:** 125-37, 1997

107. Schwartz JH, Alexander EA: Adaptation of intercalated cells along the collecting duct to systemic acid/base changes. *Kidney Int,* 78**:** 949-51, 2010

108. Verlander JW, Madsen KM, Galla JH, Luke RG, Tisher CC: Response of intercalated cells to chloride depletion metabolic alkalosis. *Am J Physiol,* 262**:** F309-19, 1992

109. Finberg KE, Wagner CA, Bailey MA, Paunescu TG, Breton S, Brown D, Giebisch G, Geibel JP, Lifton RP: The B1-subunit of the H^+ ATPase is required for maximal urinary acidification. *Proc Natl Acad Sci U S A,* 102**:** 13616-21, 2005

110. Valles P, Wysocki J, Salabat MR, Cokic I, Ye M, LaPointe MS, Batlle D: Angiotensin II increases H^+-ATPase B1 subunit expression in medullary collecting ducts. *Hypertension,* 45**:** 818-23, 2005

111. Rothenberger F, Velic A, Stehberger PA, Kovacikova J, Wagner CA: Angiotensin II stimulates vacuolar H^+ -ATPase activity in renal acid-secretory intercalated cells from the outer medullary collecting duct. *J Am Soc Nephrol,* 18**:** 2085-93, 2007

112. Laing CM, Toye AM, Capasso G, Unwin RJ: Renal tubular acidosis: developments in our understanding of the molecular basis. *Int J Biochem Cell Biol,* 37**:** 1151-61, 2005

113. Stehberger PA, Shmukler BE, Stuart-Tilley AK, Peters LL, Alper SL, Wagner CA: Distal renal tubular acidosis in mice lacking the AE1 (band3) Cl-/HCO3- exchanger (slc4a1). *J Am Soc Nephrol,* 18**:** 1408-18, 2007

114. Karet FE, Gainza FJ, Gyory AZ, Unwin RJ, Wrong O, Tanner MJ, Nayir A, Alpay H, Santos F, Hulton SA, Bakkaloglu A, Ozen S, Cunningham MJ, di Pietro A, Walker WG, Lifton RP: Mutations in the chloride-bicarbonate exchanger gene AE1 cause autosomal dominant but not autosomal recessive distal renal tubular acidosis. *Proc Natl Acad Sci U S A,* 95**:** 6337-42, 1998

115. Amlal H, Petrovic S, Xu J, Wang Z, Sun X, Barone S, Soleimani M: Deletion of the anion exchanger Slc26a4 (pendrin) decreases apical Cl(-)/HCO3(-) exchanger activity and impairs bicarbonate secretion in kidney collecting duct. *Am J Physiol Cell Physiol,* 299**:** C33-41, 2010

116. Frische S, Kwon TH, Frokiaer J, Madsen KM, Nielsen S: Regulated expression of pendrin in rat kidney in response to chronic NH_4Cl or $NaHCO_3$ loading. *Am J Physiol Renal Physiol,* 284**:** F584-93, 2003

117. Quentin F, Chambrey R, Trinh-Trang-Tan MM, Fysekidis M, Cambillau M, Paillard M, Aronson PS, Eladari D: The Cl-/HCO3- exchanger pendrin in the rat kidney is regulated in response to chronic alterations in chloride balance. *Am J Physiol Renal Physiol,* 287**:** F1179-88, 2004

118. Verlander JW, Hassell KA, Royaux IE, Glapion DM, Wang ME, Everett LA, Green ED, Wall SM: Deoxycorticosterone upregulates PDS (Slc26a4) in mouse kidney: role of pendrin in mineralocorticoid-induced hypertension. *Hypertension,* 42**:** 356-62, 2003

119. Verlander JW, Kim YH, Shin W, Pham TD, Hassell KA, Beierwaltes WH, Green ED, Everett L, Matthews SW, Wall SM: Dietary Cl(-) restriction upregulates pendrin expression within the apical plasma membrane of type B intercalated cells. *Am J Physiol Renal Physiol,* 291**:** F833-9, 2006

120. Wall SM, Kim YH, Stanley L, Glapion DM, Everett LA, Green ED, Verlander JW: NaCl restriction upregulates renal Slc26a4 through subcellular redistribution: role in Cl- conservation. *Hypertension,* 44**:** 982-7, 2004

121. Pech V, Pham TD, Hong S, Weinstein AM, Spencer KB, Duke BJ, Walp E, Kim YH, Sutliff RL, Bao HF, Eaton DC, Wall SM: Pendrin modulates ENaC function by changing luminal HCO3. *J Am Soc Nephrol,* 21**:** 1928-41, 2010

122. Kim YH, Pech V, Spencer KB, Beierwaltes WH, Everett LA, Green ED, Shin W, Verlander JW, Sutliff RL, Wall SM: Reduced ENaC protein abundance contributes to the lower blood pressure observed in pendrin-null mice. *Am J Physiol Renal Physiol,* 293**:** F1314-24, 2007

123. Kim HY, Verlander JW, Bishop JM, Cain BD, Han KH, Igarashi P, Lee HW, Handlogten ME, Weiner ID: Basolateral expression of the ammonia transporter family member Rh C glycoprotein in the mouse kidney. *Am J Physiol Renal Physiol,* 296**:** F543-55, 2009

124. Verlander JW, Miller RT, Frank AE, Royaux IE, Kim YH, Weiner ID: Localization of the ammonium transporter proteins RhBG and RhCG in mouse kidney. *Am J Physiol Renal Physiol,* 284**:** F323-37, 2003

125. Bishop JM, Verlander JW, Lee HW, Nelson RD, Weiner AJ, Handlogten ME, Weiner ID: Role of the Rhesus glycoprotein, Rh B glycoprotein, in renal ammonia excretion. *Am J Physiol Renal Physiol,* 299**:** F1065-77, 2010

126. Lee HW, Verlander JW, Bishop JM, Nelson RD, Handlogten ME, Weiner ID: Effect of intercalated cell-specific Rh C glycoprotein deletion on basal and metabolic acidosis-stimulated renal ammonia excretion. *Am J Physiol Renal Physiol,* 299**:** F369-79, 2010

127. Seshadri RM, Klein JD, Kozlowski S, Sands JM, Kim YH, Han KH, Handlogten ME, Verlander JW, Weiner ID: Renal expression of the ammonia transporters, Rhbg and Rhcg, in response to chronic metabolic acidosis. *Am J Physiol Renal Physiol,* 290**:** F397-408, 2006

128. Lee HW, Verlander JW, Bishop JM, Igarashi P, Handlogten ME, Weiner ID: Collecting duct-specific Rh C glycoprotein deletion alters basal and acidosis-stimulated renal ammonia excretion. *Am J Physiol Renal Physiol,* 296**:** F1364-75, 2009

129. Ganser AL, Forte JG: K^+-stimulated ATPase in purified microsomes of bullfrog oxyntic cells. *Biochim Biophys Acta,* 307**:** 169-80, 1973

130. Sachs G, Chang HH, Rabon E, Schackman R, Lewin M, Saccomani G: A nonelectrogenic H^+ pump in plasma membranes of hog stomach. *J Biol Chem,* 251**:** 7690-8, 1976

131. Gustin MC, Goodman DB: Isolation of brush-border membrane from the rabbit descending colon epithelium. Partial characterization of a unique K^+-activated ATPase. *J Biol Chem,* 256**:** 10651-6, 1981

132. Kaunitz JD, Sachs G: Identification of a vanadate-sensitive potassium-dependent proton pump from rabbit colon. *J Biol Chem,* 261**:** 14005-10, 1986

133. Doucet A, Marsy S: Characterization of K-ATPase activity in distal nephron: stimulation by potassium depletion. *Am J Physiol,* 253**:** F418-23, 1987

134. Garg LC, Narang N: Ouabain-insensitive K-adenosine triphosphatase in distal nephron segments of the rabbit. *J Clin Invest,* 81**:** 1204-8, 1988

135. Wingo CS: Active proton secretion and potassium absorption in the rabbit outer medullary collecting duct. Functional evidence for proton-potassium-activated adenosine triphosphatase. *J Clin Invest,* 84**:** 361-5, 1989

136. Rabon EC, McFall TL, Sachs G: The gastric [H,K]ATPase:H^+/ATP stoichiometry. *J Biol Chem,* 257**:** 6296-9, 1982

137. Geering K: FXYD proteins: new regulators of Na-K-ATPase. *Am J Physiol Renal Physiol,* 290**:** F241-50, 2006

138. Gumz ML, Duda D, McKenna R, Wingo CS, Cain BD: Molecular modeling of the rabbit colonic (HKalpha2a) H^+, K^+ ATPase. *J Mol Model,* 9**:** 283-9, 2003

139. Beggah AT, Beguin P, Bamberg K, Sachs G, Geering K: beta-subunit assembly is essential for the correct packing and the stable membrane insertion of the H,K-ATPase alpha-subunit. *J Biol Chem,* 274**:** 8217-23, 1999

140. Vagin O, Turdikulova S, Sachs G: The H,K-ATPase beta subunit as a model to study the role of N-glycosylation in membrane trafficking and apical sorting. *J Biol Chem,* 279**:** 39026-34, 2004

141. Vagin O, Denevich S, Sachs G: Plasma membrane delivery of the gastric H,K-ATPase: the role of beta-subunit glycosylation. *Am J Physiol Cell Physiol,* 285**:** C968-76, 2003

142. Codina J, Kone BC, Delmas-Mata JT, DuBose TD, Jr.: Functional expression of the colonic H^+,K^+-ATPase alpha-subunit. Pharmacologic properties and assembly with X^+,K^+-ATPase beta-subunits. *J Biol Chem,* 271**:** 29759-63, 1996

143. Sangan P, Thevananther S, Sangan S, Rajendran VM, Binder HJ: Colonic H-K-ATPase alpha- and beta-subunits express ouabain-insensitive H-K-ATPase. *Am J Physiol Cell Physiol,* 278**:** C182-9, 2000

144. Sangan P, Kolla SS, Rajendran VM, Kashgarian M, Binder HJ: Colonic H-K-ATPase beta-subunit: identification in apical membranes and regulation by dietary K depletion. *Am J Physiol,* 276**:** C350-60, 1999

145. Codina J, Delmas-Mata JT, DuBose TD, Jr.: The alpha-subunit of the colonic H^+,K^+-ATPase assembles with beta1-Na^+,K^+-ATPase in kidney and distal colon. *J Biol Chem,* 273**:** 7894-9, 1998

146. Kraut JA, Hiura J, Shin JM, Smolka A, Sachs G, Scott D: The Na^+-K^+-ATPase beta 1 subunit is associated with the HK alpha 2 protein in the rat kidney. *Kidney Int,* 53**:** 958-62, 1998

147. Shao J, Gumz ML, Cain BD, Xia SL, Shull GE, van Driel IR, Wingo CS: Pharmacological profiles of the murine gastric and colonic H,K-ATPases. *Biochim Biophys Acta,* 1800**:** 906-11, 2010

148. Buffin-Meyer B, Younes-Ibrahim M, Barlet-Bas C, Cheval L, Marsy S, Doucet A: K depletion modifies the properties of Sch-28080-sensitive K-ATPase in rat collecting duct. *Am J Physiol,* 272**:** F124-31, 1997

149. Cougnon M, Planelles G, Crowson MS, Shull GE, Rossier BC, Jaisser F: The rat distal colon P-ATPase alpha subunit encodes a ouabain-sensitive H^+, K^+-ATPase. *J Biol Chem,* 271**:** 7277-80, 1996

150. Del Castillo JR, Rajendran VM, Binder HJ: Apical membrane localization of ouabain-sensitive K^+-activated ATPase activities in rat distal colon. *Am J Physiol,* 261**:** G1005-11, 1991

151. Dherbecourt O, Cheval L, Bloch-Faure M, Meneton P, Doucet A: Molecular identification of Sch28080-sensitive K-ATPase activities in the mouse kidney. *Pflugers Arch,* 451**:** 769-75, 2006

152. Abe K, Tani K, Fujiyoshi Y: Structural and functional characterization of H^+, K^+-ATPase with bound fluorinated phosphate analogs. *J Struct Biol,* 170**:** 60-8, 2010

153. Abe K, Tani K, Fujiyoshi Y: Conformational rearrangement of gastric H^+,K^+-ATPase induced by an acid suppressant. *Nat Commun,* 2**:** 155, 2011

154. Abe K, Tani K, Nishizawa T, Fujiyoshi Y: Inter-subunit interaction of gastric H^+,K^+-ATPase prevents reverse reaction of the transport cycle. *Embo J,* 28**:** 1637-43, 2009

155. Zhou X, Wingo CS: Mechanisms of rubidium permeation by rabbit cortical collecting duct during potassium restriction. *Am J Physiol,* 263**:** F1134-41, 1992

156. Zhou X, Xia SL, Wingo CS: Chloride transport by the rabbit cortical collecting duct: dependence on H,K-ATPase. *J Am Soc Nephrol,* 9**:** 2194-202, 1998

157. Swarts HG, Koenderink JB, Willems PH, De Pont JJ: The human non-gastric H,K-ATPase has a different cation specificity than the rat enzyme. *Biochim Biophys Acta,* 1768**:** 580-9, 2007

158. Swarts HG, Klaassen CH, Schuurmans Stekhoven FM, De Pont JJ: Sodium acts as a potassium analog on gastric H,K-ATPase. *J Biol Chem,* 270**:** 7890-5, 1995

159. Codina J, Pressley TA, DuBose TD, Jr.: The colonic H^+,K^+-ATPase functions as a Na^+-dependent K^+(NH_4^+)-ATPase in apical membranes from rat distal colon. *J Biol Chem,* 274**:** 19693-8, 1999

160. Swarts HG, Koenderink JB, Willems PH, De Pont JJ: The non-gastric H,K-ATPase is oligomycin-sensitive and can function as an H^+,NH_4^+-ATPase. *J Biol Chem,* 280**:** 33115-22, 2005

161. Crowson MS, Shull GE: Isolation and characterization of a cDNA encoding the putative distal colon H^+,K^+-ATPase. Similarity of deduced amino acid sequence to gastric H^+,K^+-ATPase and Na^+,K^+-ATPase and mRNA expression in distal colon, kidney, and uterus. *J Biol Chem,* 267**:** 13740-8, 1992

162. Shull GE: cDNA cloning of the beta-subunit of the rat gastric H,K-ATPase. *J Biol Chem,* 265**:** 12123-6, 1990

163. Shull GE, Lingrel JB: Molecular cloning of the rat stomach ($H^+ + K^+$)-ATPase. *J Biol Chem,* 261**:** 16788-91, 1986

164. Muraoka A, Kaise M, Guo YJ, Yamada J, Song I, DelValle J, Todisco A, Yamada T: Canine H^+-K^+-ATPase alpha-subunit gene promoter: studies with canine parietal cells in primary culture. *Am J Physiol,* 271**:** G1104-13, 1996

165. Newman PR, Greeb J, Keeton TP, Reyes AA, Shull GE: Structure of the human gastric H,K-ATPase gene and comparison of the 5'-flanking sequences of the human and rat genes. *DNA Cell Biol,* 9**:** 749-62, 1990

166. Zhang W, Kuncewicz T, Higham SC, Kone BC: Structure, promoter analysis, and chromosomal localization of the murine H^+/K^+-ATPase alpha 2 subunit gene. *J Am Soc Nephrol,* 12**:** 2554-64, 2001

167. Sverdlov VE, Kostina MB, Modyanov NN: Genomic organization of the human ATP1AL1 gene encoding a ouabain-sensitive H,K-ATPase. *Genomics,* 32**:** 317-27, 1996

168. Schar P, Fritsch O: DNA repair and the control of DNA methylation. *Prog Drug Res,* 67**:** 51-68, 2011

169. Canfield VA, Levenson R: Structural organization and transcription of the mouse gastric H^+, K^+-ATPase beta subunit gene. *Proc Natl Acad Sci U S A,* 88**:** 8247-51, 1991

170. Canfield VA, Okamoto CT, Chow D, Dorfman J, Gros P, Forte JG, Levenson R: Cloning of the H,K-ATPase beta subunit. Tissue-specific expression, chromosomal assignment, and relationship to Na,K-ATPase beta subunits. *J Biol Chem,* 265**:** 19878-84, 1990

171. Newman PR, Shull GE: Rat gastric H,K-ATPase beta-subunit gene: intron/exon organization, identification of multiple transcription initiation sites, and analysis of the 5'-flanking region. *Genomics,* 11**:** 252-62, 1991

172. Herrmann M, Selige J, Raffael S, Sachs G, Brambilla A, Klein T: Systematic expression profiling of the gastric H^+/K^+ ATPase in human tissue. *Scand J Gastroenterol,* 42**:** 1275-88, 2007

173. Shibata T, Hibino H, Doi K, Suzuki T, Hisa Y, Kurachi Y: Gastric type H^+,K^+-ATPase in the cochlear lateral wall is critically involved in formation of the endocochlear potential. *Am J Physiol Cell Physiol,* 291**:** C1038-48, 2006

174. Callaghan JM, Tan SS, Khan MA, Curran KA, Campbell WG, Smolka AJ, Toh BH, Gleeson PA, Wingo CS, Cain BD, et al.: Renal expression of the gene encoding the gastric H^+-K^+-ATPase beta-subunit. *Am J Physiol,* 268**:** F363-74, 1995

175. Campbell-Thompson ML, Verlander JW, Curran KA, Campbell WG, Cain BD, Wingo CS, McGuigan JE: In situ hybridization of H-K-ATPase beta-subunit mRNA in rat and rabbit kidney. *Am J Physiol,* 269**:** F345-54, 1995

176. Pestov NB, Korneenko TV, Adams G, Tillekeratne M, Shakhparonov MI, Modyanov NN: Nongastric H-K-ATPase in rodent prostate: lobe-specific expression and apical localization. *Am J Physiol Cell Physiol,* 282**:** C907-16, 2002

177. Pestov NB, Korneenko TV, Radkov R, Zhao H, Shakhparonov MI, Modyanov NN: Identification of the beta-subunit for nongastric H-K-ATPase in rat anterior prostate. *Am J Physiol Cell Physiol,* 286**:** C1229-37, 2004

178. Pestov NB, Korneenko TV, Shakhparonov MI, Shull GE, Modyanov NN: Loss of acidification of anterior prostate fluids in Atp12a-null mutant mice indicates that nongastric H-K-ATPase functions as proton pump in vivo. *Am J Physiol Cell Physiol,* 291**:** C366-74, 2006

179. Pestov NB, Romanova LG, Korneenko TV, Egorov MV, Kostina MB, Sverdlov VE, Askari A, Shakhparonov MI, Modyanov NN: Ouabain-sensitive H,K-ATPase: tissue-specific expression of the mammalian genes encoding the catalytic alpha subunit. *FEBS Lett,* 440**:** 320-4, 1998

180. Ahn KY, Kone BC: Expression and cellular localization of mRNA encoding the "gastric" isoform of H^+-K^+-ATPase alpha-subunit in rat kidney. *Am J Physiol,* 268**:** F99-109, 1995

181. Ahn KY, Park KY, Kim KK, Kone BC: Chronic hypokalemia enhances expression of the H^+-K^+-ATPase alpha 2-subunit gene in renal medulla. *Am J Physiol,* 271**:** F314-21, 1996

182. Bastani B: Colocalization of H-ATPase and H,K-ATPase immunoreactivity in the rat kidney. *J Am Soc Nephrol,* 5**:** 1476-82, 1995

183. Fejes-Toth G, Naray-Fejes-Toth A: Immunohistochemical localization of colonic H-K-ATPase to the apical membrane of connecting tubule cells. *Am J Physiol Renal Physiol,* 281**:** F318-25, 2001

184. Fejes-Toth G, Naray-Fejes-Toth A, Velazquez H: Intrarenal distribution of the colonic H,K-ATPase mRNA in rabbit. *Kidney Int,* 56**:** 1029-36, 1999

185. Kraut JA, Helander KG, Helander HF, Iroezi ND, Marcus EA, Sachs G: Detection and localization of H^+-K^+-ATPase isoforms in human kidney. *Am J Physiol Renal Physiol,* 281**:** F763-8, 2001

186. Wingo CS, Madsen KM, Smolka A, Tisher CC: H-K-ATPase immunoreactivity in cortical and outer medullary collecting duct. *Kidney Int,* 38**:** 985-90, 1990

187. Codina J, Delmas-Mata JT, DuBose TD, Jr.: Expression of HKalpha2 protein is increased selectively in renal medulla by chronic hypokalemia. *Am J Physiol,* 275**:** F433-40, 1998

188. Fejes-Toth G, Rusvai E, Longo KA, Naray-Fejes-Toth A: Expression of colonic H-K-ATPase mRNA in cortical collecting duct: regulation by acid/base balance. *Am J Physiol,* 269**:** F551-7, 1995

189. Wingo CS, Armitage FE: Rubidium absorption and proton secretion by rabbit outer medullary collecting duct via H-K-ATPase. *Am J Physiol,* 263**:** F849-57, 1992

190. Ahn KY, Turner PB, Madsen KM, Kone BC: Effects of chronic hypokalemia on renal expression of the "gastric" H^+-K^+-ATPase alpha-subunit gene. *Am J Physiol,* 270**:** F557-66, 1996

191. Silver RB, Choe H, Frindt G: Low-NaCl diet increases H-K-ATPase in intercalated cells from rat cortical collecting duct. *Am J Physiol,* 275**:** F94-102, 1998

192. Sangan P, Rajendran VM, Mann AS, Kashgarian M, Binder HJ: Regulation of colonic H-K-ATPase in large intestine and kidney by dietary Na depletion and dietary K depletion. *Am J Physiol,* 272**:** C685-96, 1997

193. Wall SM, Truong AV, DuBose TD, Jr.: H^+-K^+-ATPase mediates net acid secretion in rat terminal inner medullary collecting duct. *Am J Physiol,* 271**:** F1037-44, 1996

194. Zhou X, Wingo CS: H-K-ATPase enhancement of Rb efflux by cortical collecting duct. *Am J Physiol,* 263**:** F43-8, 1992

195. Eiam-Ong S, Dafnis E, Spohn M, Kurtzman NA, Sabatini S: H-K-ATPase in distal renal tubular acidosis: urinary tract obstruction, lithium, and amiloride. *Am J Physiol,* 265**:** F875-80, 1993

196. Eiam-ong S, Laski ME, Kurtzman NA, Sabatini S: Effect of respiratory acidosis and respiratory alkalosis on renal transport enzymes. *Am J Physiol,* 267**:** F390-9, 1994

197. Silver RB, Frindt G, Mennitt P, Satlin LM: Characterization and regulation of H-K-ATPase in intercalated cells of rabbit cortical collecting duct. *J Exp Zool,* 279**:** 443-55, 1997

198. Silver RB, Mennitt PA, Satlin LM: Stimulation of apical H-K-ATPase in intercalated cells of cortical collecting duct with chronic metabolic acidosis. *Am J Physiol,* 270**:** F539-47, 1996

199. Capurro C, Coutry N, Bonvalet JP, Escoubet B, Garty H, Farman N: Cellular localization and regulation of CHIF in kidney and colon. *Am J Physiol,* 271**:** C753-62, 1996

200. Frank AE, Wingo CS, Andrews PM, Ageloff S, Knepper MA, Weiner ID: Mechanisms through which ammonia regulates cortical collecting duct net proton secretion. *Am J Physiol Renal Physiol,* 282**:** F1120-8, 2002

201. Frank AE, Wingo CS, Weiner ID: Effects of ammonia on bicarbonate transport in the cortical collecting duct. *Am J Physiol Renal Physiol,* 278**:** F219-26, 2000

202. Garg LC: Respective roles of H-ATPase and H-K-ATPase in ion transport in the kidney. *J Am Soc Nephrol,* 2**:** 949-60, 1991

203. Jaisser F, Escoubet B, Coutry N, Eugene E, Bonvalet JP, Farman N: Differential regulation of putative K^+-ATPase by low-K^+ diet and corticosteroids in rat distal colon and kidney. *Am J Physiol,* 270**:** C679-87, 1996

204. Tojo A, Tisher CC, Madsen KM: Angiotensin II regulates H^+-ATPase activity in rat cortical collecting duct. *Am J Physiol,* 267**:** F1045-51, 1994

205. El Moghrabi S, Houillier P, Picard N, Sohet F, Wootla B, Bloch-Faure M, Leviel F, Cheval L, Frische S, Meneton P, Eladari D, Chambrey R: Tissue kallikrein permits early renal adaptation to potassium load. *Proc Natl Acad Sci U S A,* 107**:** 13526-31, 2010

206. Elabida B, Edwards A, Salhi A, Azroyan A, Fodstad H, Meneton P, Doucet A, Bloch-Faure M, Crambert G: Plasma steroid profiling under ionic stress reveals that progesterone is required for efficient renal adaptation to chronic dietary K^+ restriction in male. *Kidney Int*, 2011, In Press

207. Laroche-Joubert N, Marsy S, Doucet A: Cellular origin and hormonal regulation of K^+-ATPase activities sensitive to Sch-28080 in rat collecting duct. *Am J Physiol Renal Physiol,* 279**:** F1053-9, 2000

208. Laroche-Joubert N, Marsy S, Luriau S, Imbert-Teboul M, Doucet A: Mechanism of activation of ERK and H-K-ATPase by isoproterenol in rat cortical collecting duct. *Am J Physiol Renal Physiol,* 284**:** F948-54, 2003

209. Laroche-Joubert N, Marsy S, Michelet S, Imbert-Teboul M, Doucet A: Protein kinase A-independent activation of ERK and H,K-ATPase by cAMP in native kidney cells: role of Epac I. *J Biol Chem,* 277**:** 18598-604, 2002

210. Xu X, Zhang W, Kone BC: CREB trans-activates the murine H^+-K^+-ATPase alpha(2)-subunit gene. *Am J Physiol Cell Physiol,* 287**:** C903-11, 2004

211. Yu Z, Li M, Zhang D, Xu W, Kone BC: Sp1 trans-activates the murine H^+-K^+-ATPase alpha(2)-subunit gene. *Am J Physiol Renal Physiol,* 297**:** F63-70, 2009

212. Zhang W, Kone BC: NF-kappaB inhibits transcription of the H^+-K^+-ATPase alpha(2)-subunit gene: role of histone deacetylases. *Am J Physiol Renal Physiol,* 283**:** F904-11, 2002

213. Spicer Z, Miller ML, Andringa A, Riddle TM, Duffy JJ, Doetschman T, Shull GE: Stomachs of mice lacking the gastric H,K-ATPase alpha -subunit have achlorhydria, abnormal parietal cells, and ciliated metaplasia. *J Biol Chem,* 275**:** 21555-65, 2000

214. Franic TV, Judd LM, Robinson D, Barrett SP, Scarff KL, Gleeson PA, Samuelson LC, Van Driel IR: Regulation of gastric epithelial cell development revealed in H^+/K^+-ATPase beta-subunit- and gastrin-deficient mice. *Am J Physiol Gastrointest Liver Physiol,* 281**:** G1502-11, 2001

215. Scarff KL, Judd LM, Toh BH, Gleeson PA, Van Driel IR: Gastric H^+,K^+-adenosine triphosphatase beta subunit is required for normal function, development, and membrane structure of mouse parietal cells. *Gastroenterology,* 117**:** 605-18, 1999

216. Courtois-Coutry N, Roush D, Rajendran V, McCarthy JB, Geibel J, Kashgarian M, Caplan MJ: A tyrosine-based signal targets H/K-ATPase to a regulated compartment and is required for the cessation of gastric acid secretion. *Cell,* 90**:** 501-10, 1997

217. Wang T, Courtois-Coutry N, Giebisch G, Caplan MJ: A tyrosine-based signal regulates H-K-ATPase-mediated potassium reabsorption in the kidney. *Am J Physiol,* 275**:** F818-26, 1998

218. Meneton P, Schultheis PJ, Greeb J, Nieman ML, Liu LH, Clarke LL, Duffy JJ, Doetschman T, Lorenz JN, Shull GE: Increased sensitivity to K^+ deprivation in colonic H,K-ATPase-deficient mice. *J Clin Invest,* 101**:** 536-42, 1998

219. Spicer Z, Clarke LL, Gawenis LR, Shull GE: Colonic H^+-K^+-ATPase in K^+ conservation and electrogenic Na^+ absorption during Na^+ restriction. *Am J Physiol Gastrointest Liver Physiol,* 281**:** G1369-77, 2001

220. Marney AM, Brown NJ: Aldosterone and end-organ damage. *Clin Sci (Lond),* 113**:** 267-78, 2007

221. Coruzzi P, Brambilla L, Brambilla V, Gualerzi M, Rossi M, Parati G, Di Rienzo M, Tadonio J, Novarini A: Potassium depletion and salt sensitivity in essential hypertension. *J Clin Endocrinol Metab,* 86**:** 2857-62, 2001

222. Guntupalli J, Onuigbo M, Wall S, Alpern RJ, DuBose TD, Jr.: Adaptation to low-K^+ media increases H^+-K^+-ATPase but not H^+-ATPase-mediated pHi recovery in OMCD1 cells. *Am J Physiol,* 273**:** C558-71, 1997

223. Lin SH, Halperin ML: Hypokalemia: a practical approach to diagnosis and its genetic basis. *Curr Med Chem,* 14**:** 1551-65, 2007

224. Kovacikova J, Winter C, Loffing-Cueni D, Loffing J, Finberg KE, Lifton RP, Hummler E, Rossier B, Wagner CA: The connecting tubule is the main site of the furosemide-induced urinary acidification by the vacuolar H^+-ATPase. *Kidney Int,* 70**:** 1706-16, 2006

225. Kintzer PP, Peterson ME: Treatment and long-term follow-up of 205 dogs with hypoadrenocorticism. *J Vet Intern Med,* 11**:** 43-9, 1997

226. Lynn RC, Feldman EC: Treatment of canine hypoadrenocorticism with microcrystalline desoxycorticosterone pivalate. *Br Vet J,* 147**:** 478-83, 1991

227. Lynn RC, Feldman EC, Nelson RW: Efficacy of microcrystalline desoxycorticosterone pivalate for treatment of hypoadrenocorticism in dogs. DOCP Clinical Study Group. *J Am Vet Med Assoc,* 202**:** 392-6, 1993

228. Zies DL, Gumz ML, Wingo CS, Cain BD: Characterization of the rabbit HKalpha2 gene promoter. *Biochim Biophys Acta,* 1759**:** 443-50, 2006

229. Wallmark B, Briving C, Fryklund J, Munson K, Jackson R, Mendlein J, Rabon E, Sachs G: Inhibition of gastric H^+,K^+-ATPase and acid secretion by SCH 28080, a substituted pyridyl(1,2a)imidazole. *J Biol Chem,* 262**:** 2077-84, 1987

230. Thongboonkerd V, Chutipongtanate S, Kanlaya R, Songtawee N, Sinchaikul S, Parichatikanond P, Chen ST, Malasit P: Proteomic identification of alterations in metabolic enzymes and signaling proteins in hypokalemic nephropathy. *Proteomics,* 6**:** 2273-85, 2006

231. Sweiry JH, Binder HJ: Active potassium absorption in rat distal colon. *J Physiol,* 423**:** 155-70, 1990

232. Codina J, Pressley TA, DuBose TD, Jr.: Effect of chronic hypokalemia on H^+-K^+-ATPase expression in rat colon. *Am J Physiol,* 272**:** F22-30, 1997

233. Kraut JA, Hiura J, Besancon M, Smolka A, Sachs G, Scott D: Effect of hypokalemia on the abundance of HK alpha 1 and HK alpha 2 protein in the rat kidney. *Am J Physiol,* 272**:** F744-50, 1997

234. Coruzzi P, Gualerzi M, Parati G, Brambilla L, Brambilla V, Di Rienzo M, Novarini A: Potassium supplementation improves the natriuretic response to central volume expansion in primary aldosteronism. *Metabolism,* 52**:** 1597-600, 2003

235. Kornandakieti C, Tannen RL: Hydrogen ion secretion by the distal nephron in the rat: effect of potassium. *J Lab Clin Med,* 104**:** 293-303, 1984

236. Hulter HN, Licht JH, Sebastian A: K^+ deprivation potentiates the renal acid excretory effect of mineralocorticoid: obliteration by amiloride. *Am J Physiol,* 236**:** F48-57, 1979

237. Hulter HN, Sigala JF, Sebastian A: K^+ deprivation potentiates the renal alkalosis-producing effect of mineralocorticoid. *Am J Physiol,* 235**:** F298-309, 1978

238. Hulter HN, Sebastian A, Sigala JF, Licht JH, Glynn RD, Schambelan M, Biglieri EG: Pathogenesis of renal hyperchloremic acidosis resulting from dietary potassium restriction in the dog: role of aldosterone. *Am J Physiol,* 238**:** F79-91, 1980

239. Frindt G, Palmer LG: Effects of dietary K on cell-surface expression of renal ion channels and transporters. *Am J Physiol Renal Physiol,* 299**:** F890-7, 2010

240. Nakamura S: H^+-ATPase activity in selective disruption of H^+-K^+-ATPase alpha 1 gene of mice under normal and K-depleted conditions. *J Lab Clin Med,* 147**:** 45-51, 2006

241. Gennari FJ, Weise WJ: Acid-Base Disturbances in Gastrointestinal Disease. *Clin J Am Soc Nephrol,* 3**:** 1861-1868, 2008

242. Glad H, Svendsen P, Knuhtsen S, Olsen O, Schaffalitzky de Muckadell OB: Importance of gastrin-releasing peptide on acid-induced secretin release and pancreaticobiliary and duodenal bicarbonate secretion. *Scand J Gastroenterol,* 31**:** 993-1000, 1996

243. Pimenta E, Gaddam KK, Oparil S, Aban I, Husain S, Dell'Italia LJ, Calhoun DA: Effects of dietary sodium reduction on blood pressure in subjects with resistant hypertension: results from a randomized trial. *Hypertension,* 54**:** 475-81, 2009

244. Hager H, Kwon TH, Vinnikova AK, Masilamani S, Brooks HL, Frokiaer J, Knepper MA, Nielsen S: Immunocytochemical and immunoelectron microscopic localization of alpha-, beta-, and gamma-ENaC in rat kidney. *Am J Physiol Renal Physiol,* 280**:** F1093-106, 2001

245. Wang Q, Hummler E, Nussberger J, Clement S, Gabbiani G, Brunner HR, Burnier M: Blood pressure, cardiac, and renal responses to salt and deoxycorticosterone acetate in mice: role of Renin genes. *J Am Soc Nephrol,* 13**:** 1509-16, 2002

246. Rieg T, Dominguez JA: Unravelling a role for KCNQ1 in K^+ recycling and gastric acid secretion. *J Physiol,* 587**:** 4149-50, 2009

247. Saccomani G, Helander HF, Crago S, Chang HH, Dailey DW, Sachs G: Characterization of gastric mucosal membranes. X. Immunological studies of gastric (H^+ + K^+)-ATPase. *J Cell Biol,* 83**:** 271-83, 1979

248. Binder HJ: Organization of the Gastrointestinal System. In: *Medical Physiology,* 2nd ed. edited by Boron WF, Boulpaep EL, Philadelphia, PA, Saunders Elsevier, 2009, pp 883-894

249. Bhatt K, Mi QS, Dong Z: Invited Review- microRNAs in kidneys: biogenesis, regulation and pathophysiological roles. *Am J Physiol Renal Physiol*, 2011

250. Elvira-Matelot E, Zhou XO, Farman N, Beaurain G, Henrion-Caude A, Hadchouel J, Jeunemaitre X: Regulation of WNK1 expression by miR-192 and aldosterone. *J Am Soc Nephrol,* 21**:** 1724-31, 2010

251. Amlal H, Sheriff S, Faroqui S, Ma L, Barone S, Petrovic S, Soleimani M: Regulation of acid-base transporters by vasopressin in the kidney collecting duct of Brattleboro rat. *Am J Nephrol,* 26**:** 194-205, 2006

252. Musa-Aziz R, Barreto-Chaves ML, De Mello-Aires M: Peritubular AVP regulates bicarbonate reabsorption in cortical distal tubule via V(1) and V(2) receptors. *Am J Physiol Renal Physiol,* 282**:** F256-64, 2002

253. Inui A, Asakawa A, Bowers CY, Mantovani G, Laviano A, Meguid MM, Fujimiya M: Ghrelin, appetite, and gastric motility: the emerging role of the stomach as an endocrine organ. *Faseb J,* 18**:** 439-56, 2004

254. Tuukkanen J, Vaananen HK: Omeprazole, a specific inhibitor of H^+-K^+-ATPase, inhibits bone resorption in vitro. *Calcif Tissue Int,* 38**:** 123-5, 1986

255. O'Connell MB, Madden DM, Murray AM, Heaney RP, Kerzner LJ: Effects of proton pump inhibitors on calcium carbonate absorption in women: a randomized crossover trial. *Am J Med,* 118**:** 778-81, 2005

256. Yang YX, Lewis JD, Epstein S, Metz DC: Long-term proton pump inhibitor therapy and risk of hip fracture. *Jama,* 296**:** 2947-53, 2006

257. Sheraly AR, Lickorish D, Sarraf F, Davies JE: Use of gastrointestinal proton pump inhibitors to regulate osteoclast-mediated resorption of calcium phosphate cements in vivo. *Curr Drug Deliv,* 6**:** 192-8, 2009

BIOGRAPHICAL SKETCH

Megan Michelle Greenlee was born in Memphis, Tennessee. At the age of 5, Megan and her family moved to Lakeland, FL, where she spent the remainder of her childhood. She attended Rochelle School of the Arts for middle school and Harrison Arts Center for most of high school. Megan originally had ambitions to become an opera singer. However, after a great experience in a high school chemistry class, she changed her mind. In her senior year, Megan switched to and graduated from Lakeland Senior High School in 2003. In August 2003, she entered the University of Florida as an undergraduate, receiving a B.S. in interdisciplinary studies in biochemistry and molecular biology from the University of Florida in May 2006.

In August 2006, Megan began graduate studies in the College of Medicine's interdisciplinary program in biomedical research at the University of Florida. At the 2009 Experimental Biology conference in New Orleans, LA, Megan won 2nd place for the Pfizer Pre-doctoral Excellence in Renal Research Award. She has also authored many peer-reviewed scientific reviews and manuscripts. Megan currently has one published first-author research manuscript in the Journal of the American Society of Nephrology entitled "Mineralocorticoids stimulate the expression and activity of renal H^+,K^+-ATPases." She orally presented much of this manuscript's data at the 2010 Experimental Biology meeting in Anaheim, CA.

After graduation with her Ph.D., Megan will begin a post-doctoral fellowship at Emory University in Atlanta, Georgia under the direction of Doug Eaton. Her husband, Jeremiah Mitzelfelt, will also graduate with his Ph.D. and start a post-doctoral fellowship at Emory.